A Study On Wavelet Packet Based Algorithm For Representation of Wireless Channel

M.Sc Thesis

Submitted by:

PRASETIYONO HARI MUKTI

(Student ID: 4124464)

Supervisor:

Dr. Homayoun Nikookar

Mentor:

Madan Kumar Lakshmanan, M.Sc

International Research Center for Telecommunications and Radar
Department of Electrical Engineering, Mathematics and Computer Science
Delft University of Technology
Mekelweg 4, 2628 CD Delft, The Netherlands

August, 2011

A Study on Wavelet Packet Based Algorithm For Representation of Wireless Channel

by:
Prasetiyono Hari Mukti

M.Sc Thesis

Presented to the Faculty of the Graduate School of
Technische Universiteit Delft
In Partial Fulfillment of the Requirements
for the Degree of

Master of Science in Telecommunication

Technische Universiteit Delft
August 2011

The dream today will be the reality in the future

The fact today is the dream in the past

(Hasan Al-Banna)

To my parents, Moeljono and Eti Yuliati
My sisters, Chandra and Utari

M.Sc Thesis Presentation

Date : Friday, 19th August 2011
Time : 14:00 hrs
Location : Bordewijkzaal (HB19.130), EEMCS, TU Delft
Speaker : Prasetiyono Hari Mukti

Title : A Study on Wavelet Packet Based Algorithm For Representation of Wireless Channel

Abstract – Wireless telecommunication services are growing rapidly both in terms of the underlying technology as well as in the nature of the applications. The trends point to further growth in the foreseeable future. However, the dynamic nature of the wireless channel places fundamental limitations on the performance of wireless communication system. Unlike wired channels, which are by-and-large stationary and predictable, wireless channels are extremely random and do not offer easy analysis. Therefore, in order to gain better system performance it is of great importance to accurately and efficiently map the wireless channels.

Existing wireless channel models are based on statistical impulse response methods derived from empirical analysis. Such models employ a lot of channel coefficients which affect the complexity of computation. In this context the theory of wavelets and wavelet packets, which have recently found applicability for signal processing applications, hold the promise for wireless channel modeling. Wavelet packets offer the important feature of localization in both frequency and time domains. This property can be exploited to model channels with reduced complexity.

In this thesis report, the applicability of wireless channel representation based on wavelet packet algorithm is addressed. The possibility of one-dimensional and two-dimensional wavelet packet algorithm for time-invariant and time-varying representation, respectively, is investigated. The results illustrating the efficiency of one-dimensional and two-dimensional approach are presented. To improve the performance of the proposed system, two optimization methods, namely coefficient reduction and tree pruning are implemented. Furthermore, the impact of the number of decomposition levels and the type of mother wavelet employed are also investigated. To measure the system performance, first and second order stochastic metrics such as Mean-square Error (MSE), Level-Crossing Rate (LCR) and correlation were employed.

Acknowledgement

First, I would like to acknowledge the support and advice offered by Dr. H. Nikookar for offering invaluable assistance, expertise and guidance. I would also like to thank my mentor Madan K. Lakshmanan for continued assistance, encouragement, friendship and especially his humility that really helps me a lot to discover my confidence to finish this thesis. I am also grateful to Dyonisius Dony Arianandа for his invaluable assistance to understand the subject. Moreover, I would like also to thank for the real-time measured data from Dr. Zoubir Irahhauten which are very useful for validation campaign of my thesis.

Special thanks to Prof. L.P Ligthart from TU Delft and Dr. Suhartono Tjondronegoro from ITB who have offered me the opportunity as a student of Master Double Degree Program between ITB and TU Delft. I also thank to Erasmus Mundus Mobility for Life and The Ministry of National Education of Republic of Indonesia for granting me the scholarship covering most of the educational expensed for my study at TU Delft.

I would like also thank to the member of PPI Delft (Indonesian Students Assocation Delft) for the great friendship and caring me during my study at TU Delft, especially to Mas Agung, Pandu, Kang Andri, Kang Yugi, Bang Asrof, and of course my team of double degree student, namely Rahmat, Wahyu, and Bhimo.

My infinite thanks go to my parents and family for their love, continual prayers, and encouragement for me to finish my study at TU Delft.

Finally, *all the praises and thanks be to Allah, the Lord of the mankind and all that exists.*

Delft, August 2011

Prasetiyono Hari Mukti

Contents

List of Figures

List of Tables

List of Acronyms and Abbreviations

AFD	Average Fade Duration
AR	Autoregressive
CDF	Cumulative Distribution Function
CWT	Continuous Wavelet Transform
DWT	Discrete Wavelet Transform
FFT	Fast Fourier Transform
HPF	High Pass Filter
ICWT	Inverse Continuous Wavelet Transform
IDWT	Inverse Discrete Wavelet Transform
K-L	Karhunen-Loeve
LCR	Level-Crossing Rate
LOS	Line-of-Sight
LPF	Low Pass Filter
MRA	multi-resolution analysis
MSE	Mean Square Error
NLOS	Non-Line-of-Sight
NMSE	Normalized Mean Square Error
PDF	Probability Density Function
PDP	Power Delay Profile
PL	Path Loss
QMF	Quadrature Mirror Filters
RF	Radio Frequency
RMS	Root-mean-square
STFT	Short-Time Fourier Transform
UWB	Ultra-wideband
WP	wavelet Packet
WPT	Wavelet Packet Transform

List of Major Symbols

$h(t,\tau)$	Time-varying channel impulse response
$h(t)$	Time-invariant channel impulse response
$P(\tau)$	Power Delay Profile
$PL(d)$	Path Loss
τ	Time delay
f_d	Frequency Doppler
f_c	Frequency Carrier
$\varphi(t)$	Scaling function
$\psi(t)$	Wavelet function
$g[\bullet]$	High-pass Filter function
$h[\bullet]$	Low-pass Filter function
$A(j,k)$	Approximation of wavelet
$D(j,k)$	Detail of wavelet
$\xi(\bullet)$	1D Wavelet Packet Coefficient
$\chi(\bullet)$	2D Wavelet Packet Coefficient
$H(x)$	Entropy value

1

Introduction

1.1 Background and Motivation

Since Guiglielmo Marconi demonstrated the radio ability of continuous contact with ships sailing in 1897, the technology of communication has changed dramatically. Many applications and services have evolved towards the use of new wireless communication. Many wireless communication technologies have also emerged over the time. In this period, wireless communication is enjoying its fastest growth due to enabling technologies which permit wide spread deployment. The growth of mobile communication field has come slowly in the heels of Bell Laboratories development of the celluler concept in the 1960s and 1970s. Accordingly, with the incredible development in 1970s, the wireless communication era was born.

The widely used of wireless communication technologies leads to the huge employment of radio resource which are in fact limited to be allocated to all of wireless communication technologies. This limitation usually affects to the performance of wireless communication services. Besides that, the dynamic nature of radio link is also limited the performance of wireless communication. Hence, communication system design becomes an important thing to guarantee the quality of services of each technology.

In wireless communication design, modeling the wireless channel holds significant factor to make the system works efficiently. Due to the channel characteristic vary from one environment to another, having an accurate channel characterization for each frequency band, including key parameters and a detailed mathematical model of the channel, enables the designer or user of wireless system

to predict signal coverage, achievable data rate and the specific performance attributes of alternative signaling and reception schemes.

Many channel models are developed and reported in literature. Many ways can be used to model wireless channel into mathematical fashion, such as empirical method which is derived statistically from measurement campaign at different location and condition. Another way to model a wireless channel is using the information of location geography to determine the Maxwell equation solution of the signal, which is then called deterministic method. Generally, most of such models require a lot of coefficients to map the channel and are often inaccurate which make the computation complexity is high.

In another field, wavelet theory has been one of the powerful tools in signal processing to analyze many kind of data or signal. The property of wavelet transform allows analysis of signals at different resolution to gain more information on their characteristics in fields of image processing, data compression, radar, biomedical engineering and pure mathematics.

Recently wavelet transform has also been used in the design of sophisticated digital wireless communication systems including channel modeling, transceiver design, data representation and compression, source/channel coding, interference mitigation, signal de-noising and energy efficient networking.

Many works in the field of efficient channel model representation have been proposed by many kind of representation methods. Beside that, many methods of best basis selection of the signal have been proposed. However, no one of the channel representation methods employ the property of wavelet packet algorithm combined by best basis selection

This thesis works is an attempt to employ the property of wavelet packet algorithm for efficient wireless channel representation. In order to obtain represent the channel efficiently, we need the information of the best basis of the channel to be chosen for the representation. Accordingly, the methods of best basis selection of the channel representation will be also proposed through this thesis works.

1.2 Research Objectives and Contribution

Due to the fact that most of channel models require a lot of coefficient on their representation, the possibility of representation wireless channel model based on wavelet packet transform for sparse representation is investigated. The study is divided into two stages,

1. One-dimensional wavelet packet algorithm to represent time-invariant wireless channel model.
2. Two-dimensional wavelet packet algorithm to represent time-varying wireless channel model.

Both the wavelet packet algorithms are evaluated and examined to give an insight on the performance of each algorithm to represent such wireless channel with less number of coefficients.

Besides that, in order to select the best coefficients which are used to be reconstructed, the best basis selection algorithms are also proposed in this thesis, namely

1. Coefficient reduction
2. Tree-Pruning

Those best basis selection algorithms will be evaluated and compared between each other to obtain the information of the performance of those algorithms to select the best coefficient to be reconstructed.

1.3 Organization of Thesis Work

The rest of the thesis report is organized as follows. Chapter 2 and Chapter 3 provide the fundamental theory of channel modeling and wavelet packet, respectively. Chapter 4 describes the first contribution of this thesis works, namely, the representation of channel model using one-dimensional wavelet packet. This representation is developed by applying the novelty algorithm so called coefficient reduction which uses uniformly decomposition at the beginning of the algorithm and tree pruning which uses arbitrary wavelet packet tree structure to represent channel model. These algorithms are developed under the knowledge of entropy in information theory.

The representation method which is described in chapter 4 is applied for time-invariant channel model. Unfortunately, many signals encountered in practice are varying in time. Hence, in order to deal with time-varying channel model, two-dimensional wavelet packet for representing such channel model is investigated and reported in Chapter 5. This investigation is conducted under the knowledge of wavelet packet based image processing. The algorithm which has been developed in chapter 4 is also taken into account in this investigation, afterwards.

Finally, chapter 6 concludes this thesis work and gives overview about possible future researches.

2

Wireless Channel Model

Wireless communication systems have been widely deployed to fulfill the need of consumer applications. To run these applications, wireless communication system employs radio link to transmit the information from a radio transmitter to radio receiver. The characteristics of radio link not only vary from one environment to another but also vary within the environment itself due to the effects of signal propagation. These conditions limit the performance of wireless communication. Hence, having an adequate knowledge of channel characteristic is required to guarantee good performance of wireless communication.

An overview of channel model which represents the characteristic of wireless channel will be provided in this chapter. The discussion starts in section 2.1 which tells the mechanism of signal propagation which is affected to the characteristic of wireless channel is strongly influenced. Furthermore, in order to obtain good understanding of the channel behavior, mathematical channel model is explained in section 2.2. In designing the wireless communication system, there several parameters that have to be considered. These parameters will be described in Section 2.3. Finally, due to the fact that channel characteristic is vary both in time and space, section 2.4 gives an overview on the statistical models which are related to the channel parameters.

2.1 The Propagation Mechanisms

The variation of wireless channel characteristic is caused by the multiplicity of signal propagation which travels from transmitter to receiver, called *multipath propagation* (see Figure 2.1). Line-of-sight (LOS) is the simplest propagation of

signal since such signal travels directly from the transmitter to the receiver without any obstruction. Meanwhile, Non-line-of-sight (NLOS) is a complex propagation of signal due to such signal is severely obstructed by some obstacles between transmitter and receiver, such as buildings, foliage, mountains and hill. These obstacles lead to different mechanism of signal propagation, namely reflection, diffraction, and scattering [1]. The examples of signal propagation between transmitter and receiver are depicted in Figure 2.2.

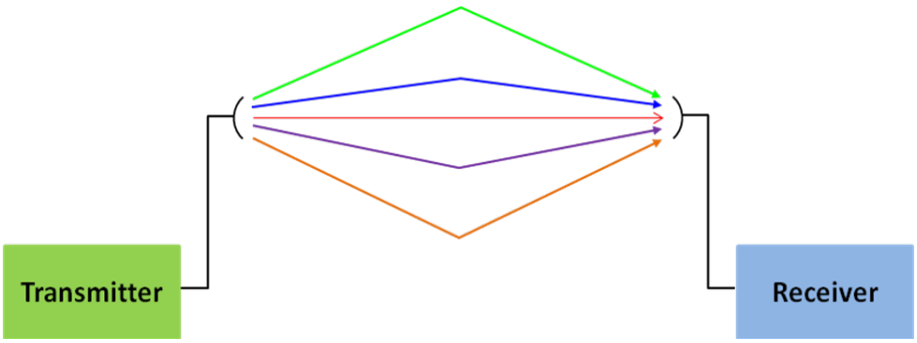

Figure 2.1 Multipath Propagation

Figure 2.2(a) represents a troposcatter radio communication link used in military applications for communication at long distances. The transmitted signal is directed toward the troposphere layer of the atmosphere, the incident wave is scattered, and some of the scattered signal energy reaches the receiver. Communication between the transmitter and the receiver can be modeled with several paths. Figure 2.2(b) represents a microwave radio link with line-of-sight (LOS) condition, which is widely used for terrestrial communications. However, occasionally, the reflected signal is also occurred from ground and atmosphere in such a way due to atmospheric conditions, creating a multipath condition. Figure 2.2(c) represents a mobile radio scenario where the received signal arrives by several paths: bounced from large objects such as buildings and local paths scattered from objects close to the receiver, such as ground or trees. Figure 2.2(d) shows a simple multipath condition for an indoor area.

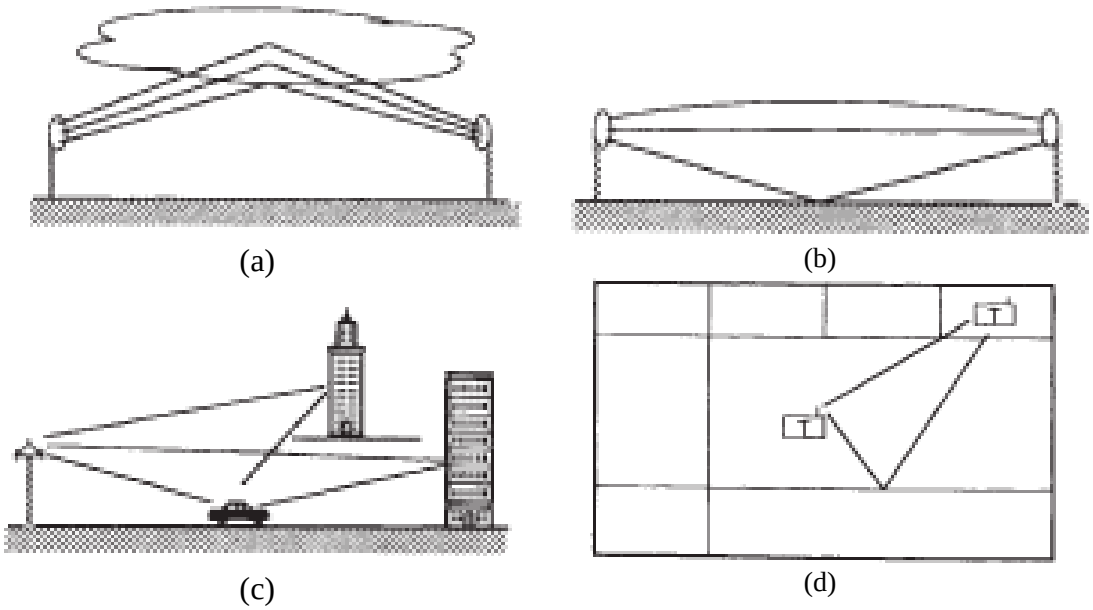

Figure 2.2 Propagation Scenarios of a signal traveling in (a) Toposcatter Propagation, (b) LOS Condition, (c) Mobile radio communication, (d) Indoor Propagation. [2]

The condition of each propagation mechanism can be explained, as follow [1],

Reflection occurs when a propagating electromagnetic wave impinges upon an object which has very large dimensions when compared to the wavelength of the propagating wave. Reflections occur from the surface of the earth and from buildings and walls.

Diffraction occurs when the radio path between the transmitter and receiver is obstructed obstructing surface are present throughout the space and even behind the obstacle, giving rise to a bending of waves around the obstacle, even when a line-of-sight path does not exist between transmitter and receiver. At high frequencies, diffraction, like reflection, depends on the geometry of the object, as well as the amplitude, phase, and polarization of the incident wave at the point of diffraction.

Scattering occurs when the medium through which the wave travels consists of objects with dimensions that are small compared to the wavelength, and where the number of obstacles per unit volume is large. Scattered waves are produced by rough surfaces, small objects, or by other irregularities in the channel. In practice, foliage, street signs, and lamp posts induce scattering in a mobile communications system.

2.2 Mathematical Modeling of Wireless Channel

The phenomena of multipath propagation cause self-replicas of signal. Each replica travels over different distances and thus suffers from different amplitude attenuation, phase shift, and arrives with different time delay. The detail of these factors will be described in a separate section, subsequently. These factors influence the received power at receiver may add destructively or constructively. Consequently, no one can predict what the signal power will be at the receiver.

In order to obtain accurate information about the characteristic of such channel, some researchers have derived mathematical model of wireless channel. These models can be classified into two domain, namely time domain and frequency domain. The main difference between time- and frequency- domain is that in the time domain use impulse response as a measure. Meanwhile, in the frequency domain, frequency domain is measured directly [2].

2.2.1 Time Domain Modeling

The time domain is a traditional measurement systems used for broadband and urban areas. This technique was first used to measure a variety of wideband radio channel [3]. In [3], Turin suggested the time-variant impulse response version of the channel model. This model is expressed as follow,

$$h(t) = \sum_{k=0}^{N-1} a_k \delta(t - t_k) e^{j\theta_k} \tag{2.1}$$

where the subscript k indices the k-th path from N paths of propagation path. Meanwhile, t represents the time occurrence of related path. The variables a, θ and δ represent path amplitude, phase and dirac-delta function, respectively.

Afterwards, due to the fact the nature of wireless channel is not stationary either in time of space, the equation (2.1) has to be expanded to meet time-varying wireless channel. To fulfill this circumstance, Hashemi in [4] proposed a time-varying channel model as a linear time-varying filter with the impulse response given as,

$$h(t,\tau) = \sum_{n=0}^{N(\tau)-1} a_n(t) \delta\left[\tau - \tau(t)\right] e^{j\theta_n(t)} \tag{2.2}$$

where t and τ are the observation time and application of the impulse, respectively. The function of $N(\tau)$ represents the number of multipath components. Meanwhile, $a_n(t)$, $\tau_n(t)$ and $\theta_n(t)$ are the random time-varying amplitude, arrival time, and phase sequences, respectively, of related path, and $\delta(\bullet)$ is the Dirac delta function. This mathematical model is a wideband model that can be used to obtain the response of the channel to the transmission of any signal [4].

Wideband model, usually, is used for the application which needs high data rates or inherently wideband transmission. Besides that, based on the application of communication system there are other systems which can be considered, that are narrowband and ultra-wideband communication.

In case of narrowband communication system, a signal with small bandwidth centered around a single frequency is used to excite the channel. Such channel can be expressed as

$$Ae^{j\theta} = \sum_{k=1}^{K} a_k e^{j\theta_k} \tag{2.3}$$

Where A and θ are the amplitude and phase of the received signal.

The equation (2.3) describes that the channel considered as narrowband only provide information on the power fluctuation caused by the signal arriving from a number of different paths. Whereas, equation (2.2) describes that if the channel considered as wideband then the multipath delay spread and phase of signal arrival can be extracted from the measurement.

2.2.2 Frequency Domain Modeling

In the preceding discussion, the time domain mathematical model has been described. However, there is a shortcoming in the implementation of time domain modeling due to the complexity of computation. Hence, another way to model the channel with simple method, namely frequency domain modeling which uses Autoregressive (AR) model. This model was first introduced by Howard et al. [5].

The basic idea of AR modeling is that the frequency response $H(f_n)$ of the channel at frequency $f = f_n$ can be modeled by an AR process. The AR model has the advantage that it can statistically represent the channel with a minimum number

of parameters. Accordingly, the measured frequency responses can be regenerated in an easier way, important for computer simulation. The model can be expressed as:

$$H(f_n, x) = \sum_{i=1}^{p} a_i H(f_{n-i}, x) + V(f_n) \tag{2.4}$$

where $H(f_i)$ is the *n*-th sample of the complex frequency domain measurement and $V(f_n)$ is a complex white noise process representing the error between the actual frequency response value at frequency f_n and its estimate based on the last *p* samples of the frequency response [2]. Taking the *z*-transformation of equation (2.4), the AR process $H(f_n, x)$ can be viewed as the output of a linear filter with transfer function

$$G(z) = \frac{1}{1 - \sum_{i=1}^{p} a_i z^{-i}} = \prod_{i=1}^{p} \frac{1}{(1 - p_i z^{-i})} \tag{2.5}$$

excited by $V(f_n)$. With this method only *p* poles are required to characterize the frequency response of the channel. The geometry of the poles is important. The delay associated with a pole is determined by the angle of that pole and the distance of a pole to the unit circle represents the power at the corresponding delay.

2.3 Channel Parameters for system design

In the campaign of wireless channel design, the knowledge on the parameters which are affected to the system performance is important. This knowledge can lead to the reliability of the system against to the obstruction.

2.3.1 Power Delay Profile

When such channel is considered as multipath time-invariant channel, the average received signal power as function of excess time delay is called the power delay profile (PDP). Using the impulse response in (2.1), the profile can be obtained as

$$P(\tau) = E\left\{|h(t)|^2\right\} = \sum_{n=0}^{N-1} \overline{a_n^2}\, \delta(\tau - \tau_n) \tag{2.6}$$

Usually later paths of the power delay profile experience more attenuation and accordingly the power delay profile are generally decreasing function of excess delay.

2.3.2 Path Loss, shadowing and Fading

As described in previous section that due to several obstacles between transmitter and receiver the average received power at the receiver will be vary. The variation of signal can be classified into three types, that are path loss, shadowing and multipath fading. Figure 2.3 illustrates the ratio of the received-to-transmit power in dB versus log-distance for the combined effects of path loss, shadowing, and multipath.

Variation due to path loss occurs over very large distances (100-1000 meters), whereas variation due to shadowing occurs over distances proportional to the length of the obstructing object (10-100 meters in outdoor environments and less in indoor environments). Since variations due to path loss and shadowing occur over relatively large distances, this variation is sometimes refered to as *large-scale propagation effects*. Variation due to multipath occurs over very short distances, on the order of the signal wavelength, so these variations are sometimes refered to as *small-scale propagation effects* [6].

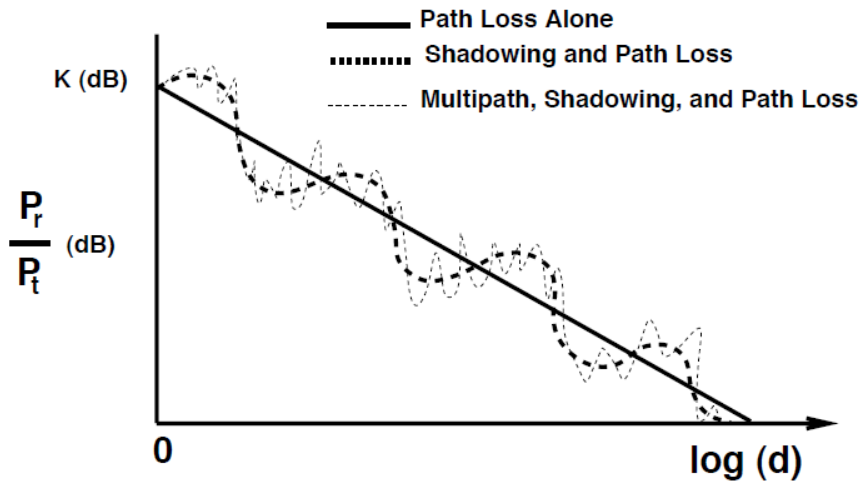

Figure 2.3 Path loss, shadowing and Multipath [6]

Path loss model

Path loss is defined as the radio of the transmit signal power to the receiver signal power. Path loss is happened due to dissipation of the power radiated by the transmitter over certain distance as well as effects of the propagation channel. Generally, path loss model is assumed has same path loss value a given transmitter-receiver distance [1],[6]. Accordingly, path loss model is a function of distance which exponentially increases with the increasing of distance between transmitter and receiver. This function of path loss $PL(d)$ can be express as

$$PL(d) \propto \left(\frac{d}{d_0} \right)^{\alpha} \tag{2.7}$$

Where d and d_0 are distance between transmitter and receiver, and the reference distance (corresponding to a point located in the far-field of the antenna, usually $d_0 = 1$ m). Meanwhile, α is the path loss exponent. The path loss exponent indicates how fast the signal power is decaying as function of distance and usually depends on the type of propagation environment. In logarithmic scale, equation (2.7) can be transformed as

$$PL_{[dB]}(d) = PL_{[dB]}(d_0) + 10\alpha \log_{10}\left(\frac{d}{d_0} \right) \tag{2.8}$$

Besides that definition, according to Friss Free Space Equation, path loss can be also considered as the attenuation of RF energy between the transmitter and receiver according to an inverse-square law. The received power expressed in terms of transmitted power is attenuated by a factor $PL(d)$, which can be also expressed as [1]

$$PL(d) = \frac{P_r}{P_t} = G_t G_r \left(\frac{\lambda}{4\pi d} \right)^2 \tag{2.9}$$

where P_r and P_t is received and transmitted signal power, respectively, G_t and G_r is antenna gain of transmitter and receiver, respectively, λ is wavelength, and d is distance between transmitter and receiver.

Shadowing

In many cases, path loss model is often not valid if the users who have equal distance to the receiver but placed at different locations. The users in this condition do not always receive similar signal power as resulted from path loss model but vary significantly. This slow signal fluctuation is known as shadowing or shadow fading. Based on this condition, shadow fading can be also defined as the long-term average changes in the received signal strength caused by changes in the relative position of large objects between transmitter and receiver.

Researchers have found that a good agreement of signal power variations around the average path-loss can be obtained with the lognormal distribution (i.e. Gaussian distribution in logarithmic scale) [4]. So, the shadowing effect is usually modeled as a lognormal random process, meaning that the path-loss model can be described by:

$$PL_{[dB]}(d) = PL_{[dB]}(d_0) + 10\alpha \log_{10}\left(\frac{d}{d_0}\right) + X_\sigma \qquad (2.10)$$

Where X_σ is a zero-mean Gaussian random variable in logarithmic scale with standard deviation σ.

Multipath Fading

Multipath fading is the rapid instantaneous changes in the received signal power caused by constructive and destructive interferences between replicas of the transmitted signal. This condition can be happened since the wavelength of transmitted signal is very small compared to distance; hence small movement can produce phase shifts of each replica that result in large variation in their coherent sum. Consequently, after superposition of all path signals, it affects the resulting overall received signal.

In statistical modeling, shadowing effect in a large area can be represented by log-normal distribution. While small-scale fading is usually called ***Rayleigh fading*** because if the multiple reflective paths are large in number and there is no line-of-sight signal component, the envelope of the received signal is statistically described by a power density function of Rayleigh, when there is a dominant non-fading signal

component present, such as a line-of-sight propagation path, the small-scale fading envelope is described by a power density function of **Rician [1]**.

2.3.3 RMS Delay spread

Due to the multipath propagation of a signal over fading multipath channel, arrival time of each path in the receiver can be also varied of that to another path. The arrival time of each path is equal to the distance over signal velocity, in this case equal to the light velocity. The difference arrival time from the earliest to the latest path is called *maximun excess delay*, as shown in Figure 2.4. In some case, considering that parameter is not the best indicator of how any given system would perform on the channel. This is because the same excess delay spread in different channel can exhibit very different profiles of signal intensity. Therefore, a better measure of delay spread is the root mean square (rms) delay spread, τ_{rms}, which is the second central moment of the channel impulse response [2] or power delay profile [1]. It can be mathematically expressed as

$$\tau_{rms} = \sqrt{\overline{\tau^2} - \left(\overline{\tau}\right)^2} \tag{2.11}$$

with,

$$\overline{\tau^n} = \frac{\sum_k a^2{}_k \tau^n{}_k}{\sum_k a^2{}_k} = \frac{\sum_k P(\tau_k)\tau^n{}_k}{\sum_k P(\tau_k)}$$

where a_n, P_n and τ_n are the amplitude, power and delay characteristics, respectively.

The first derivation of this parameter is *coherence bandwidth*. The coherence bandwidth, is a defined relation derived from the RMS delay spread, τ_{rms}. Coherence bandwidth is a statistical measure of the range of frequencies over which the channel can be considered "flat", which mean a channel which passes all spectral components with approximately equal gain and linear phase. In other words, coherence bandwidth is the range of frequencies over which two frequency components have a strong potential for amplitude correlation. Two sinusoids with frequency separation greater than are affected quite differently by the channel. If the coherence bandwidth

is defined as the bandwidth over which the frequency correlation function is above 90%, then the coherence bandwidth is approximately [1]

$$B_c \approx \frac{1}{50\,\tau_{rms}}$$

And if the definition is related to the frequency correlation function above 50%, then the coherence bandwidth is approximately [1]

$$B_c \approx \frac{1}{5\,\tau_{rms}}$$

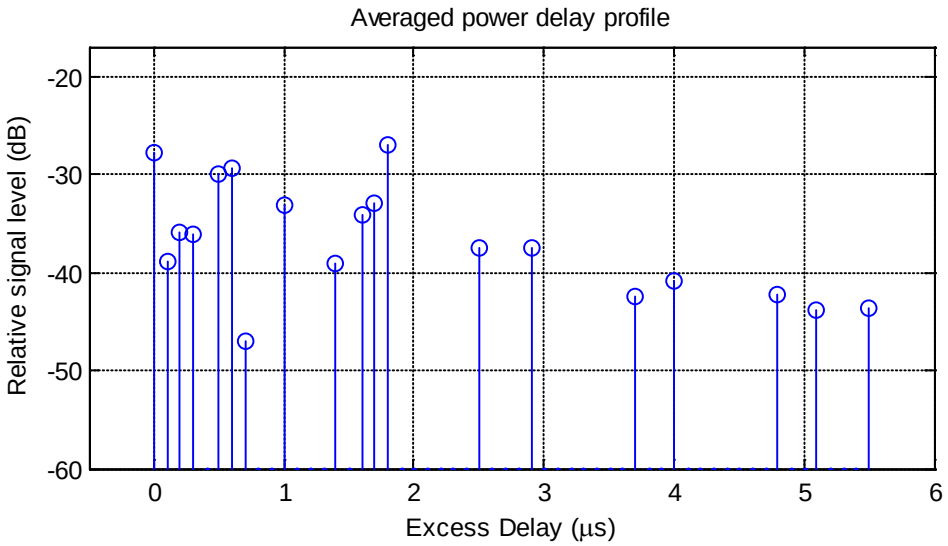

Figure 2.4 Delay Spread Profile

From approximated value of the coherence bandwidth, we can classify the behaviours of channel based on that definition and is compared to the transmitted signal bandwidth, that are

1. Frequency-selective fading, this behavior occurs when the transmitted signal bandwidth is larger than the coherence bandwidth.
2. Flat fading, this behavior occurs when the transmitted signal bandwidth is smaller than the coherence bandwidth.

2.3.4 Doppler Spectrum

Beside the attenuated power in the receiver, there is another parameter which can be derived when transmitting a sine wave over a fading multipath channel, that is

Doppler frequency shift. This parameter comes from the fundamental of physics that whenever a transmitter and a receiver are in relative motion, the received carrier frequency is shifted relative to the transmitted carrier frequency. The shifting of the frequency carrier observed at the receiver can be expressed by

$$f_d = \frac{v_m}{c} f_c$$

where v_m is the relative motion speed of the portable terminal toward or away to the fixed terminal and f_c is transmitted frequency carrier. The Doppler frequency shift f_d is either positive or negative depending on whether the transmitter is moving toward or away from the receiver.

In a realistic channel environment, due to the multipath propagation, the velocity of movement of each arriving path is different from that of another path. Thus, instead of being subjected to a simple Doppler shift, we refer to as the *Doppler spectrum*. This effect can be viewed as a spreading of the transmitted signal frequency, and can referred generally as *Doppler spread* of the channel. Beside the movement of transmitter and receiver, Doppler spread can also occur when person or objects moves within the propagation path between fixed transmitter and receiver.

The behavior described above describes the channel in a local area, they do not provide information about time-varying nature of channel caused by by relative motion between a transmitter and receiver, or by movement of objects within the channel. Since the channel characteristics are dependent on the positions of the transmitter and receiver, time variance in this case is equivalent to spatial variance. One of the parameters that can be used to describe this behavior is *coherence time*.

In time-frequency domain analysis, the Coherence time, T_c, is the time domain dual of Doppler spread in frequency domain and is used to characterize the time varying nature of the frequency dispersiveness of the channel in the time domain. The Doppler spread and coherence time are inversely proportional to one another. That is,

$$T_c = 1 \big/ f_d$$

where f_d is maximum doppler spread given by $f_d = v/\lambda$.

The coherence time is defined as a a statistical measure of the time duration over which the channel impulse response is essentially invariant, and quantifies the similarity of the channel response at different times. In other words, coherence time is the time duration over which two received signals have a strong potential for amplitude correlation. If the coherence time is defined as the time over which the time correlation function is above 50%, then the coherence time is approximately

$$T_c = \frac{9}{16\pi f_d}$$

A popular rule of thumb for modern digital communications is to define the coherence time as the geometric mean of the two equations above. That is,

$$T_c = \sqrt{\frac{9}{16\pi f_d^{\,2}}}$$

The coherence time parameter, T_c, indicates the rate of the channel changes. If we compare that parameter to the transmitted signal duration, we can classify as follow

1. Slow fading, this behavior occurs when the transmitted signal duration is smaller than the coherence time. In other word, the channel behaves in a correlated manner is long compared to the time duration of a transmission symbol.
2. Fast fading, this behavior occurs when the transmitted signal duration is greater than the coherence time. In other word, the channel response impulse changes rapidly within the signal duration due to a correlated manner is short compared to the time duration of a symbol.

2.3.5 Fading Rate and Fading Duration

In wireless communication system, many mobile devices have a certain level of sensitivity to receive the signal from transmitter with good performance. In order to guarantee the quality of received signal in the receiver, level of sensitivity must be taken into account in designing a system due to the fact that multipath propagation cause signal power fluctuation in the receiver. Hence, two parameters of second-order statistic are developed to measure the rate of fading signal below a given signal

level and duration of a fading signal below a given level. These parameters were first derived by Lee in [11].

Fading Rate

Fading rate which is also referred as Level-Crossing Rate (LCR) is defined as the expected rate of fading, normalized to the local RMS signal level, crosses a specified level in a positive-going direction [1]. In case of Rayleigh fading, the number of level-crossing N_α at a given signal level α can be expressed as

$$\begin{aligned} LCR = N_\alpha &= \int_0^\infty \hat{A} p\left(A, \hat{A}\right) d\hat{A} \\ &= \sqrt{2\pi} f_d \alpha \exp\left(-\alpha\right) \end{aligned} \tag{2.12}$$

Where f_d is the maximum Doppler shift and $\alpha = A / A_{rms}$ is the value of the specified A, normalized to the local rms amplitude of the fading envelope. Whereas, $p\left(A, \hat{A}\right)$ is a joint probability density function of A and its slope $\hat{A}$. A slope $\hat{A}$ is a time derivation of A which can be expressed as

$$\hat{A} = \frac{dA}{\tau}$$

Fading Duration

The average fade duration is defined as the average period of time for which the received signal stays below a specified level A. For Rayleigh fading, the average fade duration, AFD, is given as

$$\begin{aligned} \overline{\tau} &= \frac{1}{LCR} \Pr\left[a \le A\right] \\ &= \frac{\exp\left(\alpha^2\right) - 1}{\sqrt{2\pi}\alpha f_d} \end{aligned} \tag{2.13}$$

Where $\Pr\left[a \le A\right]$ is the probability that the received signal a is less than A which given as

$$\begin{aligned} \Pr\left[a \le A\right] &= \int_0^A p\left(a\right) \\ &= 1 - \exp\left(-\rho^2\right) \end{aligned}$$

2.4 Statistical Model for Channel Parameters

The nature of wireless channel is completely random, not only in time but also in space. Modeling such channel mathematically is not sufficient, so that many researchers develop the channel model based on statistical method obtained from empirical analysis. This modeling is affected to the channel parameters which are also modeled statistically. In this subsection, the statistical model of each parameter will be described.

2.4.1 Path amplitude

Rayleigh Distribution

In mobile radio channels, the Rayleigh distribution is the most accepted model for small-scale rapid amplitude fluctuations in absence of the LOS component. The probability density function (PDF) is given by:

$$f(x) = \frac{x}{\sigma^2}\exp\left(-\frac{x^2}{2\sigma^2}\right) \tag{2.14}$$

Where σ is the rms value of the received signal voltage, and σ^2 is the time-averaged power of the received signal. The mean and variance of Rayleigh are $\sigma/\sqrt{\pi/2}$ and $\sigma(2-\pi/2)$, respectively.

Rician Distribution

Different to the Rayleigh Channel, in some cases, the line-of-sight (LOS) signal is involved in the amplitude fluctuation. In this case, Rayleigh distribution for modeling such amplitude is not valid; hence Rician distribution is proposed to model such amplitude which is also happened in small-scale propagation. The PDF of Rician distribution is given as

$$f(x) = \frac{x}{\sigma^2}\exp\left(-\frac{x^2+A^2}{2\sigma^2}\right)I_0\left(\frac{Ax}{\sigma^2}\right) \tag{2.15}$$

where A is the LOS component amplitude and I_0 is the zero-order modified Bessel function of the first kind expressed as:

$$I_0 = \frac{1}{2\pi}\int_{-\pi}^{+\pi} e^{x\cos\phi}d\phi \tag{2.16}$$

Usually, a parameter K_{rice} which is called as Rice factor is introduced to describe the Rice distribution, and is defined as:

$$K_{rice} = \frac{A}{2\sigma} \tag{2.17}$$

In case of $A = 0$, the Rician distribution becomes the Rayleigh distribution.

Log-normal Distribution

In multipath fading, not only small-scale propagation that has to be taken into account but also large-scale propagation. In large-scale propagation the distance between transmitter and receiver is much larger than signal wavelength. The fluctuation of received signal due to large-scale propagation can modeled as log-normal distribution. The PDF of this distribution is given by

$$f(x) = \frac{1}{\sigma x\sqrt{2\pi}} \exp\left[-\frac{(\ln x - \mu)^2}{2\sigma^2} \right] \tag{2.18}$$

Where $\ln x$ has a normal (Gaussian) distribution, and the parameters μ and σ^2 are the mean and variance, respectively.

Nakagami Distribution

In Rayleigh distribution, the length of scatter vectors are nearly equal and their phase are random. However, in real life, the length of scatter vector is actually random. So that, Rayleigh distribution is not quite suitable to model such fading. To fulfill this circumstance, the Nakagami distribution, which is also known as *m*-distribution, is proposed. The PDF is given as [8]

$$f(x) = \frac{2m^m x^{2m-1}}{\Gamma(m)\Omega^m} \exp\left[-\frac{mx^2}{\Omega^2} \right] \tag{2.19}$$

Where $\Omega = E\left[x^2\right]$, $m = \left[E\left(x^2\right)\right]^2 \Big/ \mathrm{var}\left(x^2\right) \geq 0.5$ and $\Gamma(\bullet)$ is the Gamma function defines as

$$\Gamma(m) = \int_0^\infty t^{m-1} \exp(-t)\, dt \tag{2.20}$$

The Nakagami Distribution reduces to the Rayleigh distribution for $m = 1$.

Weibull Distribution

The probability density function (PDF) of Weibull Distribution is expressed as

$$f(x) = \frac{\beta}{b}\left(\frac{x}{b}\right)\exp\left[-\left(\frac{x}{b}\right)\beta\right] \tag{2.21}$$

where β and b are the shape and scale factors, respectively. The distribution reduces to the exponential distribution for $\beta = 1$, and to the Rayleigh distribution for $\beta = 2$.

2.4.2 Path Arrival time model

As described in the preceding section, the signal experiences multiple paths because of many obstacles. The multiplicity of propagation path causes different path lengths of each replica. Hence, arrival time of each replica in the receiver is also different. The sequence of arrival time, which is also called excess delay, in the receiver can be modeled as Poisson distribution [3][4]. In this distribution, the probability of l arriving paths within an interval of T seconds is given as [9]

$$P(L = l) = \frac{\mu^l e^{-\mu l}}{l!} \tag{2.22}$$

Where $\mu = \int_T \lambda(t)dt$ is the Poisson parameter, and $\lambda(t)$ is the mean arrival rate at time t. Another distribution related to the arrival time sequence is the inter-arrival time sequence, defined as the difference between two successive arrival paths where $x_i = \tau_i - \tau_{i-1}$. For a standard Poisson process, the differences are exponentially distributed:

$$f(x) = \lambda e^{-\lambda x} \tag{2.23}$$

Analysis of time of arrival of multipath components of the indoor and mobile data base has shown that standard Poisson model does not provide a good fit [10]. This mismatch is probably due to the fact that scatterers inside a building (causing multipath dispersion) are not randomly located. Patterns in their location give rise to deviations from a standard Poisson model, which is based on purely random arrival times [10]. A more realistic model is the "modified Poisson" or $\Delta - K$ model. This

model which takes into account the clustering properties of multipath components was first suggested by G.L.Turin [3] and was successfully used in analysis [10].

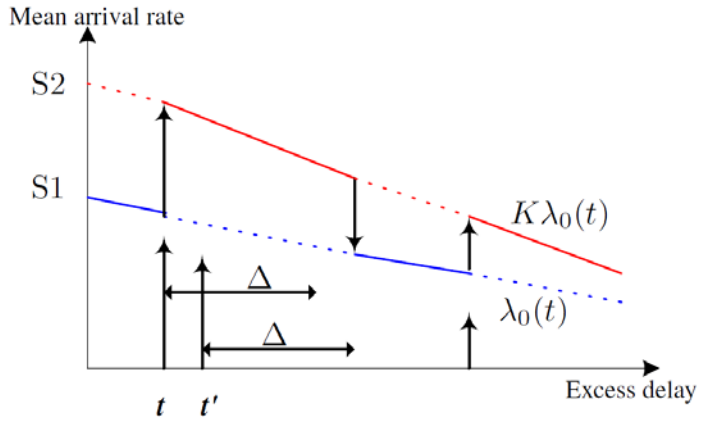

Figure 2.5 Modified Poisson Process

The model tries to create the correlation between radio wave arrivals by means of two parameters, K and Δ [10]. As we can see in Figure 2.5, the model has two states: S_1 and S_2. The first is the initial state, where the mean arrival rate of the paths is $\lambda_0(t)$. As soon as a path reaches the receiver, the process makes a transition to state S_2, where the mean arrival rate is $K\lambda_0(t)$. If no path arrives in the next Δ seconds, then the process comes back to S_1. However, if a path arrives at time t' before the interval is out, then it is restarted. The model can therefore be described by a series of transitions between the two states. If the parameter $\Delta = 0$ or $K = 1$, the model reverts to the standard Poisson process. For $K > 1$, an incidence of a path at time t increases the probability of receiving another path in the next Δ interval (i.e., the process shows a clustering property). On the other hand, if $K < 1$, the probability of a path occurrence in the Δ seconds after a path arrived at time t is decreased (i.e., the paths arrive more evenly than in a standard Poisson process) [10].

2.4.3 Phase Model

Besides the arrival time, multipath propagation is also affected to the phase of the transmitted signal. The signal phase is critically sensitive to path length and changes by a factor of 2π as the path length changes by a wavelength. Small changes (in order of meters) in the position of receiver yields in a great change in

phase. When one considers an ensemble of points, therefore, it is reasonable to expect uniform distribution; i.e., on a global basis, θ_n, has a Uniform $[0, 2\pi)$ distribution. For small sampling distances, however, great deviations from uniformity may occur. Furthermore, phase values are strongly correlated if the channel's impulse response is sampled at the sampling rate (tens to hundreds of kilobits per second). Phase values at a fixed delay for a given site are therefore correlated [4]. Adjacent detectable multipath components of the same profile, on the other hand, have independent phases since their excess range (excess delay multiplied by speed of light) is longer than a wavelength, even for very high resolution (a few nanoseconds) measurements [4].

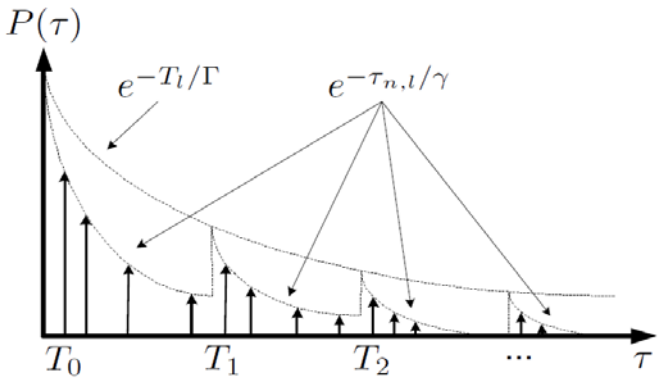

Figure 2.6 Power Delay Profile with double exponential model

2.4.4 Power Delay Profile models

The behavior of the averaged received power as function of excess time delay follows mostly an exponential decreasing function since the later paths of the profile experience more attenuation after traveling over larger distances [4]. However, for indoor environments another model is introduced based on measurements [12],[13]. This model refers to the double exponential model based on clustering, i.e., the received components arrive in clusters, in terms of arriving angles and delays. In Figure 2.6, a scheme showing the double exponential model is presented. T_l refers to the arrival time of the first path in the *l*-th cluster, $\tau_{n,l}$ refers to the arrival time of the *n*-th path in the *l*-th cluster and Γ and γ are the ray and cluster time decay constants of the power delay profiles, respectively.

3

Wavelet Theory

The wavelet transform is a powerful tool used to gain insight on a signal. It has been widely used in many applications of signal processing, such as image processing, data compression and the design of sophisticated digital wireless communication systems. The power of wavelet transform comes from the fact that the basis functions of the transform have compact support in time (or space) and are localized in frequency. Furthermore, the technique allows analysis of signals at different resolutions which often correspond to the natural behavior of the process one wants to understand.

In this chapter, an overview of fundamental concepts of wavelet theory is provided. Section 3.1 describes the principle of signal representation and its progression. In this section, an overview on time-frequency localization is also described. Two types of wavelet transform, namely Continuous Wavelet Transform (CWT) and Discrete Wavelet Transform (DWT) are explained in section 3.2 and section 3.4, respectively. Meanwhile, section 3.3 presents the important basic of the wavelet theory, which is called multi-resolution analysis (MRA). The implementation of discrete wavelet transform in terms of filter banks is elaborated in section 3.5. An important variant of the wavelet transform known as Wavelet Packet Transform is presented in section 3.5.2. In section 3.5 and section 3.5.2, the signal reconstruction using filter banks is also described. Finally, a review on wavelet properties a few popular wavelet families are given in section 3.7.

3.1 Representation of Signals

In real life, many signals are constituted by the series of linear function, which is usually called *basis function*. Mathematical signal representation is a way to describe information of such signal in term of their basis function. A mathematical transform is usually a linear expression where any given signal $f(x)$ in space S is expressed as a linear combination of a set of known signals $\{\varphi_i\}_{i\in Z}$ as [13]

$$f(x)=\sum_i \alpha_i \varphi_i \tag{3.1}$$

In (3.1), α_i are the expansion coefficients (of weights) which tell how much of the component φ_i is available in the original signal $f(x)$. The space S can be finite dimensional like (e.g. $\mathbb{R}^n, C^n$) or infinite dimensional (e.g. l^2, L^2)

In the case of all signals $x\in\mathbb{Z}$ can be expanded as in (3.1), then there will also exist a dual set $\{\overline{\varphi}_i\}_{i\in Z}$ such that the expansion coefficient α_i in (3.1) can be computed as

$$\alpha_i=\left\langle f(x),\overline{\varphi}_i\right\rangle \tag{3.2}$$

Where $\langle\ ,\ \rangle$ represents an inner product operation. An important particular case is when the set $\{\varphi_i\}_{i\in Z}$ is orthonormal and complete, since then we have an orthonormal basis for S and the basis and its dual are the same, that is, $\varphi_i=\overline{\varphi}_i$. Then

$$\left\langle \varphi_i,\varphi_j\right\rangle=\delta[i-j] \tag{3.3}$$

where $\delta[i]=1$ if $i=0$, and 0 otherwise. If the set is complete and the vectors φ_i are linearly independent but not orthonormal, then we have a biorthogonal basis, and the basis and its dual satisfy

$$\left\langle \varphi_i,\overline{\varphi}_j\right\rangle=\delta[i-j] \tag{3.4}$$

The choice on the right set of basis functions depends on the type of signal to be represented and the application in hand.

3.1.1 The Development on Signal Representation

The most popular way to represent the signal is *Fourier Transform*. This transformation is a variant of Fourier series expansion, which was proposed by Jean Baptiste Joseph Fourier in the early 19^{th} century and published in the *Théorie Analytique de la Chaleur* (*The Analytical Theory of Heat*) in the year 1822 [15]. Fourier transform is used to decompose non-periodic functions with finite energy, which can be expressed in terms of trigonometric basis function as

$$F(\omega) = \int_{-\infty}^{\infty} f(t) e^{-j\omega t} dt, \tag{3.5}$$

And the reverse Fourier Transform can be expressed as

$$f(t) = \frac{1}{2\pi} \int_{-\infty}^{\infty} F(\omega) e^{j\omega t} d\omega, \tag{3.6}$$

Where t stands for time, $\omega = 2\pi f$ stands for frequency, and $f(\bullet)$ denotes the signal in time domain and the $F(\bullet)$ denotes the transformed signal in frequency domain. Since the Fourier transform analyses time-based signal to provide frequency information, the operation is regarded as frequency-amplitude decomposition.

Eventhough, the Fourier Transform offers excellent frequency resolution, but do not provide an information concerning the frequency content *locally* in time, which means when one frequency is occurred and when for others are known. The Fourier analysis only tells whether a certain frequencies occur or not, it does not tell when that frequency is occurred [16].

It is therefore important to have a representation that gives both time and frequency information of the signal studied. Due to this drawback, Dennis Gabor adapted the Fourier transform to analyze a signal in certain only a small section of the signal at a time, which is then called the *Short-Time Fourier Transform (STFT)*. In STFT, the signal is windowed into small segments (taken to be stationary) which are then studied independently [17]. For a window function $w(t)$, the STFT operation maps a signal or function $f(t)$ into a two-dimensional function of time τ and frequency f and can be defined as [18]:

$$STFT\{x(t)\} \triangleq X(\tau, f) = \int_t \left[x(t) w(t-\tau) \right] e^{-2\pi f t} dt \tag{3.7}$$

The STFT is a compromise between time and frequency-based views of a signal [19]. A trade off between the time and frequency resolution is enabled in STFT by altering the dimensions of the window function. Smaller windows offer better time resolution but poorer frequency resolution. On the other hand if the size of the window is enlarged to allow better frequency resolution, the time resolution is compromised. These conditions are illustrated in Figure 3.1 in terms of time-frequency plane.

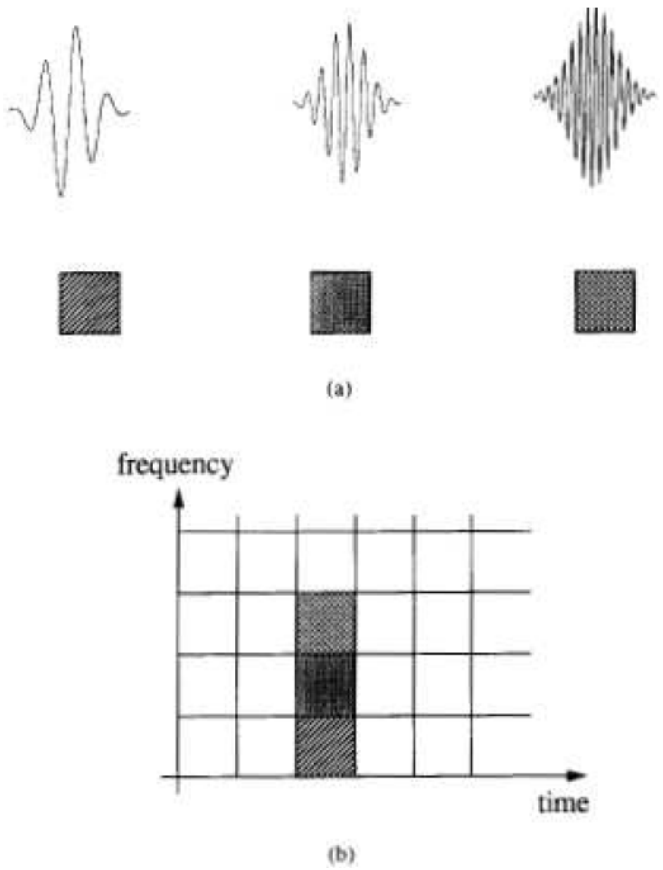

Figure 3.1 Problem encountered in Short Time Fourier Transform (STFT) (a) the same window size is applied to signal with difference frequency (b) the same resolution at all locations in time frequency plane caused by the use of single window [20]

From Figure 3.1, the drawback of STFT can be seen due to STFT suggests the use of same window for each collection samples, so the frequency resolution for the whole frequency range is uniform. Many signals require a more flexible approach, one where the window size can be varied to accurately determine both time and frequency.

One of the alternatives that can be used to solve this circumstance is wavelet analysis. In wavelet analysis, the window which will be used to transform the signal depends on the detail contained in the information [21]. Besides that, the use of irregular shape wavelet offers better tool to represent sharp changes and local features [22].

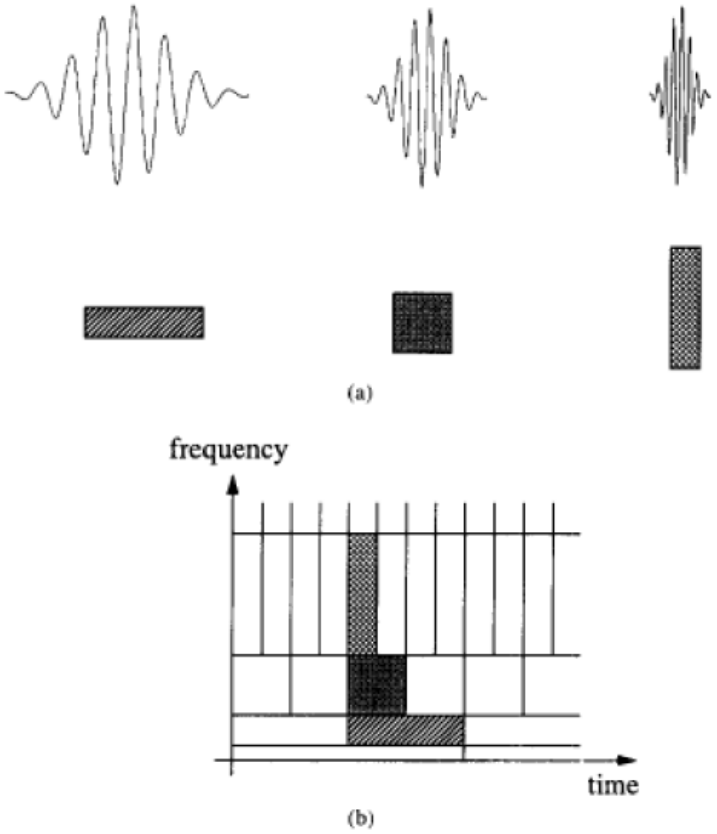

Figure 3.2 Dynamic resolution in time-frequency plane offered by Wavelet Transform (a) the basis functions and corresponding time-frequency resolution (b) time-frequency resolution in time-frequency plane [23]

The wavelet transform is a multi-resolution analysis (MRA) mechanism where an input signal is decomposed into different frequency components, and then each component is studied with resolutions matched to its time-scales, as shown in Figure 3.1 (a). Figure 3.1 (b) illustrates the time-frequency tiling concept that is employed by wavelet transform. Each block Figure 3.1 (b) covers one coefficient of the wavelet transform in the time-frequency plane. It is clear from this figure that for higher frequencies, the blocks have narrow width but long height illustrating good time resolution but poor frequency resolution. On the other hand, the blocks at low

frequencies have broad width but short height illustrating poor time resolution but good frequency resolution.

3.2 Continuous Wavelet Transform

The First wavelet based transform which is similar to STFT in time-frequency localization is Continuous Wavelet Transform (CWT). Different to STFT which has a constant resolution at all times and frequencies, CWT has a good time and poor frequency resolution at high frequencies, and good frequency and poor time resolution at low frequency. The CWT can be defined as an expansion of continuous function in terms of two variables; scale, j and shift, k, called wavelets $\psi(t)$. This expansion was firstly introduced by Mortlet and Grossman [24], [25]. They showed that a continuous-time function $f(t)$ in space $L^2(\mathbb{R})$ can be represented by a set of function $\{\psi_{k,s}(t)\}$ obtained by shifting k and scaling s of function $\psi(t)$, known as mother wavelets. The CWT of any signal $f(t)$ can be expressed as [26],

$$CWT_x^{\psi}(j,k) \triangleq \gamma_x^{\psi}(j,k) = \frac{1}{\sqrt{j}} \int_{-\infty}^{\infty} f(t).\psi_{j,k}{}^*(t)\, d \qquad (3.8)$$

Where

$$\psi_{j,k}(t) = \frac{1}{\sqrt{|j|}} \psi\left(\frac{t-k}{j}\right) \qquad (3.9)$$

In equation (3.8), $\gamma_f^{\psi}(j,k)$ can be referred as the CWT coefficients of the continuous signal which are obtained from the sum of various scaled and shifted version of mother wavelets, as shown in equation (3.9). Scaling parameter j describes how a wavelet basis function is stretched or contracted. While, the shifting variable, also known as translation parameter, represents the location of the wavelet in time.

The relation shows in (3.9) underlines an enormous advantage offered by wavelet transform by allowing it to provide dynamic resolution capability through the use of short basis function (contracted version) to obtain good time domain analysis and long basis function to get fine frequency domain analysis.

Furthermore, after analyze the signal of interest, the original signal wants to be reconstructed or synthesized. Such original signal can be reconstructed using inverse CWT (ICWT) given as,

$$f(t) = \int_j \int_k \gamma_f^{\psi}(k,s) \frac{1}{j^2} \tilde{\psi}\left(\frac{t-k}{j}\right) dkds \tag{3.10}$$

In (3.10), $\tilde{\psi}(t) = c_{\psi}^{-1}\psi(t)$, where

$$c_{\psi} = \int_{-\infty}^{\infty} \frac{\left|\Psi(\omega)\right|^2}{|\omega|} d\omega \tag{3.11}$$

In (3.11), $\Psi(\omega)$ is defined as the Fourier Transform of $\psi(t)$.

3.3 Multi-resolution Analysis

An important fundamental in the field of wavelets was Multi-resolution Analysis (MRA) framework develop by Mallat [24] and Meyer [27]. According to Burrus, in [28], there are two main components in the multi-resolution formulation of wavelet analysis, namely scaling and wavelet functions. The MRA allows characterization of $\psi(t) \in L^2(\mathbb{R})$ that result in an orthonormal basis. The scaling function can be defined as

$$\varphi(t) = \varphi(t-k), \quad k \in \mathbb{Z} \;\; \varphi \in L^2 \tag{3.12}$$

In (3.12), the subspace $L^2(\mathbb{R})$ represents square integrable functions in Hilbert space while k implies discrete step translation. The subspace that is spanned by linear combination of the scaling function in (3.12) and its translated version is imaginable. However, it can be easily found that the size of the subspace can be increased by manipulating the scale of the scaling function. This manipulation results in two dimensional functions that are generated by basic scaling function through both scaling s and translation k as follows

$$\varphi_{j,k}(t) = 2^{j/2}\varphi\left(2^j t - k\right), \quad j,k \in \mathbb{Z} \;\; \varphi \in L^2 \tag{3.13}$$

From (3.13) it is clear that the scaling function can be expressed as a linear combination of the half scale scaling function and its shifted versions which are orthogonal to each other. In this case, the space spanned by the scaling function with

larger scale is included in the space spanned by the scaling function with smaller scale. In other word, the space spanned by the scaling function with larger scale is a subspace of the space spanned by the scaling function with smaller scale. In order to clarify this idea we can define V_0 as a subspace spanned by the set of basis functions in (3.12).

Then we can also construct $\varphi_k(t)$ for $k=0$ via the following way,

$$\varphi[n]=\sum_k h[i]\sqrt{2}\varphi(2n-i), \quad n\in\mathbb{Z} \tag{3.14}$$

Since $\varphi(t)$ in (3.14) is expressed as linear combination of its shifted half scale versions, $h[i]$ defines the weight of each half scale component. If V_1 is a subspace spanned by set of scaling functions $\varphi(2n-i)$, it is clear that $V_0 \subset V_1$. In general, the subspace V_j can be defined as

$$V_j=\overline{span}\left\{\varphi\left(2^j t\right)\right\}=\overline{span}\left\{\varphi_{j,k}(t)\right\} \tag{3.15}$$

Therefore, the multiresolution analysis can be defined as a nesting of closed subspaces as follows [29]

$$\{0\}\subset\ldots\subset V_{-2}\subset V_{-1}\subset V_0\subset V_1\subset V_2\subset\ldots\subset L^2 \tag{3.16}$$

It is obvious that as j goes to infinity V_j enlarges to cover all energy signals. On the other hand, as j goes to minus infinity V_j shrinks down to cover only the zero signal. The difference between space spanned by scaling function and its half scale version is expressed as the orthogonal complement. This orthogonal complement is spanned by the corresponding wavelet function. This means, if we have a certain scaling function with particular scale, the space spanned by that scaling function can be decomposed into a subspace and its orthogonal complement. The subspace is spanned by the scaling function with double scale of the previous scaling function while the orthogonal complement is spanned by the corresponding wavelet function. Therefore we can define the space spanned by wavelet W_j as

$$V_{j+1}=V_j\oplus W_j \tag{3.17}$$

By performing repetition on (3.17), we may formulate:

$$\begin{aligned} V_{j+1} &= \left(V_{j-1} \oplus W_{j-1}\right) \oplus W_j \\ &= \left(V_{j-2} \oplus W_{j-2}\right) \oplus W_{j-1} \oplus W_j \\ &= \left(V_{j-3} \oplus W_{j-3}\right) \oplus W_{j-2} \oplus W_{j-1} \oplus W_j \\ &= \left(V_0 \oplus W_0\right) \oplus W_1 \oplus \cdots \oplus W_{j-2} \oplus W_{j-1} \oplus W_j \\ \text{with}: V_0 &\perp W_0 \perp W_1 \perp \ldots \perp W_{j-2} \perp W_{j-1} \perp W_j \end{aligned} \tag{3.18}$$

As a consequence of (3.18), the entire square integrable functions in Hilbert space can later be represented as

$$L^2\left(\mathbb{R}\right) = V_0 \oplus W_0 \oplus W_1 \oplus W_2 \oplus \ldots \tag{3.19}$$

The visualization of space V_j and W_j described by (3.17)-(3.18) are illustrated in Figure 3.3.

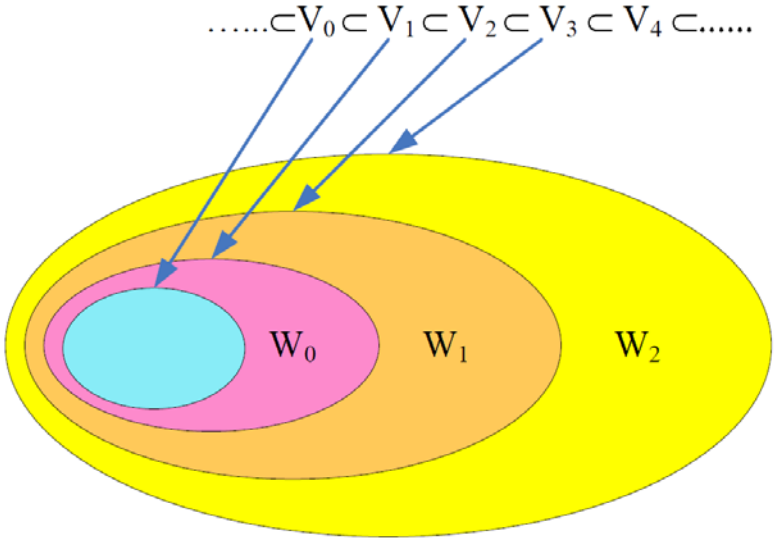

Figure 3.3 Illustration of MRA concepts and nested subspaced

The next step would be to express the wavelet function $\psi(t)$ in multi-resolution concept. Since it is clear from (3.17) that $W_0 \subset V_1$ and by taking (3.14) into consideration, the wavelet function $\psi(t)$ can be expressed as:

$$\psi[n] = \sum_k g[i]\sqrt{2}\varphi(2n-i), \quad n \in \mathbb{Z} \tag{3.20}$$

Function $g[i]$ in (3.20) defines the weight of each half scale component. Since V_0 and W_0 are orthogonal to each other, $\psi(t)$ is orthogonal to $\varphi(t)$. This means

there should be special relationship between weight coefficients $h[i]$ in (3.14) and $g[i]$ in (3.20) to ensure the orthogonality. This relationship is given by [26]:

$$g[i] = (-1)^n h[L-1-i], \quad \text{for } h[i] \text{ with length of } L \tag{3.21}$$

As for the case of scaling function in(3.13), the wavelet functions can be manipulated through scaling and translation as follows,

$$\psi_{j,k}(t) = 2^{j/2}\psi\left(2^j t - k\right), \quad j,k \in \mathbb{Z} \ \ \psi \in L^2 \tag{3.22}$$

Finally, based on the philosophy illustrated above, we can give visual illustration of signal decomposition. Given signal $f(t) \in V_0$, we can apply signal decomposition on $f(t)$ as follows [29],

$$\begin{aligned} f(t) &= D_1(t) + A_1(t) \\ &= D_1(t) + D_2(t) + A_2(t) \\ &= D_1(t) + D_2(t) + D_3(t) + A_3(t) \\ &= D_1(t) + D_2(t) D_3(t) + D_4(t) + A_4(t) \end{aligned} \tag{3.23}$$

where $D_j(t) \in W_{-j}$ and $A_j(t) \subset V_{-j}$

In(3.23), $D_j(t)$ is the detail at level j while $D_j(t)$ is recognized as the approximation at level j. Hence, the scaling function corresponds to the approximation of a signal while the wavelet function describes the detail version of the signal at particular level of decomposition.

3.4 Discrete Wavelet Transform

In practical, processing a signal to obtain more data using the Continuous wavalet tranform and its synthesis is not efficient because many redundancies exist. This condition also affects to the performance of computation which is limited by processing rate and memory capacity.

Therefore, the discrete wavelet transform (DWT) which will be discussed in this section is preferred. DWT is developed based on multi-resolution analysis and it basically can be used to decompose any function $f(t) \in L^2(\mathbb{R})$ into scaling and wavelet basis function spanning the entire $L^2(\mathbb{R})$. Assuming an orthogonal

transform, the forward discrete wavelet transform (DWT) of a discrete signal or function $f[n]\{n=0,1,2,\ldots,M\}$ belonging to $L^2(\mathbb{Z})$ is defined as

$$\begin{aligned} A[j,k] &= \langle f[n], \varphi_{j,k}[n] \rangle \\ &= \sum_n f[n]\varphi_{j,k}[n] \\ &= \sum_n f[n] 2^{j/2} \varphi_{j,k}\left[2^j n - k\right] \end{aligned} \tag{3.24}$$

$$\begin{aligned} D[j,k] &= \langle f[n], \psi_{j,k}[n] \rangle \\ &= \sum_n f[n]\psi_{j,k}[n] \\ &= \sum_n f[n] 2^{j/2} \psi_{j,k}\left[2^j n - k\right] \end{aligned} \tag{3.25}$$

Notation $\langle\ ,\ \rangle$ denotes the inner product between two functions. $A[j,k]$ and $D[j,k]$ in equation (3.24) and (3.25) are approximation and details coefficients of which denote the weight of scaling function $\varphi_{j,k}[n]$ and wavelet function $\psi_{j,k}[n]$, respectively.

After analyzing such discrete signal, the original signal can be also reconstructed or synthesized using inverse DWT (IDWT) given as

$$f[n] = \sum_{k=-\infty}^{\infty} A[j_0,k] 2^{j_0/2} \varphi\left[2^{j_0} n - k\right] + \sum_{j=j_0}^{\infty} \sum_{k=-\infty}^{\infty} D[j,k] 2^{j/2} \varphi\left[2^j n - k\right] \tag{3.26}$$

The parameter j_0 in (3.26) is an integer which sets the coarsest level of approximation of the function *f*[*n*]. The details of the which are filled by its projection onto the wavelet spaces W_j.

3.5 Filter Banks Representation

The possibility of implementing DWT algorithm using a set of filter banks was firstly studied by Mallat in [24]. In his work, Mallat showed that it is possible to perform DWT decomposition and reconstruction using 2-channel filter banks through a hierarchical algorithm known as the pyramidal algorithm. The algorithm meant that results of wavelet theory could be developed entirely using filter banks.

3.5.1 Analysis Filter Banks

To analyze DWT using a set of filter banks, firstly consider two basis discrete functions which are used in multi-resolution analysis (MRA), namely scaling function $\varphi[n]$and wavelet function $\psi[n]$. The scaling function $\varphi[n]$ basically can be expressed as a linear combination of $\varphi[2n]$, meanwhile the wavelet function $\psi[n]$, as the orthogonal complement of $\varphi[n]$, can be also expressed as $\psi[2n]$, which reside in the upper half band.

From the description above, it is logical to associate coarse version of a signal with low frequency component and the detail version with high frequency component. Projection of signal with respect to scaling and wavelet basis function can logically be actualized through low pass and high pass filtering. Since multiple-level signal analysis based on DWT is nothing but signal decomposition into different frequency bands, successive high pass and low pass filtering of the time domain signal can be employed. These successive filtering should be implemented based on (3.14) and (3.20) famously recognized as two-scale equation. In order to find the exact relationship between DWT and the filtering process, we modify two equation (3.14) and (3.20) by replacing $n \to 2^j n - k$ in order to obtain more general form of two scale equation. The general form of two-scale equation for scaling function with scale j and translation k is represented as:

$$\begin{aligned}\varphi\left[2^j n-k\right] &= \sum_i h[i]\sqrt{2}\varphi\left[2\left(2^j n-k\right)-i\right] \\ &= \sum_i h[i]\sqrt{2}\varphi\left[2^{j+1}n-2k-i\right] \\ &= \sum_m h[m-2k]\sqrt{2}\varphi\left[2^{j+1}n-m\right],\ \ m,n\in\mathbb{Z} \text{ and } m=2k+i\end{aligned} \tag{3.27}$$

Similarly, considering wavelet function in (3.20), can be also represented in two scale equation as

$$\begin{aligned}\psi\left[2^j n-k\right] &= \sum_i h[i]\sqrt{2}\psi\left[2\left(2^j n-k\right)-i\right] \\ &= \sum_i h[i]\sqrt{2}\psi\left[2^{j+1}n-2k-i\right] \\ &= \sum_m h[m-2k]\sqrt{2}\psi\left[2^{j+1}n-m\right],\ \ m,n\in\mathbb{Z} \text{ and } m=2k+i\end{aligned} \tag{3.28}$$

Based on equations (3.27) and (3.28), the DWT coefficients, $A[j,k]$ and $D[j,k]$, in equation (3.24) and (3.25) can redefined as,

$$\begin{aligned}
A[j,k] &= \left\langle f[n], \varphi_{j,k}[n] \right\rangle \\
&= \sum_n f[n] \varphi_{j,k}[n] \\
&= \sum_n f[n] 2^{j/2} \varphi_{j,k}\left[2^j n - k\right] \\
&= \sum_n f[n] 2^{j/2} \sum_m h[m-2k] \sqrt{2} \varphi\left[2^{j+1} n - m\right] \\
&= \sum_m h[m-2k] \sum_n f[n] 2^{(j+1)/2} \varphi\left[2^{j+1} n - m\right] \\
&= \sum_m h[m-2k] A[j+1,k], \quad m \in \mathbb{Z}
\end{aligned} \tag{3.29}$$

$$\begin{aligned}
D[j,k] &= \left\langle f[n], \psi_{j,k}[n] \right\rangle \\
&= \sum_n f[n] \psi_{j,k}[n] \\
&= \sum_n f[n] 2^{j/2} \psi_{j,k}\left[2^j n - k\right] \\
&= \sum_n f[n] 2^{j/2} \sum_m h[m-2k] \sqrt{2} \psi\left[2^{j+1} n - m\right] \\
&= \sum_m h[m-2k] \sum_n f[n] 2^{(j+1)/2} \psi\left[2^{j+1} n - m\right] \\
&= \sum_m h[m-2k] D[j+1,k], \quad m \in \mathbb{Z}
\end{aligned} \tag{3.30}$$

Equations (3.29) and (3.30) show that the DWT coefficient for scaling and wavelet function at particular scale j can be calculated from linear combination of DWT coefficient from higher scale, $j+1$. These equations also inform us that a convolution between DWT coefficients at scale $j+1$ with filter having impulse response $h[i]$ and $g[i]$ followed by down sampling each output with factor 2 will produce new scaling and wavelet DWT coefficients at scale j. As a result, the filtering representation of DWT is realized by developing half-band low pass filter H and high pass filter G. The low pass filter H and high pass filter G have weight values $h[i]$ in (3.14) and $g[i]$ in (3.20), respectively, as their impulse responses. The term half-band is used here since $h[i]$ in (3.14) and $g[i]$ in (3.20) are related according to (3.21) which ensures the orthogonality between scaling and wavelet

function. The filters satisfying (3.21) are also commonly known as the Quadrature Mirror Filters (QMF).

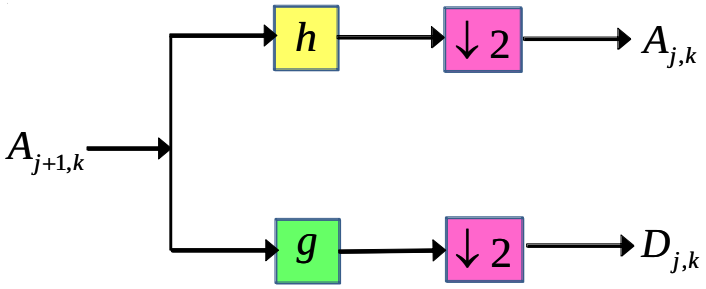

Figure 3.4 2-channel Analysis Filter Bank

Figure 3.4 illustrates a representation of equation (3.24) and (3.25) by a 2-channel filter banks. The 2-channel filter bank first splits the input signal in two parts and filters one part with filter h and other with filter g. Both filtered signals are then subsampled by 2 and resulting signals are forwarded to the output of the 2-channel filter bank. Each output signal will therefore contain half the number of samples and will span half of the frequency band compared to the input signal. It should be noticed that the number of samples at the input of the filter bank equals the number of samples at the output.

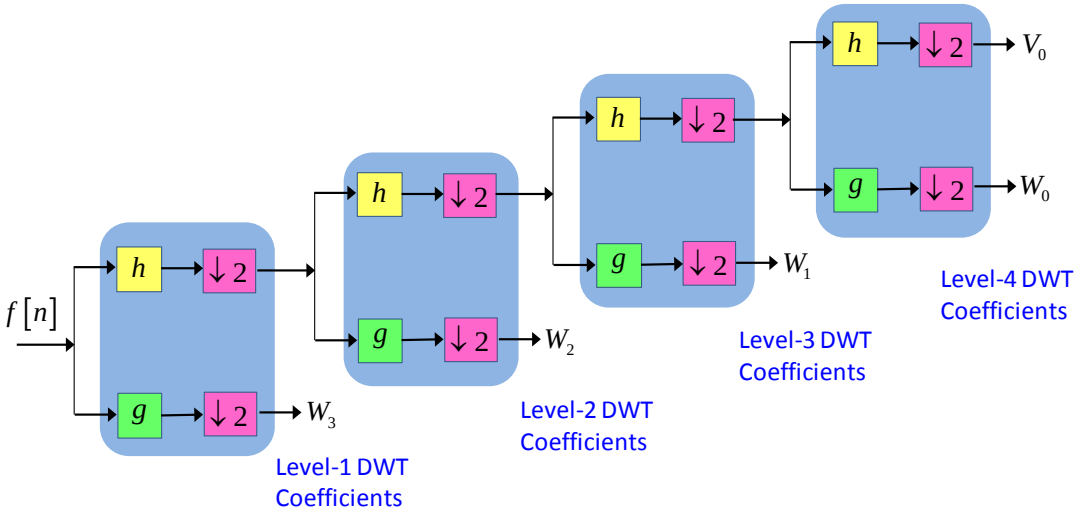

Figure 3.5 The implementation of 4 stages Analysis Filter Banks

The complete representation of the DWT can be obtained by iteration of the 2-channel filter bank and taking repeatedly scaling DWT coefficients A as input. The number of stages in iteration process will determine the DWT resolution and therefore the number of channels.

The example of a two band analysis tree with four stages is graphically shown by Figure 3.5. The input signal f has 512 samples and contains frequencies that lie between 0 and π. The resulting decompositions together will still contain 512 samples and span the same frequency band as the original signal but these will be decomposed in different DWT coefficients.

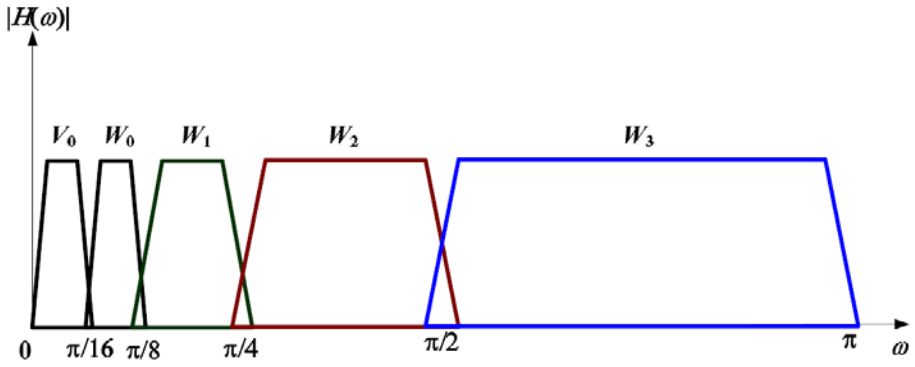

Figure 3.6 Frequency Bands for the 4-stage Analysis Tree

The subband structure of wavelet decomposition in frequency domain can be calculated using Fourier transformation. For the previous example of 4-stage analysis tree the corresponding subband structure is illustrated in Figure 3.6.

3.5.2 Synthesis Filter Banks

The reconstruction formula is derived by considering a signal in the $j+1$ scaling space $f[n] \in V_{j+1}$ as [28]:

$$f[n] = \sum_{k=-\infty}^{\infty} A[j+1,k]\varphi_{j+1,\beta}[n] = \sum_{k=-\infty}^{\infty} A[j+1,k]\sqrt{2^{j+1}}\psi[2^{j+1}n-k] \qquad (3.31)$$

This can be expressed in terms of the next scale as [28]:

$$f[n] = \sum_{k=-\infty}^{\infty} A[j,k]\sqrt{2^{j}}\varphi[2^{j}n-k] + \sum_{k=-\infty}^{\infty} D[j,k]\sqrt{2^{j}}\varphi[2^{j}n-k] \qquad (3.32)$$

Substituting the 2-scale equations (3.27) and (3.28) into (3.32), we get

$$\begin{aligned} f[n] = &\sum_{k=-\infty}^{\infty} A[j,k]\sum_{m} h[m-2\beta]2^{(j+1)/2}\varphi[2^{j+1}n-m] \\ &+ \sum_{k=-\infty}^{\infty} D[j,k]\sum_{m} g[m-2\beta]2^{(j+1)/2}\varphi[2^{j+1}n-m] \end{aligned} \qquad (3.33)$$

Multiplying both sides of equation (3.33) by $\varphi\left[2^{j+1}n-k'\right]$ and taking the summation allows us to describe the DWT coefficients at higher scales by those of the lower scale [28]:

$$A(j+1,k)=\sum_m A(j,k)h[k-2m]+\sum_m D(j,k)g[k-2m] \qquad (3.34)$$

The equation (3.34) shows that the DWT coefficient for scaling and wavelet function at particular scale $j+1$ can be reconstructed from linear combination of DWT coefficient from higher scale, j.

Introducing, two new variables $\hat{h}[i]$ and $\hat{g}[i]$ which are time-reversed versions of $h[i]$ and $g[i]$. The relations between those notation are $\hat{h}[i]=h[-i]$ and $\hat{g}[i]=g[-i]$. Figure 3.7 2-channel Synthesis Filter Bank illustrates a representation of equation (2.37) by a 2-channel synthesis filter banks.

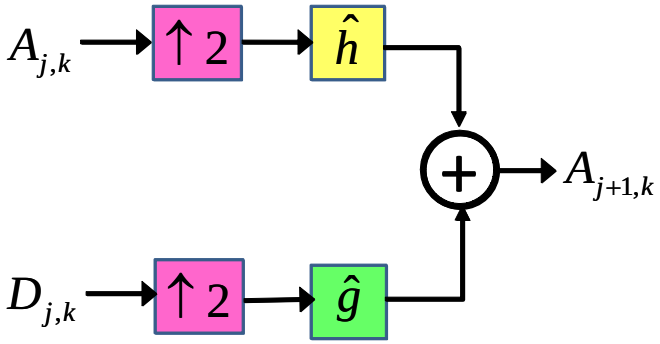

Figure 3.7 2-channel Synthesis Filter Bank

The 2-channel synthesis filter bank performs operations which are exactly opposite to those of analysis filter bank discussed in the previous section. The wavelet and scaling DWT coefficients are first upsampled by factor 2 and after that the wavelet function DWT coefficients are filtered with HPF $\hat{g}[i]$ while scaling function DWT coefficients are filtered with LPF $\hat{h}[i]$. The two filtered signals are then added to each other to construct DWT coefficients at higher scale.

The decomposition of a signal in terms of coefficients is called discrete wavelet transform. In order to reconstruct the original signal from coefficients we can apply inverse wavelet transform, abbreviated IDWT. The IDWT can be efficiently implemented by iterating the 2-channel synthesis filter bank in the same

manner like we have done in the previous paragraph for the 2-channel analysis filter bank. The example of 4-stages synthesis tree is illustrated in figure Figure 3.1.

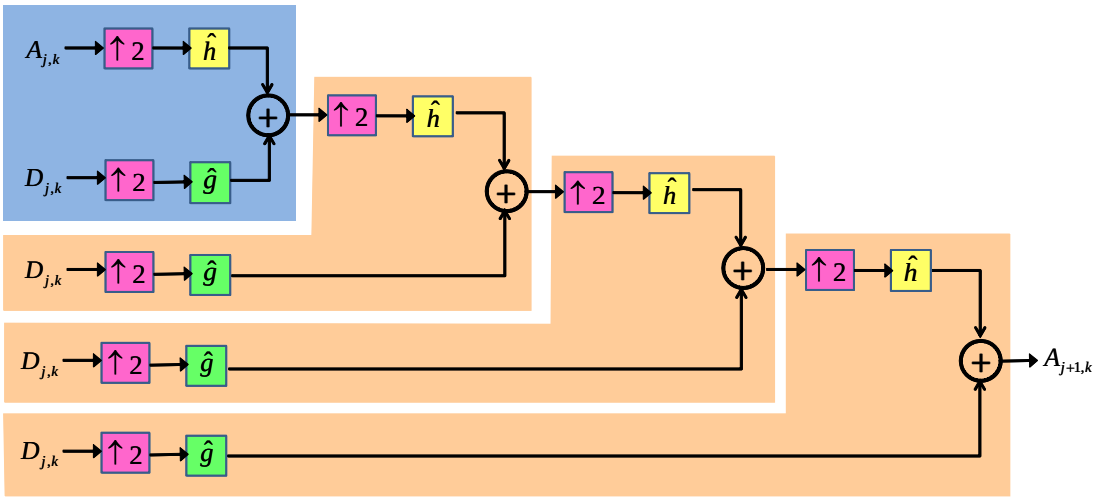

Figure 3.8 4-stages Syntehesis Tree

3.6 Wavelet Packet Transform

The implementation of wavelet transform in terms of filter banks is usually non-uniform, which means that only the output of low pass filters that are decomposed iteratively. On the other side, decomposition on both low and high frequencies component is also possible. This process is then referred as wavelet packet transform. The original investigation on the topic was carried out by Coifman and Meyer [30]. And it was followed by Wickerhauser [31]-[32] who constructed uniform wavelet packet trees and demonstrated its operation for acoustic signal compression. Since low and high frequencies component are decomposed in the same way, the wavelet packet transform has uniform frequency resolution. Figure 3.9 shows the frequency bands for 3-stage wavelet packet tree.

The filter bank structure for wavelet packet transform usually expands to a full binary tree, yields a set of wavelet packet coefficients. These wavelet packet coefficient is notated as χ_l^p which refer to the certain level l of the node in the tree structure and the current position p of the node at a given level. Wavelet packet decomposition recursively splits each parent node in two orthogonal subspaces W_l^p located at the next level [33]:

$$W_l^p = W_{l+1}^{2p} \oplus W_{l+1}^{2p+1} \tag{3.35}$$

The subspaces given in equation (3.35) are those spanned by the basis functions of wavelet packets:

$$W_l^p = \overline{span\left\{2^{l/2}\chi_l^p\left(2^l t - k\right)\right\}} \tag{3.36}$$

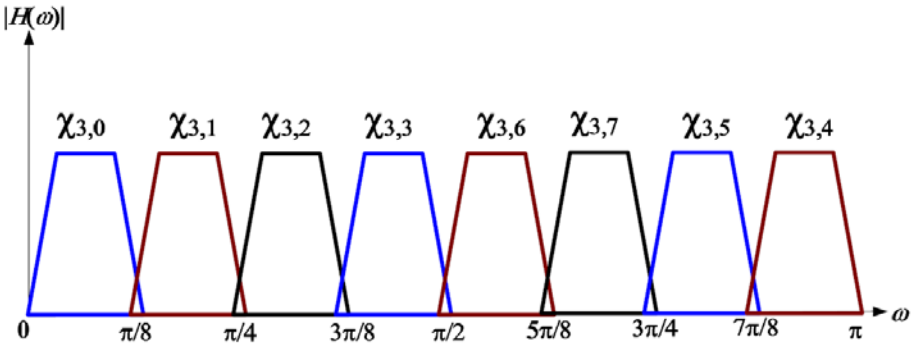

Figure 3.9 Frequency Bands for 3-stages Wavelet Packet Tree

In order to obtain wavelet packet coefficients χ at a certain level of tree, the wavelet and scaling filter are convolved with wavelet packets coefficients from a previous level. This process is perform repeatedly for all wavelet packets until the full binary tree is obtained to desired depth. The wavelet packets coefficients $\chi_{l+1}^{2p}(k)$ are generated using the scaling filter and coefficients $\chi_{l+1}^{2p+1}(k)$ are created using the wavelet filter [33][34]:

$$\begin{aligned}\chi_{l+1}^{2p}(k) &= \sum_m h[m-2k]\chi_l^p \\ \chi_{l+1}^{2p+1}(k) &= \sum_m g[m-2k]\chi_l^p\end{aligned} \tag{3.37}$$

The equation (3.37) shows the recursive equation for wavelet packets generation. In the regular DWT decomposition for each additional level we need only to perform single iteration of 2-channel filter bank while in wavelet packet transform the number of iterations is exponentially proportional to the number of levels. Therefore, the wavelet packet transform has higher computational complexity when compared to regular DWT. By utilization of fast filter bank algorithm wavelet packet transform requires $O(N\log(N))$ operation, similar to FFT while DWT needs only $O(N)$ calculation [35]. Figure 3.10 illustrates the full binary tree for the 3-stages wavelet packet analysis.

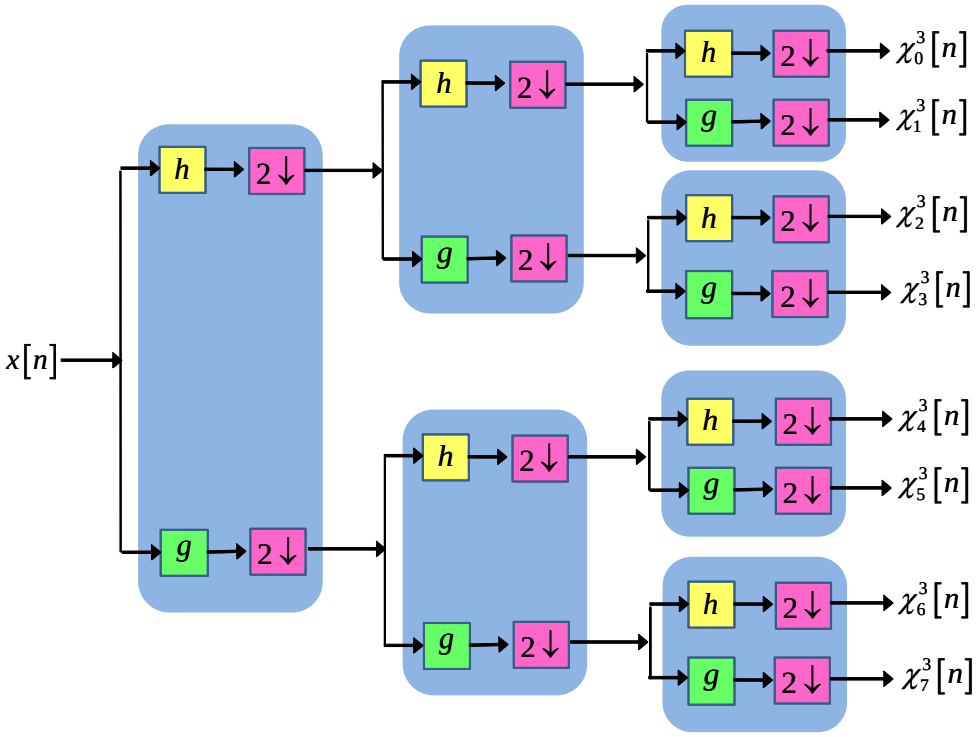

Figure 3.10 3-Stages Wavelet Packet Analysis Tree

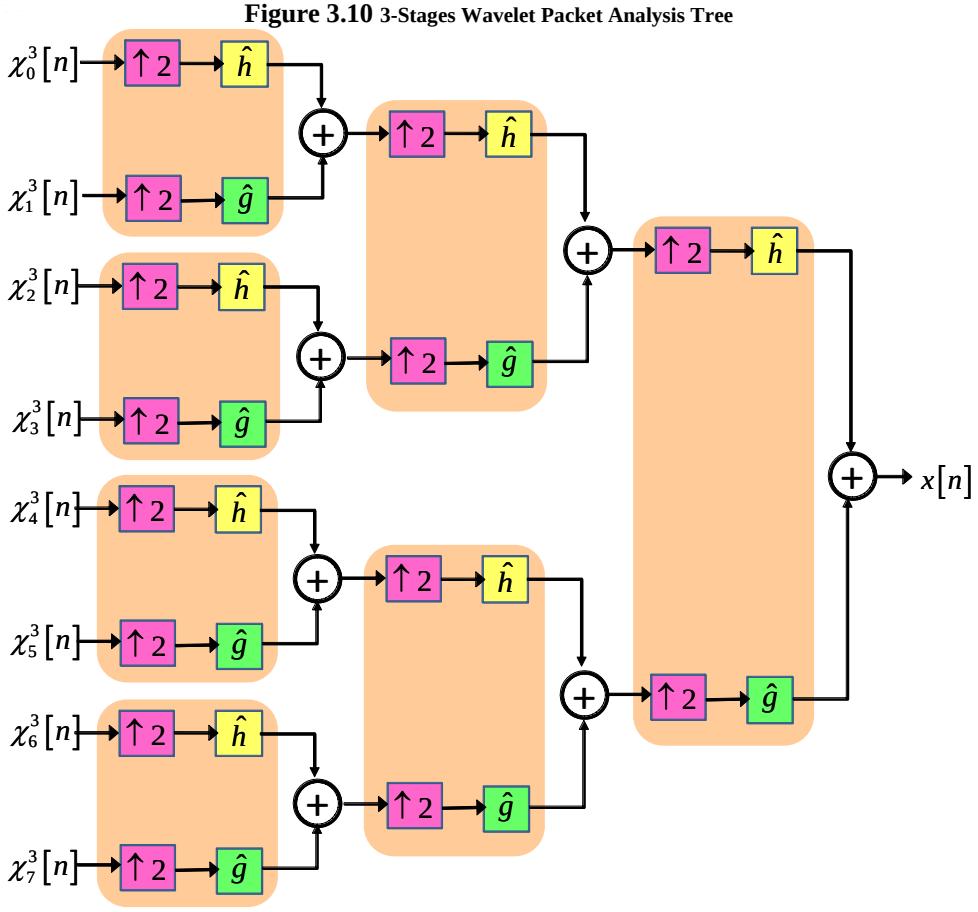

Figure 3.11 3-Stages Wavelet Packets Synthesis Tree.

The reconstruction of wavelet packets is also performed in an iterative method. For each pair of wavelet packets coefficients at level *l* of the tree we can calculate wavelet packets coefficients at the previous level *l*-1 by:

$$\chi_l^p(k) = \sum_m \chi_{l+1}^{2p}(k)\, h[m-2k] + \sum_m \chi_{l+1}^{2p+1}(k)\, g[m-2k] \qquad (3.38)$$

An example of 3-stages Wavelet Packet Synthesis Tree is depicted in Figure 3.11

3.7 Wavelet Properties

Each wavelet has specific characteristics that make it more suitable for one application than other. Therefore during design a system, a system designer should consider the different wavelet properties to meet the system requirements. There are several properties that have to be taken into account for designing a wavelet system, such as orthogonality, compact support, symmetry, and smoothness. Here we shall discuss a few important ones.

A. Orthogonality

Orthogonality holds an important characteristic that can be used to ensure perfect reconstruction. For communication system, the orthogonality of wavelet is required.

B. Compact support

Compact support is defined by the length of the filter. In order to reduce the complexity of computational, shorter filters are preferred to be chosen. However, when determine the length of filter, we have also to consider another wavelet property which is related to the filter length, such as orthogonality or regularity.

C. Symmetry

Symmetrical wavelets have as feature that transform of the mirror of an image is the same to the mirror of the wavelet transform. None of the orthogonal wavelets except Haar wavelet is symmetric. Although, requiring symmetric wavelets involuntarily means that wavelets are not orthogonal there are some applications that prefer symmetric wavelets above orthogonal

ones. For instance image compression techniques like JPEG2000 uses biorthogonal symmetric wavelets. Because by compression of an image we discard one part of the wavelet coefficients containing high detail, the perfect reconstruction has become impossible anyhow. The fulfillment of symmetry property in JPEG2000 on the other hand results in more natural, smooth images.

D. Regularity

The regularity is a measure of smoothness of the wavelet that can helps to reduce the number of non-zero coefficient in the high-pass sub-bands and it is one of the easiest ways to determine if a scaling function is fractal. The smoothness is actually defined by the continuous differentiability of the scaling function. There are two ways in which smoothness can be defined: local by the Hölder measure and global by the Sobolev measure.

3.8 Wavelet Families

Haar

It is the first and simplest of all wavelets. Haar wavelet is discontinuous, and resembles a step function.

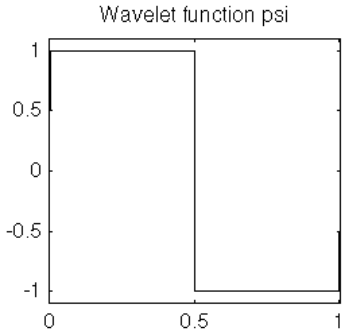

Daubechies

These compactly supported orthonormal wavelets that are popularly used in discrete wavelet analysis. The names of the Daubechies family wavelets are written db*N*, where *N* is the order, and db the “surname” of the wavelet. The db1 wavelet is the same as Haar wavelet.

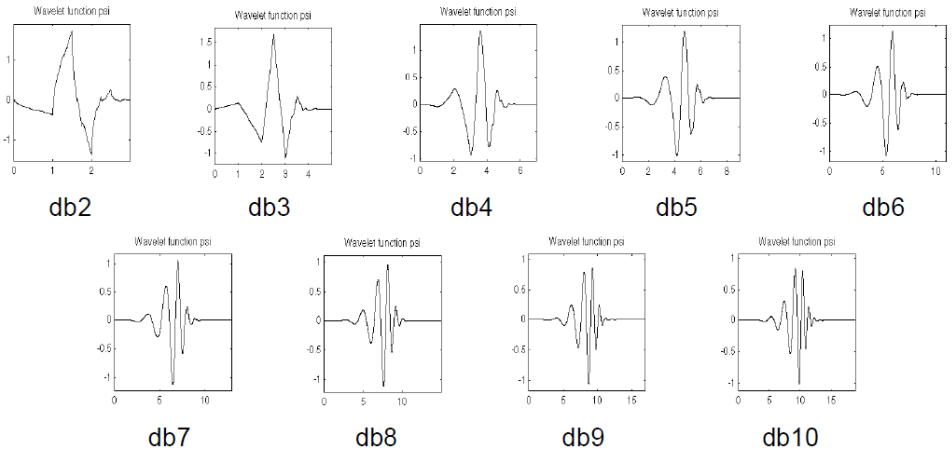

Coiflets

Coiflets are another variation on Daubechies wavelets. They have orthonormal wavelet basis with vanishing moments. Built by I. Daubechies at the request of R. Coifman. The wavelet function has 2*N* moments equal to 0 and the scaling function has 2*N*-1 moments equal to 0. The two functions have a support of length 6*N*-1.

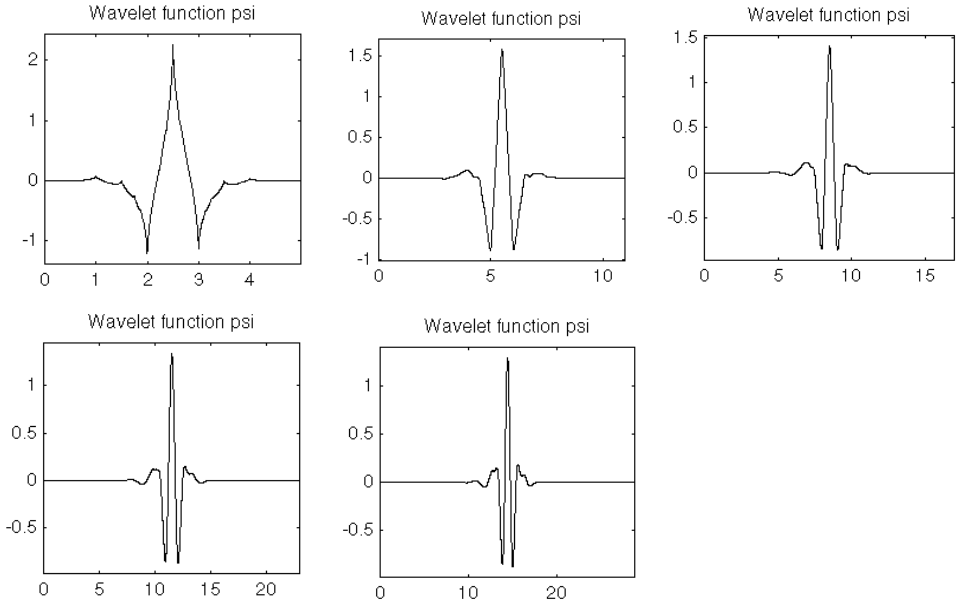

Biorthogonal

This family of wavelets exhibits the property of linear phase, which is needed for signal and image reconstruction. By using two wavelets, one for decomposition and the other for reconstruction instead of the same single one, interesting properties are derived.

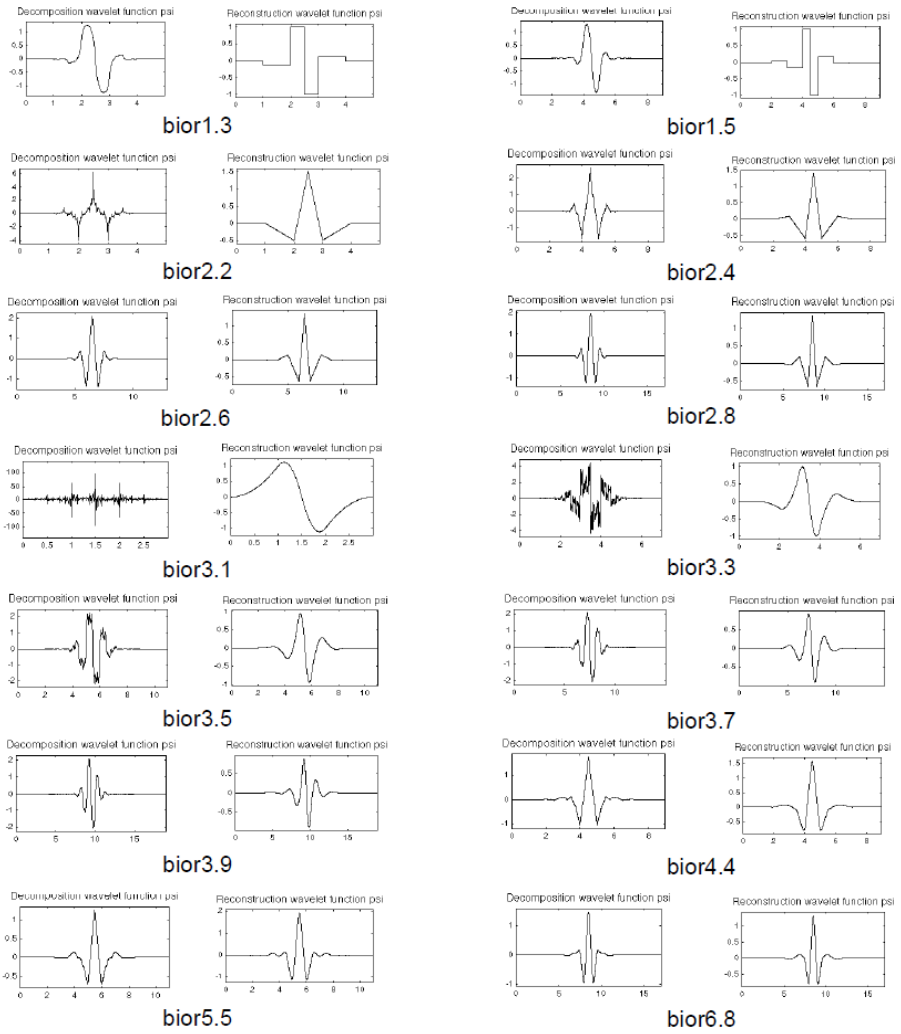

Mexican Hat

This wavelet has no scaling function and is derived from a function that is proportional to the second derivative function of the Gaussian probability density function.

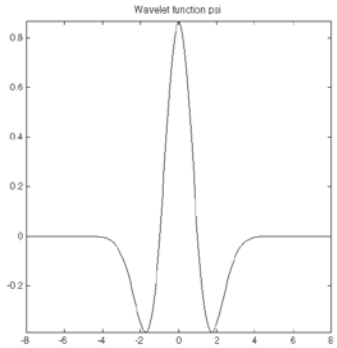

Symlets

The symlets are nearly symmetrical wavelets and are modifications to the *db* family. The properties of the two wavelet families are similar.

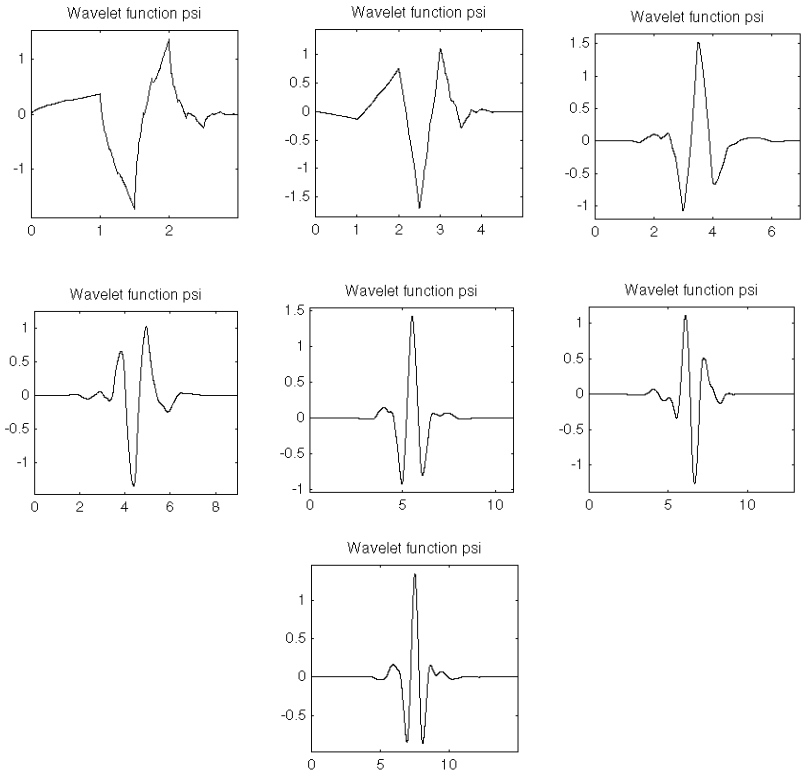

Morlet

This wavelet has no scaling function, but is explicit.

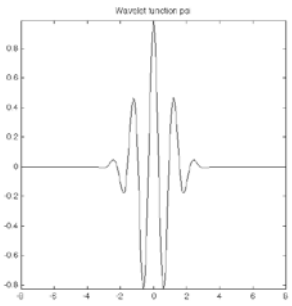

4

Wavelet Packet Based Algorithm for Representation of Time-Invariant Wireless Channel

The representation of wireless channel using one-dimensional wavelet packet algorithm will be elaborated in this chapter. All of algorithms, which will be discussed in this chapter, are developed based on the theory of entropy. The contents of the chapter are organized as follows: The discussion on current development of wireless channel representation will be elaborated in section 4.1. In section 4.2, a discussion on how a wireless channel can be represented using algorithm based on wavelet packet is presented. The proposed algorithms are divided into two mechanisms, namely coefficient reduction and tree pruning. These proposed algorithms for wireless channel representation are entirely based on entropy value. Section 4.3 talks about the simulation setup used. The performance of each those algorithms is analyzed in Section 4.4. Finally, section 4.5 summarizes the entire discussion on one-dimensional wavelet packet algorithm to represent wireless channel efficiently.

4.1 Channel Model Representation

Many applications rely on wireless communication technology. This technology uses radio link as wireless channels to transmit the information. However, no one can completely predict the performance of the wireless channels due to the dynamic nature of radio link which are extremely random and unpredictable. This condition is affected by channel effects such as reflection, refraction, scattering and motion of objects. Therefore, in order to achieve better system performance, the channel has to be mapped into simple form to understand its

behavior. There are many models in literature to represent the behavior of wireless channel such as reported in [36]-[38]. Most of these methods rely on statistical impulse response of the channel obtained from empirical analysis. Such models require a lot of coefficients to map the channel which also influence the complexity of computation.

Numerous alternative methods to represent channel models efficiently have been proposed. For example, in [39], Nikookar proposed a method to represent a channel model using Karhunen-Loeve (K-L) decomposition. This method relies on the correlation of the received signal to select the best basis of the signal. However, the price paid in terms computational complexity is still high, thereby making it unviable.

In this context the theory of wavelets and wavelet packets, which have recently found applicability for signal processing applications, hold immense promise for wireless channel modeling. Wavelet packets offer localization of information in both frequency and time domains. This property can be exploited to model channels with reduced the complexity by selecting the best basis of the signal.

Best basis selection based on wavelet packet was first introduced by Coifman in [40] for data compression and widely used in many applications [41]-[43]. The application of wavelet packet based on channel modeling has also been reported in [44]-[46]. In [44] and [45], Zhang suggested a method to represent a time-varying channel using two sets of wavelet packet. However, the use-cases considered in this work are preliminary. In [46], Sadough and Jaffrot use Mean Square Error (MSE) and Entropy as performance metrics to evaluate a Wavelet Packet model for UWB channels. They also compare the performance of wavelet packet based approach to Karhunen-Loeve (K-L) decomposition method.

4.2 Wavelet Packet Based Channel Representation

This section describes the system which will be applied to represent the wireless channel efficiently. The idea behind the proposed system is to represent an unknown wireless channel in terms of a set of known wavelet packet bases. Since the wavelet packet decomposition offers a high degree of time-frequency localization, the method guarantees an excellent approximation of the channel conditions. Once

the channel is mapped onto the WP bases, those WP components which contain significant information alone can be retained. This provides for sparse representation and accurate reconstruction of information. The proposed system is evaluated using performance metrics, such as correlation and level crossing rate, which have hitherto not been considered in the literature thus.

The proposed system primarily performs three major tasks, namely, wavelet packet (WP) decomposition, selection of best WP representation and WP reconstruction. WP Decomposition and WP reconstruction are implemented using filter banks. To select the best WP representation, two methods are employed –

a) *Coefficient-reduction*, where the channel is uniformly decomposed using WP transform and the best components are selected based on their entropy values,
b) *Tree-pruning*, where an arbitrary decomposition of the input is conducted to arrive at the WP tree structure with lowest entropy [33].

A. Wavelet Packet Decomposition

The theory of wavelet packet allows for sparse representation of information. This is done by decomposition of signal into orthogonal WP bases. These WP bases are obtained from multistage tree structure of Quadrature Mirror Filter (QMF) banks [18], [26] . The starting stage of the WP decomposition is to consider a two-channel filter bank consisting of a low-high pass filter pair $\{h[n], g[n]\}$. These filters have finite impulse responses (FIR) and share a tight relationship given as [18], [26]:

$$g\left[L-1-m\right]=\left(-1\right)^{m} h\left[m\right] \tag{4.1}$$

Furthermore, they also have adjoints or duals which are their complex conjugate time reversed variants given by [26]:

$$h'\left[m\right]=h^{*}\left[-m\right] \text{ and } g'\left[m\right]=g^{*}\left[-m\right] \tag{4.2}$$

The filter-pair $\{h'[m], g'[m]\}$ are called the analysis filters and are used to generate the wavelet packet carriers for modulation of data at the transmitter end. On the other hand the combination $\{h[m], g[m]\}$ is called the synthesis filters and is used to derive the wavelet packet carrier duals for demodulation of data at the receiver end. The

wavelet packet bases $\{\xi_l^p\}$ from these QMF filters can be derived recursively through a Multi Rate Analysis as [26]:

$$\begin{aligned}\xi_{l+1}^{2p}(t) &= \sqrt{2}\sum_m h[m]\xi_l^p(2t-m)\\ \xi_{l+1}^{2p+1}(t) &= \sqrt{2}\sum_m g[m]\xi_l^p(2t-m)\end{aligned} \tag{4.3}$$

In (4.3) the superscript *p* stands for coefficient index at any given tree depth *l*. The number of WP components *M* that can be derived from *l* iterations is given by $M = 2^l$ .The decomposition level can be chosen according to the desired resolution. It has been shown that the WP algorithm can be implemented in $O(N\log(N))$ operations [35].

B. Best Wavelet Packet Representation Selection

The main task of the system for representing wireless channel using wavelet packet algorithm is to know how to utilize wavelet packet bases to represent the input signal efficiently. This task is necessary because not all of bases, which are obtained from WP Decomposition, contain valid information on the signal. The information about the significance of those bases can be evaluated by using entropy of each base. Based on this value, one can identify whether each of these bases can be selected for reconstructing such signal or ignored. Consequently, only few WP bases are needed to represent the input signal.

Entropy[1] which is used in the theory of information is measure of an uncertainty condition associated with a random variable which quantifies the expected value of the average information contained in a message. To represent the value of entropy, Shannon formulates the equation which is given as follow [50],

$$H = -K\sum_{i=1}^{n} p_i \log_2 p_i \tag{4.4}$$

where *K* is a positive constant and p_i is the probability of a certain state i.

The quantity H has a number of interesting properties which further substantiate it as a reasonable measure of choice or information [50].

[1] The terms of entropy has been known before the invention of Shannon in information theory and widely used in thermodynamics to represent an irreversible energy in the system.

1. $H = 0$ occurs if and only if all the p_i but one are zero, this one having the value unity. Thus only when we are certain of the outcome does H vanish. Otherwise H is positive.
2. For a given n, H is a maximum and equal to $\log n$ when all the p_i are equal (i.e., $\frac{1}{n}$). This is also intuitively the most uncertain situation.

From the definition which is given in (4.4) (see Figure 4.1), one can say when the probability of an event is likely to be equal to another, then the entropy of this event is high. For instance, a series of coin tosses with a fair coin has maximum entropy. On the other hand, a string of coin tosses with a two-headed coin has zero entropy, since the coin will always come up heads. From this description, one can conclude that when the uncertainty is high, the entropy will also be high.

This concept of entropy will be considered as the basis of development of Wavelet Packet Algorithm for representing wireless channel.

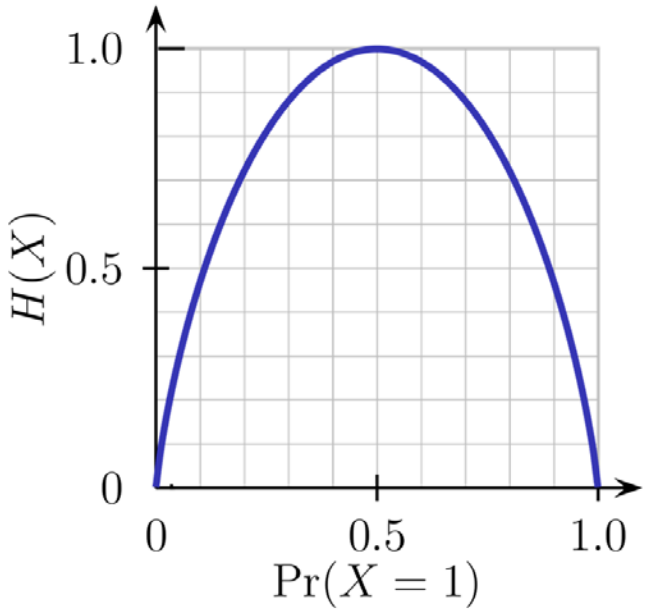

Figure 4.1 Entropy in the case of two possibilities p and $(1-p)$

As mentioned above that there are two methods which will be proposed for selecting the best wavelet packet representation.

1. Coefficient Reduction

Following the knowledge that not all of wavelet packet bases are necessary to reconstruct an input signal, the *coefficient-reduction* method becomes one of alternative method for selecting the best wavelet bases to be reconstructed.

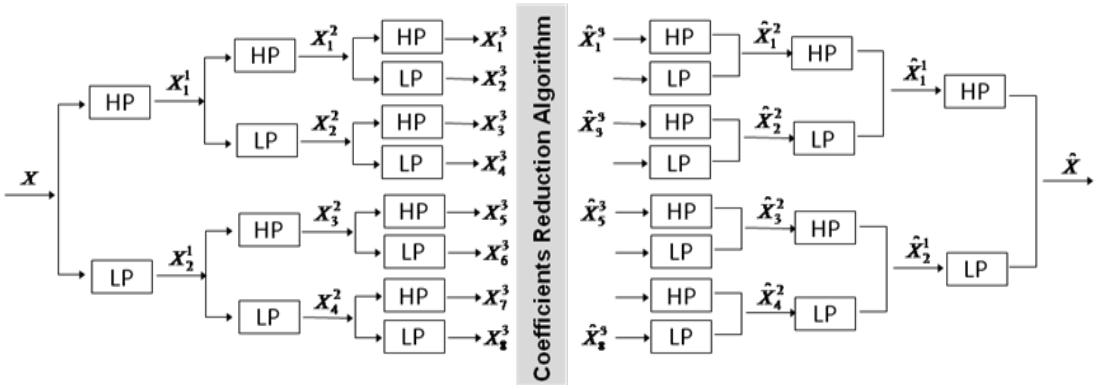

Figure 4.2 Coefficient Reduction Block Diagram.

This method begins with a uniform decomposition of input signal to obtain a set of WP bases. After a set of WP Bases are obtained, the entropy of each bases are measured to determine which bases has significant information for reconstruction. Furthermore, only WP bases which have significant information are selected to be reconstructed for representing such input signal. The selection of WP bases is conducted by choosing a set of WP bases which have lower value of entropy related to the desired resolution. The block diagram of this method is depicted in Figure 4.2.

The process of this method can be formulated as follow. Assuming the WP Bases coefficient is $C_k(t) = \xi_{l_{\max}}^{p}(t)$ and the entropy value of each base is $I_k = -\sum_n (p_n \times \log p_n)$ with *k* indicates the *k*-th bases coefficient and *n* indicate the *n*-th component of *k*-th bases coefficient in maximum depth of decomposition l_{max}, while p is the probability of component *n*-th occurred in bases *k*-th. Then, based on the desired accuracy and scarcity of signal/channel representation, the best bases can be chosen as

$$C'_k = \begin{cases} C_k & \text{, if k} \in \text{desired accuracy} \\ 0 & \text{, otherwise} \end{cases} \tag{4.5}$$

2. Tree Pruning

Another method to represent the signal efficiently is called *tree pruning*. This method was first introduced by Coifman in [40] and expanded by Ramchandran in [51]. Both of these works have similar objective that is to represent the input efficiently by using less coefficient with a small error. Lately, Lindsay in [33] also followed this path to optimize wavelet packet signal in noise environment. The method for efficient wireless channel representation will also follow these works.

Different from the *coefficient reduction algorithm*, instead of decomposing the input uniformly and evaluate the entropy at the end of decomposition, *tree pruning algorithm* decompose input signal arbitrarily to obtain WP tree structure and measure the entropy value of each node which is obtained from WP decomposition at each level of decomposition.

Besides that, in *tree pruning algorithm* the selection of best basis is conducted from the beginning of WP decomposition until certain level of decomposition. In this process, there are two conditions that have to be considered, that are [33]

a. *Forward-lock*, means that such node is not decomposed anymore and keep at such node.
b. *Forward-tuning*, means that the decomposition of such node is continued to next level of decomposition.

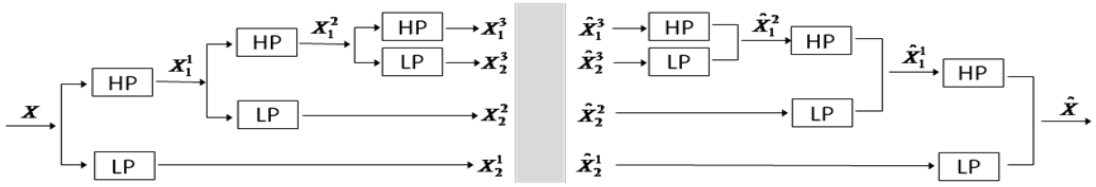

Figure 4.3 Tree Pruning Block Diagram

The complete process of this algorithm as follow. The signal is passed through the QMF to be decomposed into WP Bases and calculate the entropy value of each base at every level of decomposition. Consider each node *N*, at every stage of decomposition. A node *N* is split into two nodes N_1 and N_2 if and only if the sum of the entropy of N_1 and N_2 is lower than the entropy of *N*, otherwise if the sum of the entropy of N_1 and N_2 is larger than the entropy of *N*, the node N_1 and N_2 are rejoined

to be node *N*. This process is repeated until none of the nodes can be split anyfurther and locked for further spliting [33], [40]. This process can be expressed as,

$$N_{l+1} = \begin{cases} \left\{ N_{l+1}^{2p}, N_{l+1}^{2p+1} \right\} & , \ if \quad I_{l+1}^{p} + I_{l+1}^{p+1} < I_l \\ N_l & , \ if \quad I_{l+1}^{p} + I_{l+1}^{p+1} > I_l \end{cases} \tag{4.6}$$

Here the superscripts *p* and *l* indicate the index and the level of node *N*, while *I* indicates the entropy value of node with index *p* and *l*.

C. Wavelet Packet Reconstruction

The reconstruction of wavelet packets is also performed in an iterative method. After up sampling each pair of wavelet packets coefficients at level *l* of the tree by two, we can calculate wavelet packets coefficients at the previous level *l*-1 by:

$$\xi_l^p[\beta] = \sum_m \xi_{l+1}^{2p}[m] h[\beta - 2m] + \sum_m \xi_{l+1}^{2p+1}[m] g[\beta - 2m] \tag{4.7}$$

The complete procedure for the wavelet packet based channel representation is described in Algorithm 1.

Algorithm 1: Wavelet Packet algorithm for signal representation.

1. Choose type of channel to be represented, such as
   a. Rayleigh Distribution Data
   b. Rician Distribution Data
   c. Real Process Analysis
2. Wavelet Packet Algorithm Setup
   a. Set Type of Wavelet Filter
   b. Set Levels of Decomposition
3. Calculate entropy value of each wavelet packet branches
4. Set number of wavelet packet coefficient which will be reduced
5. Choose number of the lowest branches which will be eliminated proportionally to point 4.
6. Set eliminated branches to zero
7. Reconstruct the rest of wavelet packet coefficient to be considered as reconstructed signal for the representation.
8. Comparing the reconstructed signal to the original signal.

4.3 Simulation Setup

To evaluate the ability of the proposed wavelet packet algorithms to accurately represent channels stochastic metrics such as Normalized Mean Square Error (NMSE), Correlation and Level Crossing Rate (LCR) value are employed. Each of those parameters can be defined as follow

(a) Mean Square Error (MSE)

MSE is a second order of error, which quantifies the difference between values implied by an estimator and the true values of the quantity being estimated [52]. The equation of MSE is given as

$$MSE_{1D} = E\left[\left|y(n) - \hat{y}(n)\right|^2\right] \tag{4.8}$$

where y and $\hat{y}$ are the function of original and reconstructed signal, respectively. For comparing all of performance in this simulation with equal standard, all of MSE values are normalized to the maximum one, which then called *Normalized Mean Square Error (NMSE).*

(b) Correlation

Correlation ratio is a measure of the relationship between two sets of data. This parameter is referred to first statistical moment to quantify the dependence of a data to another [53]. In term of two dimensional data, correlation can be defined as follow

$$r = \frac{\sum_{i=1}\left(y_i - \overline{y}\right)\left(\hat{y}_i - \overline{\hat{y}}\right)}{\sqrt{\left(\sum_i \left(y_i - \overline{y}\right)^2\right)\left(\sum_{i=1}\left(\hat{y}_i - \overline{\hat{y}}\right)^2\right)}} \tag{4.9}$$

where $\overline{y}$ and $\overline{\hat{y}}$ are the mean value of two-dimensional original and reconstructed signal, respectively. For comparing all of performance in this simulation with equal standard, all of correlation values are normalized to the maximum one.

(c) Level crossing rate (LCR) is defined as the expected number of a given signal crosses certain level of signal threshold [11]. The threshold levels considered in these comparisons are defined from the minimum to the maximum value of original signal amplitude.

Some of the scenarios which will be tested to measure all of performance paramaters above with all of the possible number of coefficient reduction. Such scenarios are,

(a) different level characteristic for constant wavelet filter

(b) different wavelet filter characteristic for constant decomposition.

While, especially for LCR parameter, the simulation is conducted with only one number of coefficient reduction, and will be compared the performance of several number of coefficient reduction, afterwards. Besides that, we will also use cumulative distribution function (CDF) as a metric to learn about the characteristics of the signal.

The description above is conducted for coefficient reduction method. The scenario which will be used for tree pruning method is similar to the initial method but added with comparing the performance in term of NMSE between coefficient reduction and tree pruning with same number of reconstructed branches.

4.4 Numerical Results

4.4.1 Coefficient Reduction Algorithm

In this subsection, the results of channel representation based on wavelet packet algorithm with coefficient reduction technique will be described. The explanation are classified based on the type of input and scenarios in each type of input.

4.4.1.1 Rayleigh Distribution Data Input

The behavior of nature cannot be predicted by anyone and is usually modeled statistically due to their randomness. This condition implies to the wireless channel which is influenced by the nature. Hence, modeling such channel can be also represented statistically. One of the randomness in the channel is amplitude that can be represented using Rayleigh Distribution. In order to evaluate the ability of the proposed algorithm to represent the time-invariant wireless channel, Rayleigh Distribution is considered as an input to the algorithm with the data length of 512, as show in Figure 4.4.

There are several variables which have to be determined in the proposed algorithm to yield efficient wireless channel representation, i.e. level of decomposition and mother of wavelet. Hence, in the subsequent parts, these variables will be observed over different number of coefficient which are used to be reconstructed.

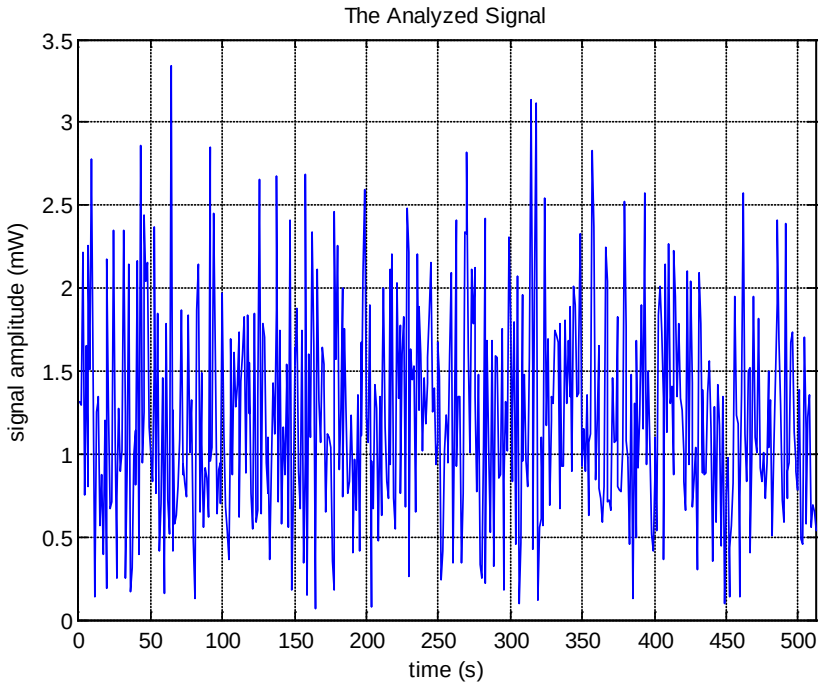

Figure 4.4 Rayleigh Distribution as an input of 1D Wavelet Packet Based Algorithm

A. Level of Decomposition

In this part, the effect of decomposition level to the performance of signal reconstruction through the proposed algorithm are observed over the number of coefficients which are used to be reconstructed. Mother of wavelet which is used in this simulation is Daubechies10. The reason of choosing Daubechies10 as a mother wavelet is that Daubechies10 has a support of minimum size for a given vanishing moment [40]. This simulation uses NMSE and correlation as a metric of performance evaluation. Figure 4.5 and Figure 4.7 show the results of performance evaluation of the proposed algorithm for different level of decomposition in terms of these parameters, respectively. The numerical representative of some such values are shown in Table 4.1 and Table 4.2.

Figure 4.5 shows the error value between original and reconstructed signal. From this figure, generally, we can see that there is no significant effect of different decomposition level to the reconstructed signal. However, if consider the zoomed version of this figure as depicted in Figure 4.6(a), there is still small differences on the effect of decomposition level. Besides that, Figure 4.7 shows the dependence between original and reconstructed signal. From this figure, we see that 6-level of

decomposition gives high correlation which means that still there is similarity between original and reconstructed signal, but the complexity is also high.

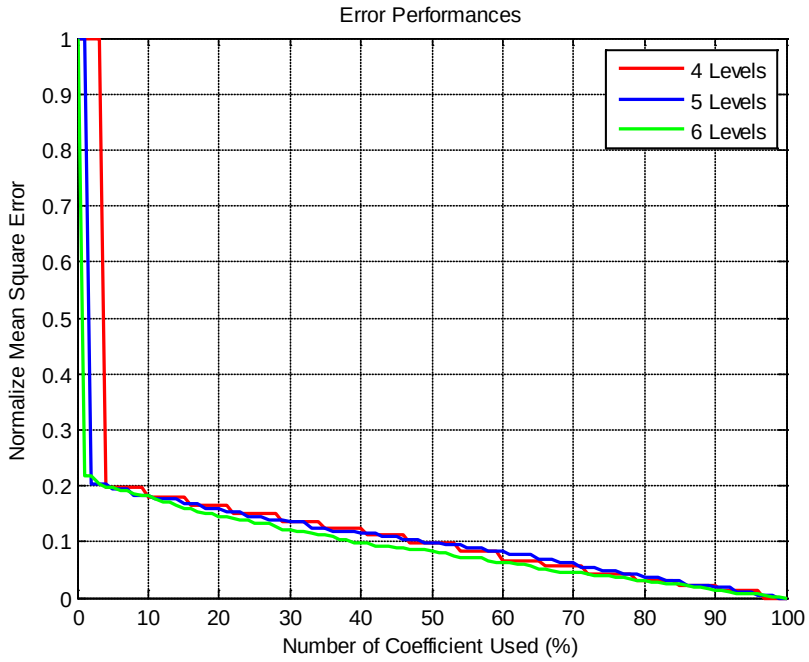

Figure 4.5 Normalized Mean Square Error (NMSE) for Rayleigh Distribution data with different level of decomposition on 1D Wavelet Packet Algorithm

Table 4.1 Representative of some values NMSE for Rayleigh Distribution data with different level of decomposition on 1D Wavelet Packet Algorithm

Level	40%	45%	50%	55%	60%
4	0.124926	0.111765	0.097765	0.082712	0.066312
5	0.116088	0.110295	0.096623	0.089702	0.082537
6	0.097134	0.089174	0.081958	0.072889	0.063545

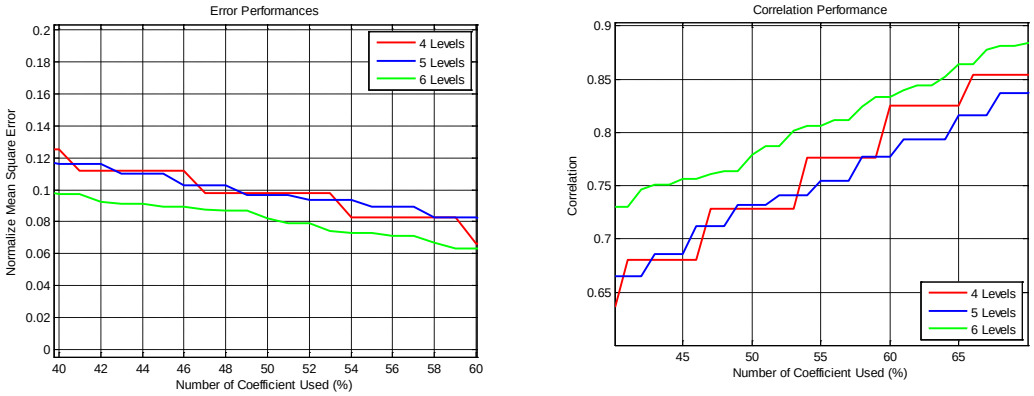

(a) (b)

Figure 4.6 Zoomed version of (a) NMSE and (b) correlation for Rayelgih distribution data with different level of decomposition on 1D Wavelet Packet Algorithm

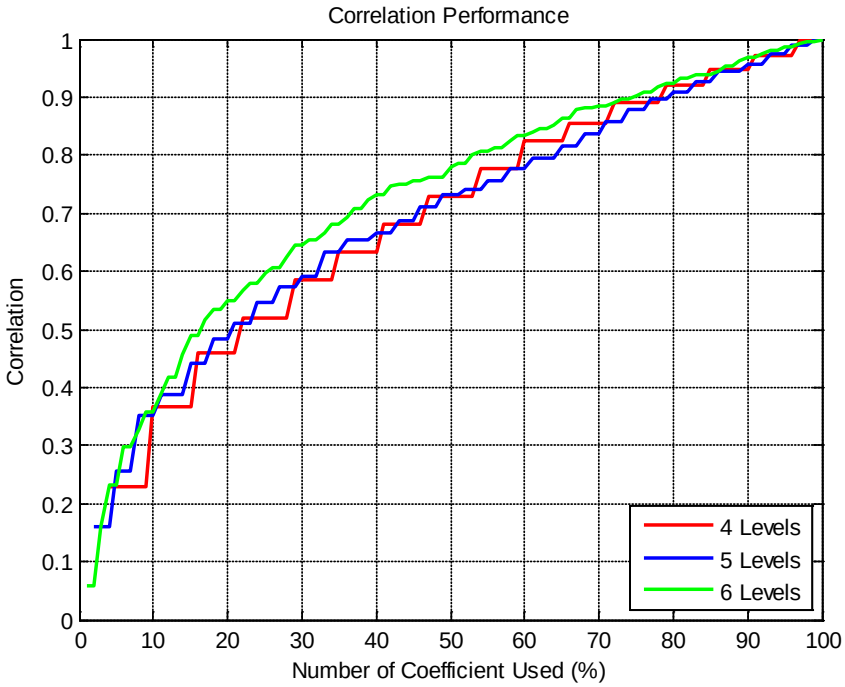

Figure 4.7 Correlation for Rayleigh Distribution Data with different level of decomposition on 1D Wavelet Packet Algorithm

Table 4.2 Representative of some values Correlation for Rayleigh Distribution data with different level of decomposition on 1D Wavelet Packet Algorithm

Level	40%	45%	50%	55%	60%
4	0.632786	0.68083	0.728352	0.776392	0.825563
5	0.665458	0.685991	0.732251	0.754583	0.777055
6	0.730575	0.756276	0.778847	0.806296	0.833658

B. Wavelet Filter

Besides the level of decomposition which affects the performance of the proposed algorithm, as mentioned in the preceding part, there is also another variable that has to be considered, namely the mother wavelet. In order to have adequate knowledge for getting the best signal reconstruction, we also need to analyze the behavior of the reconstructed signal for different type of wavelet and different length of filter. The analysis is obtained through the simulation.

Different from previous part, in this part several types of mother wavelet are used over different number of coefficients which are used at constant decomposition level of 5. The type of mother wavelets and its filter length are shown in Table 4.3. The reason of choosing 5 as level of decomposition is that (see Figure 4.5 and Figure

4.7) 5 levels of decomposition gives optimum performance in terms of complexity and accuracy than 6 or 4 levels. It is reasonable since the complexity of computation increase align with the increasing of decomposition level.

Table 4.3 Filter length of certain wavelet filter

Wavelet Type	Filter Length
Daubechis 10	20
Daubechis 20	40
Symlet 10	20
Symlet 20	40
Coiflet 2	12
Coiflet 3	18
Bi-ortoghonal 3.5	12
Bi-orthogonal 6.8	18

This simulation also uses NMSE and correlation as a metric of performance evaluation. Figure 4.8 and Figure 4.10 show the results of performance evaluation of the proposed algorithm for different type of mother wavelet in terms of these parameters, respectively. The numerical representative of some such values are shown in Table 4.4 and Table 4.5, respectively.

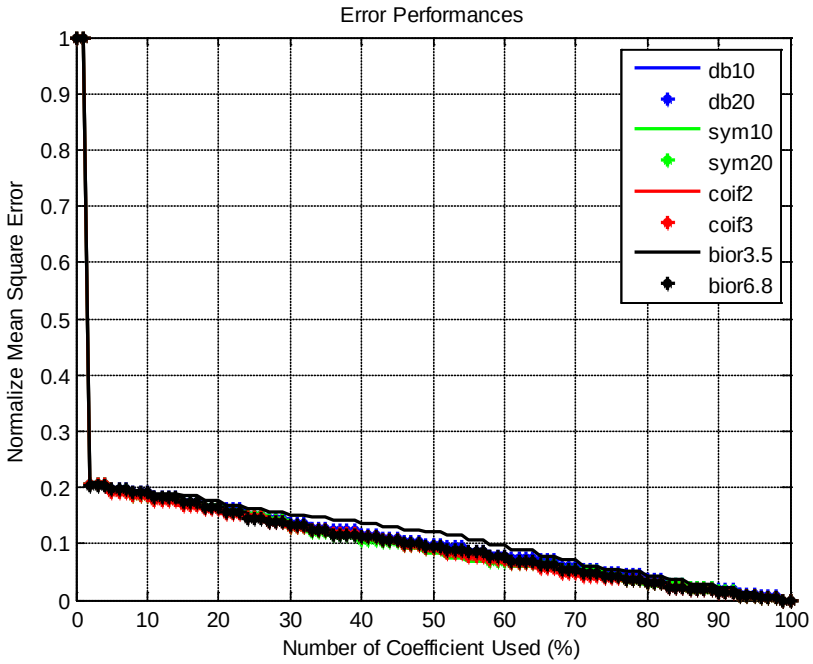

Figure 4.8 Normalized Mean Square Error (NMSE) for Rayleigh Distribution data with different type of wavelet filter on 1D Wavelet Packet Algorithm

Figure 4.8 shows the error value between original and reconstructed signal. From this figure, generally, the results for different type of wavelets and filter length are still quite similar. Even if the zoomed version of NMSE in Figure 4.9(a) is considered, the results is almost similar except for mother wavelet of Biorthogonal3.5. In this context, there is a difference when Biorthogonal3.5 and Biorthogonal6.8 are applied to the system as mother wavelet in the decomposition process. The differences are also seen when coiflets wavelet mothers are applied and compared to others. For example, if we consider coiflet2 which has filter length of 12, the accuracy of reconstruction is quite similar to the two initial wavelet mothers but different with bi-orthogonal 3.5 which also has same length of filter. These differences can be also clearly seen in figure Figure 4.10, and its zoomed version in Figure 4.9(b).

Table 4.4 Representative of some values NMSE for Rayleigh Distribution data with different type of wavelet filter on 1D Wavelet Packet Algorithm

Wavelet	40%	45%	50%	55%	60%
Daubhecies10	0.116088	0.110295	0.096623	0.089702	0.082537
Daubhecies20	0.1163	0.110994	0.097921	0.085965	0.078446
Symlett10	0.107342	0.10031	0.084275	0.069087	0.064776
Symlett20	0.108126	0.103046	0.092526	0.080602	0.068693
Coiflet2	0.111637	0.10391	0.088841	0.076311	0.070872
Coiflet3	0.112935	0.106689	0.091842	0.076788	0.070213
Bi-orthogonal3.5	0.137032	0.12942	0.121907	0.105645	0.09676
Bi-orthogonal6.8	0.112012	0.106687	0.094466	0.085193	0.078761

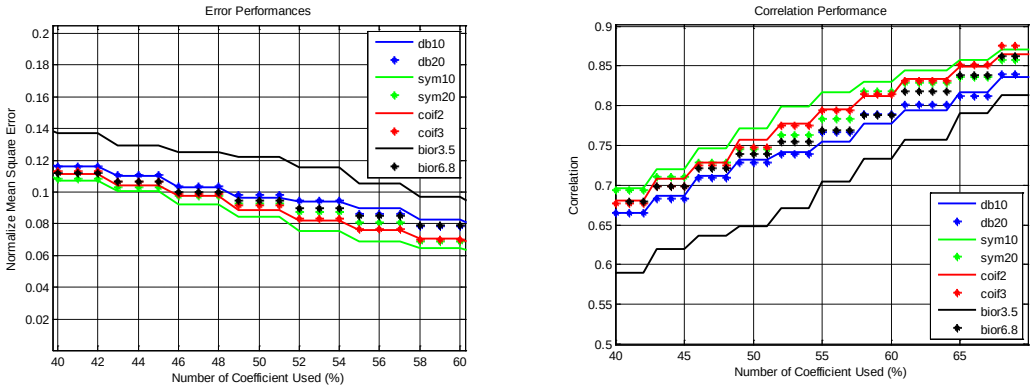

(a) (b)

Figure 4.9 Zoomed version of (a) NMSE and (b) correlation for Rayelgih distribution data with type of wavelet filter on 1D Wavelet Packet Algorithm

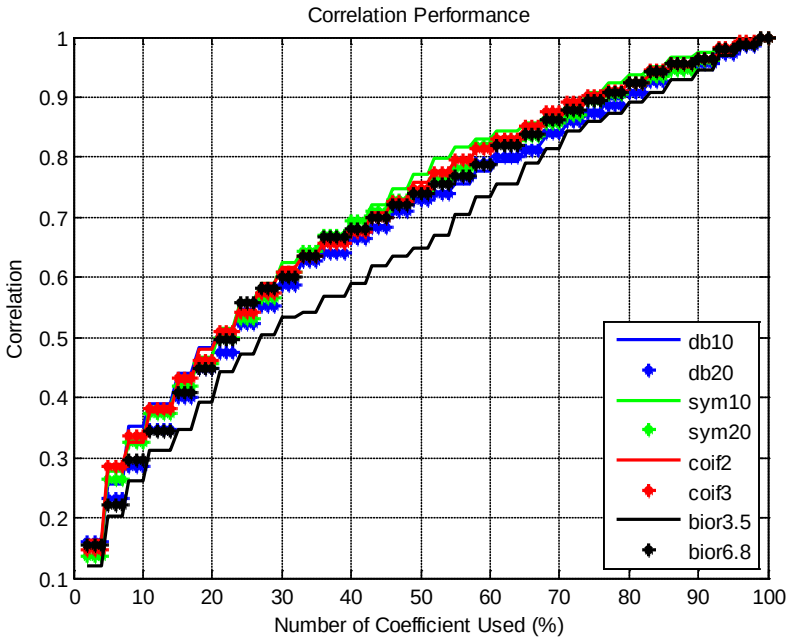

Figure 4.10 Correlation for Rayleigh Distribution data with different type of wavelet filter on 1D Wavelet Packet Algorithm

Table 4.5 Representative of some values Correlation for Rayleigh Distribution data with different type of wavelet filter on 1D Wavelet Packet Algorithm

Wavelet	40%	45%	50%	55%	60%
Daubhecies10	0.665458	0.685991	0.732251	0.754583	0.777055
Daubhecies20	0.664552	0.683457	0.727938	0.766357	0.789566
Symlett10	0.696163	0.720019	0.771562	0.817461	0.830024
Symlett20	0.693593	0.710922	0.745549	0.782987	0.818705
Coiflet2	0.681119	0.707824	0.757203	0.795947	0.812202
Coiflet3	0.676545	0.698373	0.747648	0.794524	0.814157
Bi-orthogonal3.5	0.589243	0.619979	0.647937	0.704123	0.733452
Bi-orthogonal6.8	0.679871	0.698386	0.739179	0.768692	0.788524

C. LCR Parameter

Beside the accuracy of signal reconstruction, we also have to know the characteristic of reconstructed signal against to the certain level of signal power thresholds which is considered as level crossing rate, as shown in Figure 4.11, Figure 4.12 and Figure 4.13 for different level of decomposition, type and length of wavelet filter, and the number of coefficient which are used, respectively.

Figure 4.11 shows the characteristic of reconstructed signal which use LCR as a consideration parameter for different level of decomposition with wavelet mother of Daubechis10 and 75% of significant coefficient are used in reconstruction process.

Meanwhile, the characteristic of different wavelet type which are applied in decomposition process can also be seen in Figure 4.12. This process considers decomposition level of 5 and 75% of significant coefficient are used in reconstruction process. From the results which are shown in Figure 4.11 and Figure 4.12, we can see that there are not significant influences of decomposition level and type of wavelet in decomposition process to the behavior of level crossing rate of reconstructed signal. The LCR parameter is chosen to be considered in this thesis since this parameter gives us the information about the rate of signal fluctuation against to the certain power threshold level. In the system design, this information are very useful on determining the received power sensitivity at the receiver.

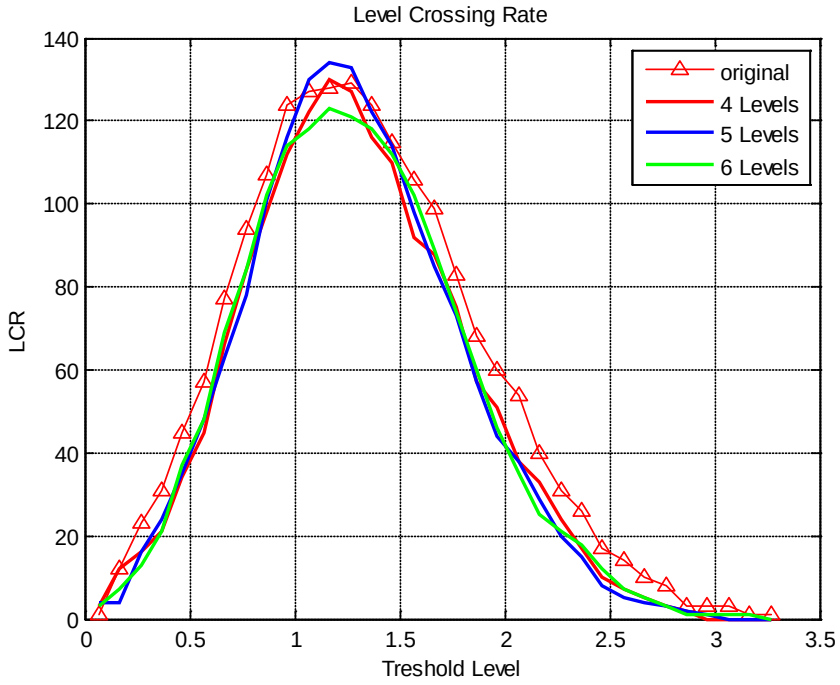

Figure 4.11 LCR for Rayleigh Distribution Data with different level of decomposition on 1D Wavelet Packet Algorithm

Finally, the original and reconstructed is depicted in Figure 4.14. This comparison is conducted under the simulation of 75% significant coefficients which are used with daubechies10 as mother wavelet and 5 levels of decomposition. We can see that the reconstructed signal is quite similar to the original with normalized mean square error (NMSE) is 0.0903.

To ensure that the reconstructed signal still has similar data distribution with the original, the cumulative distribution function (CDF) is considered and depicted in Figure 4.15.

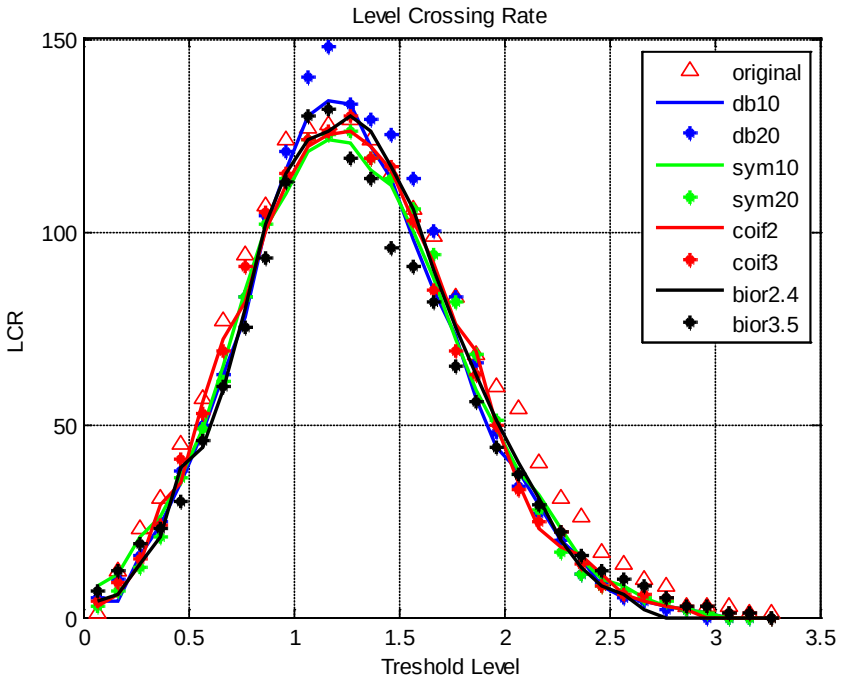

Figure 4.12 LCR for Rayleigh Distribution Data with different type of wavelet filter on 1D Wavelet Packet Algorithm

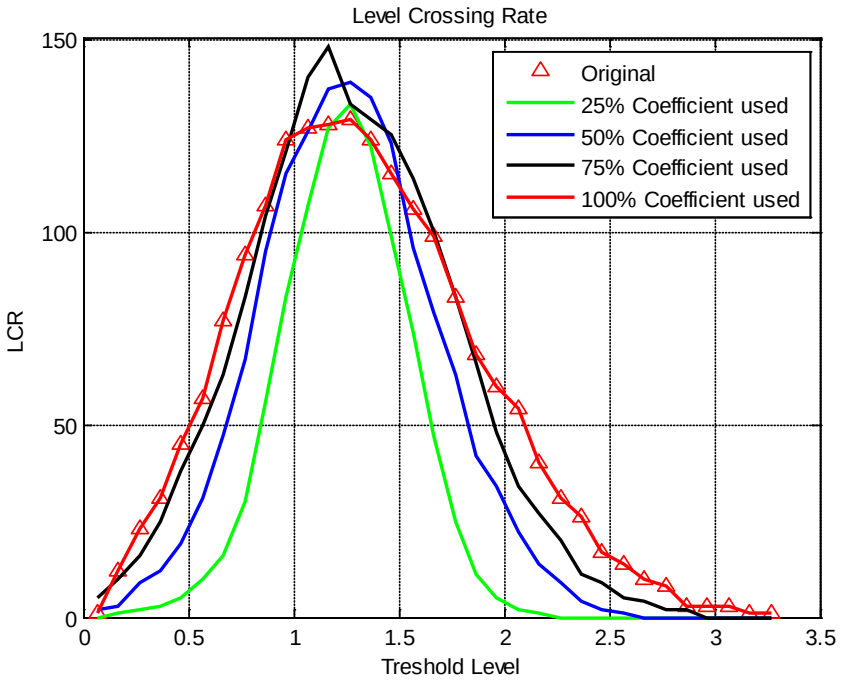

Figure 4.13 LCR for Rayleigh Distribution Data with different number of coefficient which are used on 1D Wavelet Packet Algorithm

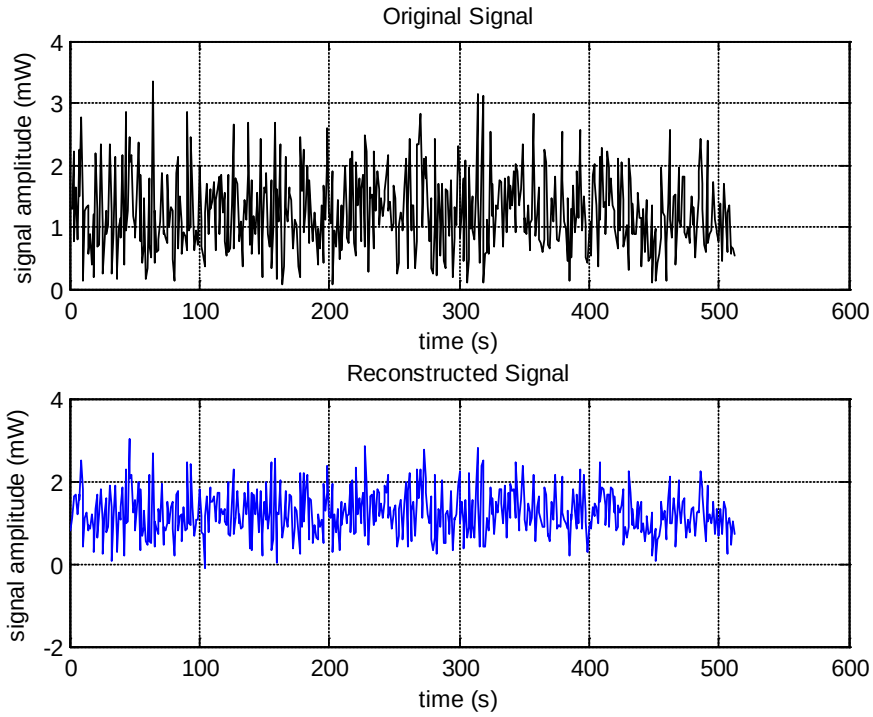

Figure 4.14 Comparsion between original and reconstructed signal for Rayleigh distribution data.

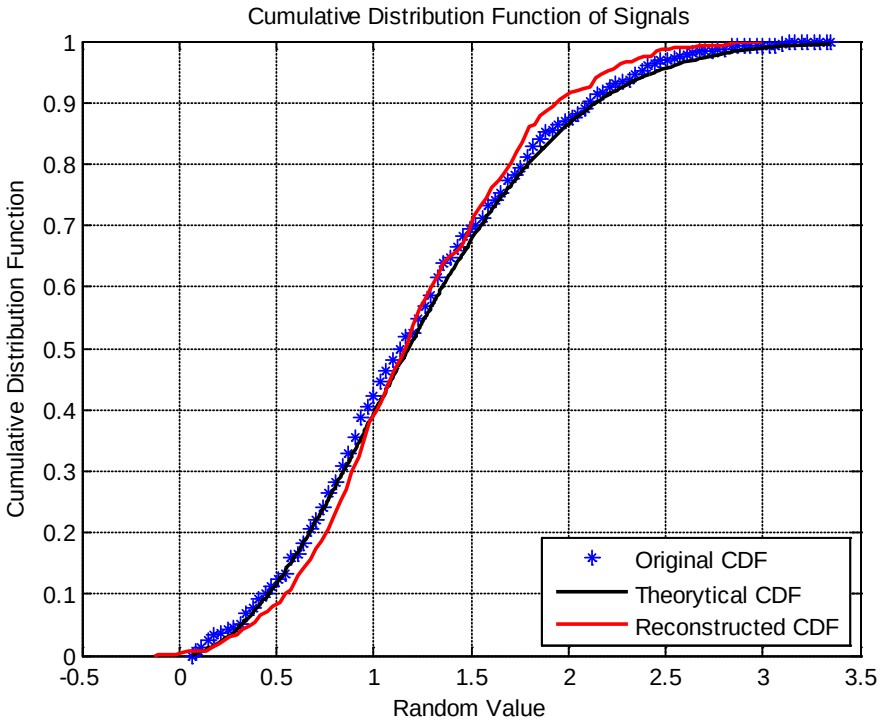

Figure 4.15 CDF for Rayleigh Distribution Data on 1D Wavelet Packet Algorithm

4.4.1.2 Rician Distribution Data Input

The signal representation which is considered in the preceding sub-section assumes that the direct signal is totally blocked by the obstacle. However, in real nature, the direct signal is occasionally received by the receiver which cannot be represented by Rayleigh distribution. In order to give proper representation, Ricean Distribution becomes an alternative to represent the received signal which has not only reflected signal but also direct signal. Consequently, this kind distribution is also used as an input to the proposed algorithm with data length of 512 as shown in Figure 4.16.

Similar to the preceding sub-section, there are several variables which have to be determined in the proposed algorithm to yield efficient wireless channel representation, i.e. level of decomposition and mother of wavelet. Hence, in the subsequent parts, these variables will be observed over different number of coefficient which are used to be reconstructed. All of scenario which are used in this simulation are totally to the previous one.

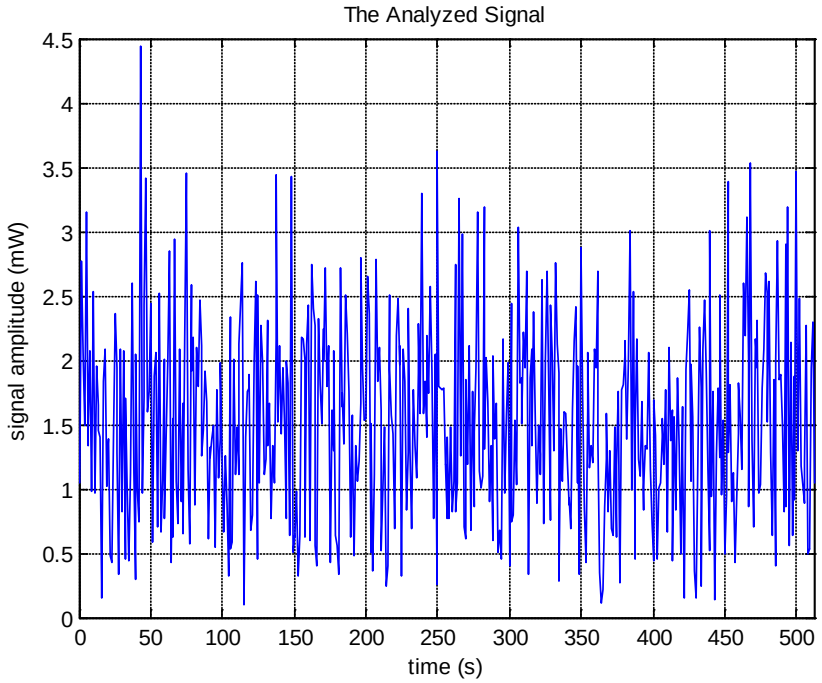

Figure 4.16 Ricean Distribution as an input of 1D Wavelet Packet Based Algorithm

A. Level of Decomposition

In this part, the effect of decomposition level to the performance of signal reconstruction through the proposed algorithm are observed over the number of coefficients which are used to be reconstructed. Mother of wavelet which is used in this simulation is Daubechies10. The reason of choosing Daubechies10 as a mother wavelet is that Daubechies10 has a support of minimum size for a given vanishing moment [40]. This simulation uses NMSE and correlation as a metric of performance evaluation. Figure 4.17 and Figure 4.19 show the results of performance evaluation of the proposed algorithm for different level of decomposition in terms of these parameters, respectively. The numerical representative of some such values are shown in Table 4.6 and Table 4.7.

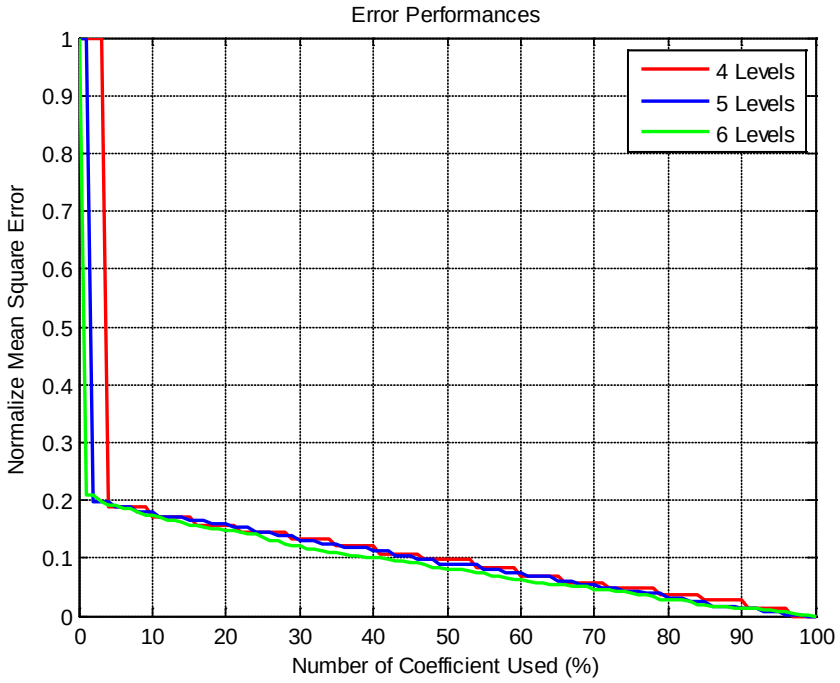

Figure 4.17 Normalized Mean Square Error (NMSE) for Ricean Distribution data with different level of decomposition on 1D Wavelet Packet Algorithm

Figure 4.17 shows the error value between original and reconstructed signal. From this figure, generally, we can see that the performance reconstructed signal is almost same for different level of decomposition. Even if the zommed version of this figure in Figure 4.18(a) is considered, the differences are still not significant to the performance of the proposed system. Besides that, Figure 4.19 shows the dependence between original and reconstructed signal. From this figure, we see that 6-level of

decomposition gives high correlation which means that still there is similarity between original and reconstructed signal, but the complexity is also high.

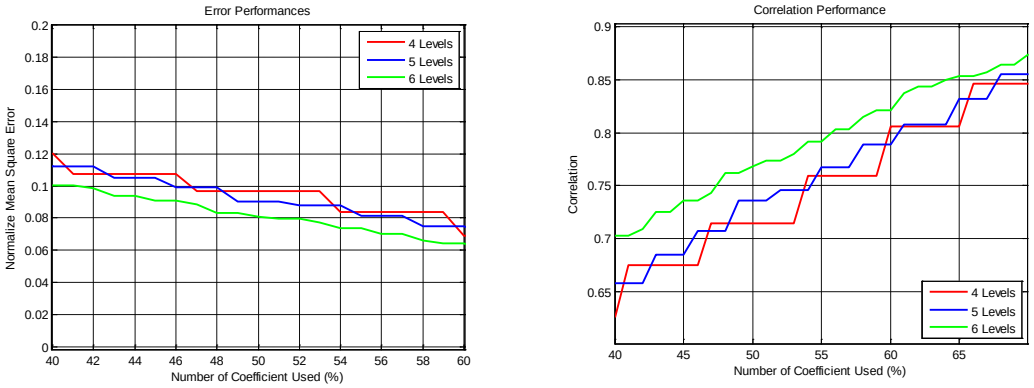

(a) (b)

Figure 4.18 Zoomed version of (a) NMSE and (b) correlation for Ricean distribution data with different level of decomposition on 1D Wavelet Packet Algorithm

Table 4.6 Representative of some values NMSE for Ricean Distribution data with different level of decomposition on 1D Wavelet Packet Algorithm

Level	40%	45%	50%	55%	60%
4	0.120408	0.107559	0.096858	0.083701	0.069241
5	0.112289	0.10496	0.090531	0.081392	0.074724
6	0.100011	0.090728	0.081094	0.073871	0.064194

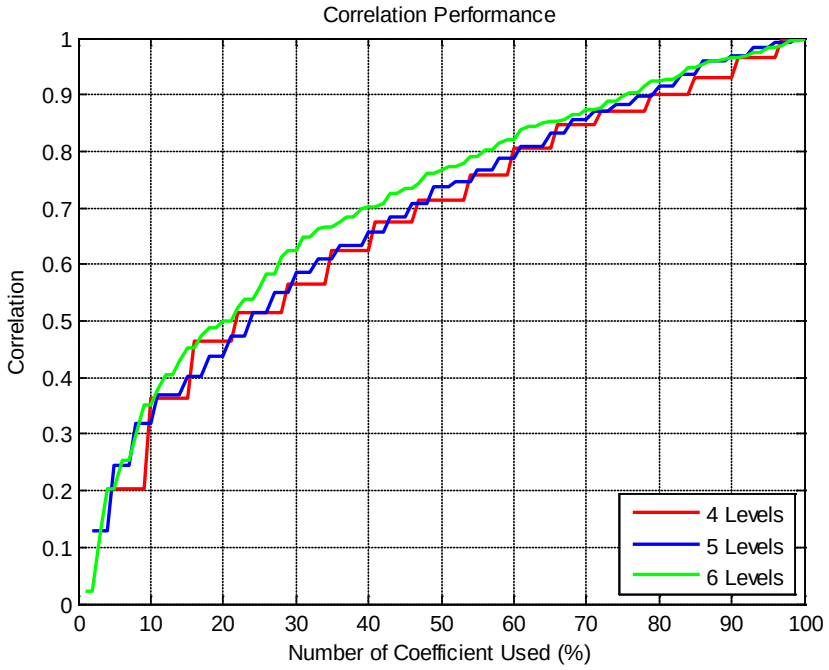

Figure 4.19 Correlation for Ricean Distribution data with different level of decomposition on 1D Wavelet Packet Algorithm

Table 4.7 Representative of some values Correlation for Ricean Distribution data with different level of decomposition on 1D Wavelet Packet Algorithm

Level	40%	45%	50%	55%	60%
4	0.625296	0.675254	0.714162	0.759352	0.806095
5	0.657545	0.685036	0.736388	0.767147	0.788855
6	0.703169	0.73582	0.768042	0.791468	0.821806

B. Wavelet Filter

Besides the level of decomposition which affects the performance of the proposed algorithm, as mentioned in the preceding part, there is also another variable that has to be considered, namely the mother wavelet. In order to have sufficient knowledge to obtain the best signal reconstruction, we also have to analyze the behavior of the reconstructed signal for different type of wavelet and different length of filter. The analysis is obtained through the simulation.

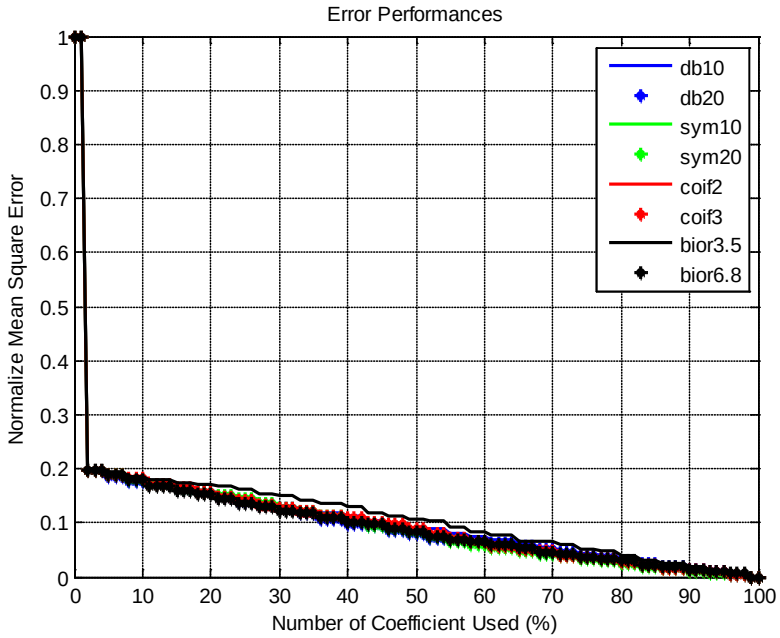

Figure 4.20 Normalized Mean Square Error (NMSE) for Ricean Distribution data with different type of wavelet filter on 1D Wavelet Packet Algorithm

Different from previous part, in this part several types of mother wavelet are used over different number of coefficients which are used at constant decomposition level of 5. The type of mother wavelets and its filter length are shown in Table 4.3. The reason of choosing 5 as level of decomposition is that (see Figure 4.5 and Figure

4.7) 5 levels of decomposition gives optimum performance in terms of complexity and accuracy than 6 or 4 levels.

This simulation also uses NMSE and correlation as a metric of performance evaluation. Figure 4.20 and Figure 4.22 show the results of performance evaluation of the proposed algorithm for different type of mother wavelet in terms of these parameters, respectively. The numerical representative of some such values are shown in Table 4.8 and Table 4.9, respectively.

Figure 4.20 shows the error value between original and reconstructed signal. From this figure, generally, the results for different type of wavelets and filter length are still quite similar. Even if the zoomed version of NMSE in Figure 4.21(a) is considered, the results are almost similar except for mother wavelet of Biorthogonal3.5. In this context, there is a difference when Biorthogonal3.5 and Biorthogonal6.8 are applied to the system as mother wavelet in the decomposition process. The differences are also seen when coiflets wavelet mothers are applied and compared to others. For example, if we consider coiflet2 which has filter length of 12, the accuracy of reconstruction is quite similar to the two initial wavelet mothers but different with bi-orthogonal 3.5 which also has same length of filter. These differences can be also clearly seen in Figure 4.22, and its zoomed version in Figure 4.21 (b).

Table 4.8 Representative of some values NMSE for Ricean Distribution data with different type of wavelet filter on 1D Wavelet Packet Algorithm

Wavelet	40%	45%	50%	55%	60%
Daubhecies10	0.112289	0.10496	0.090531	0.081392	0.074724
Daubhecies20	0.098491	0.093601	0.079625	0.069174	0.066004
Symlett10	0.104744	0.099478	0.085716	0.073993	0.064877
Symlett20	0.104162	0.096416	0.08322	0.065046	0.059023
Coiflet2	0.100007	0.093711	0.083892	0.072635	0.066269
Coiflet3	0.108316	0.102024	0.088952	0.070929	0.06687
Bi-orthogonal3.5	0.13011	0.118513	0.106091	0.093251	0.083954
Bi-orthogonal6.8	0.099913	0.096575	0.082434	0.069776	0.065112

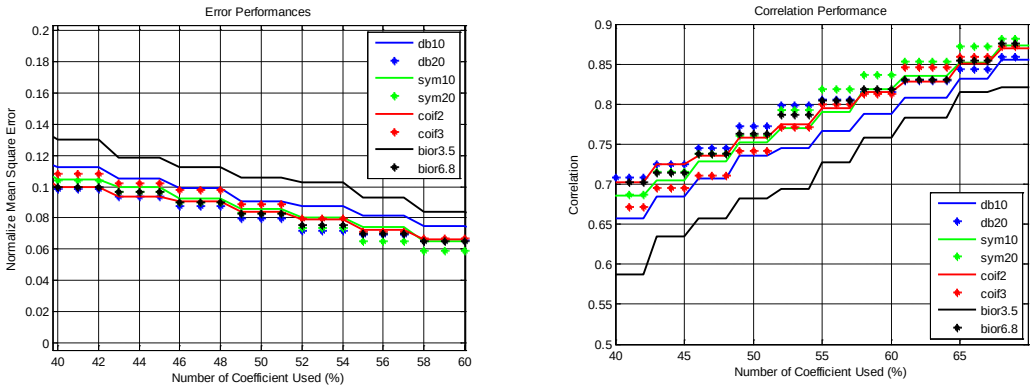

(a) (b)

Figure 4.21 Zoomed version of (a) NMSE and (b) correlation for Ricean distribution data with different type of wavelet filter on 1D Wavelet Packet Algorithm

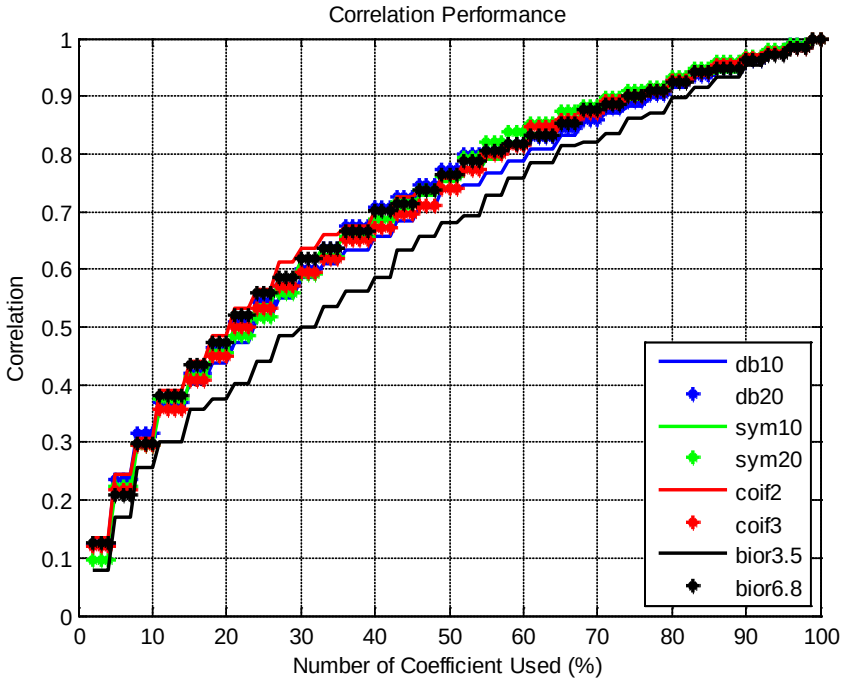

Figure 4.22 Correlation for Ricean Distribution data with different type of wavelet on 1D Wavelet Packet Algorithm

C. LCR Parameter

Beside the accuracy of signal reconstruction, we also have to know the characteristic of reconstructed signal against to the certain level of signal power thresholds which is considered as level crossing rate, as shown in Figure 4.23, Figure 4.24 and Figure 4.25 for different level of decomposition, type and length of wavelet filter, and the number of coefficient which are used, respectively.

Table 4.9 Representative of some values NMSE for Ricean Distribution data with different type of wavelet filter on 1D Wavelet Packet Algorithm

Wavelet	40	45	50	55	60
Daubhecies10	0.657545	0.685036	0.736388	0.767147	0.788855
Daubhecies20	0.70834	0.725602	0.772847	0.806285	0.816171
Symlett10	0.685569	0.704737	0.752522	0.790942	0.819587
Symlett20	0.687747	0.715675	0.760889	0.819088	0.837496
Coiflet2	0.702842	0.725141	0.75864	0.795295	0.815297
Coiflet3	0.67225	0.695522	0.741552	0.800689	0.813411
Bi-orthogonal3.5	0.587423	0.634905	0.681938	0.727504	0.759033
Bi-orthogonal6.8	0.703213	0.715122	0.763467	0.804323	0.818864

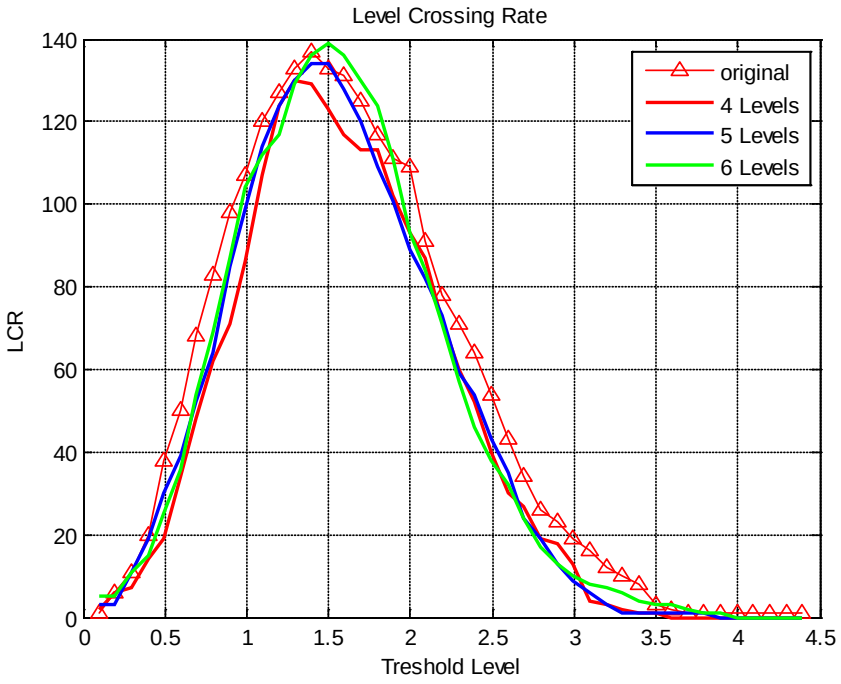

Figure 4.23 LCR for Ricean Distribution Data with different level of decomposition on 1D Wavelet Packet Algorithm

Figure 4.23 shows the characteristic of reconstructed signal which use LCR as a consideration parameter for different level of decomposition with wavelet mother of Daubechis10 and 75% of significant coefficient are used in reconstruction process. Meanwhile, the characteristic of different wavelet type which are applied in decomposition process can also be seen in Figure 4.24. This process considers decomposition level of 5 and 75% of significant coefficient are used in reconstruction process. From the results which are shown in Figure 4.23 and Figure 4.24, we can see that there are not significant influences of decomposition level and

type of wavelet in decomposition process to the behavior of level crossing rate of reconstructed signal.

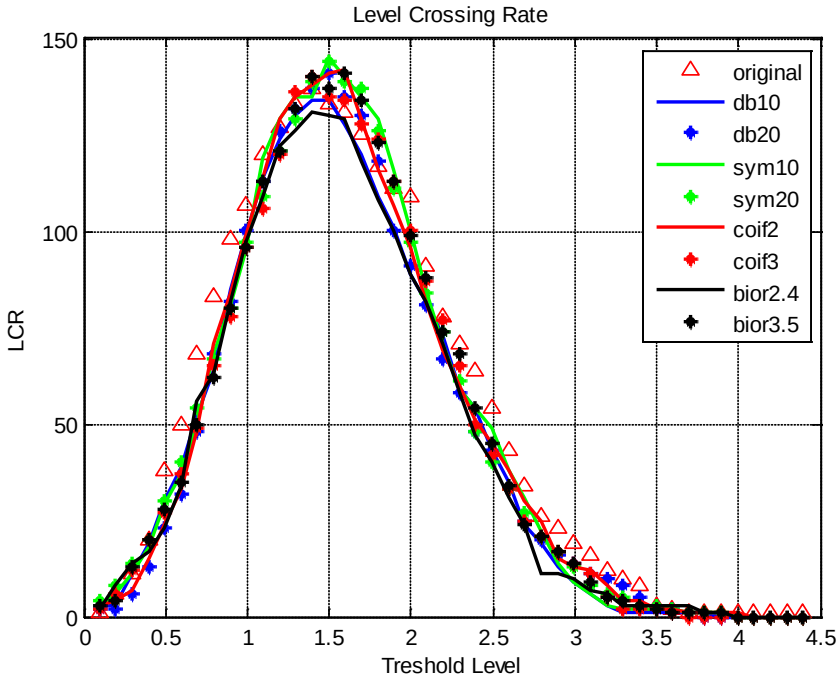

Figure 4.24 LCR for Ricean Distribution Data with different type of wavelet filter on 1D Wavelet Packet Algorithm

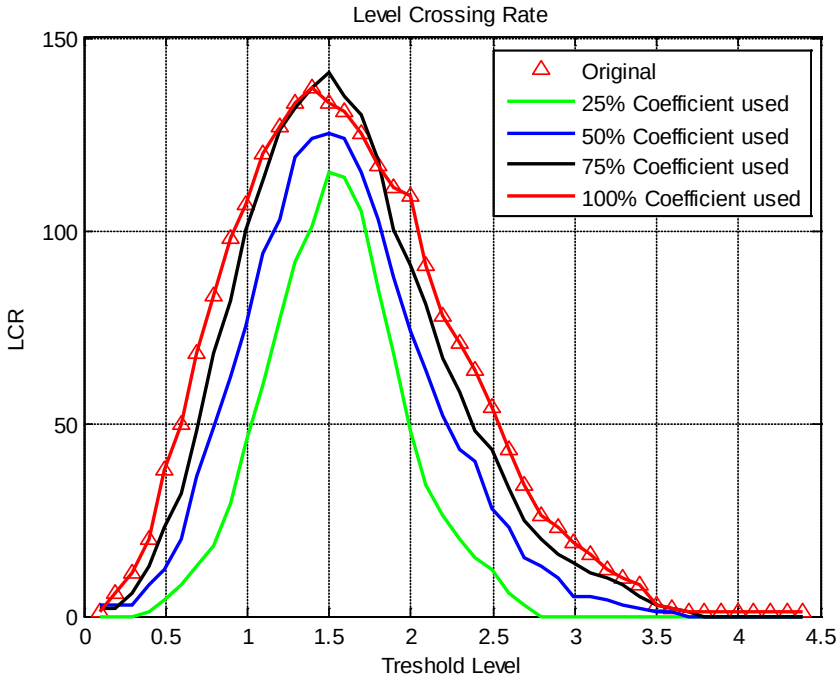

Figure 4.25 LCR for Ricean Distribution Data with different number of coefficient which are used on 1D Wavelet Packet Algorithm

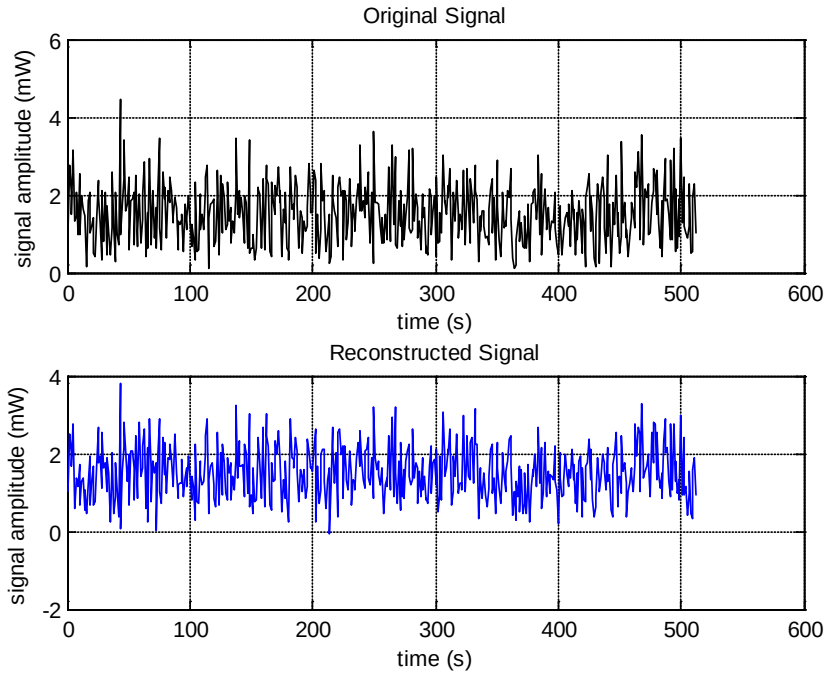

Figure 4.26 Comparsion between original and reconstructed signal for Ricean distribution data on 1D Wavelet Packet Algorithm

Finally, the original and reconstructed is depicted in Figure 4.26. This comparison is conducted under the simulation of 75% significant coefficients which are used with daubechies10 as mother wavelet and 5 levels of decomposition. We can see that the reconstructed signal is not much different from the original signal with normalized mean square error (NMSE) is 0.1262.

4.4.1.3 Real Process Analysis

This simulation is conducted to observe the capability of wavelet packet algorithm to represent the signal as a combination of Rayleigh and Poisson Distributions. This kind of signal is observed due to the fact that the fluctuated signal at receiver is influenced by the delay of signal arrival time (arrival time, sometimes, can be modeled as Poisson Distribution).

The scheme which are used to produce such signal as depicted beside as follow,

$$x(t) = \sum_{t \in \mathbb{Z}} x_1(t)$$
$$x(t+\tau) = \sum_{t \in \mathbb{Z}} x(t+\tau) + x_2(t) \qquad (4.10)$$

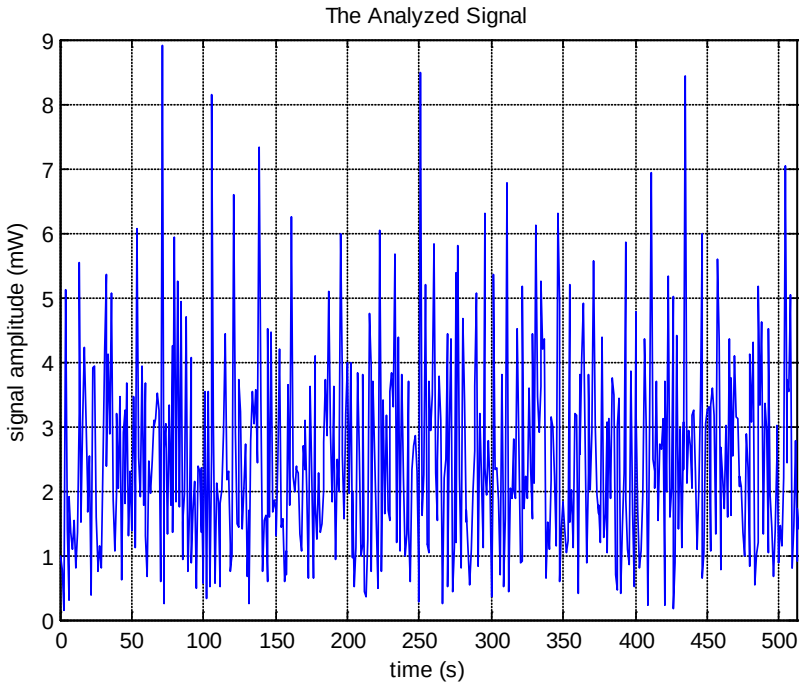

Figure 4.27 The Real Process Input for 1D Wavelet Packet Algorithm

In equation (4.10), $x_1(t)$ represents the arrival signal follows the Rayleigh Distribution, meanwhile $x_2(t)$ represents the second arrival signal follows Rayleigh Distribution which is delayed at τ follow Poisson Distribution. The sequential process of $x(t)$ is depicted in Figure 4.28.

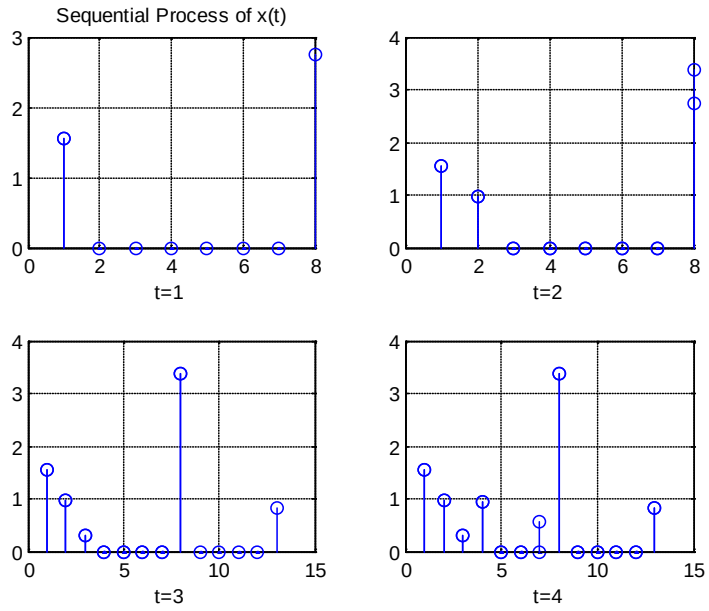

Figure 4.28 The sequential process

A. Level of Decomposition

In this part, the effect of decomposition level to the performance of signal reconstruction through the proposed algorithm are observed over the number of coefficients which are used to be reconstructed. Mother of wavelet which is used in this simulation is Daubechies10. The reason of choosing Daubechies10 as a mother wavelet is that Daubechies10 has a support of minimum size for a given vanishing moment [40]. This simulation uses NMSE and correlation as a metric of performance evaluation. Figure 4.29 and Figure 4.30 show the results of performance evaluation of the proposed algorithm for different level of decomposition in terms of NMSE and correlation, respectively.

Figure 4.29 shows the error value between original and reconstructed signal. From this figure, generally, we can see that there is no significant effect of different decomposition level to the reconstructed signal. Besides that, Figure 4.30 shows the dependence between original and reconstructed signal which not much different for every level of decomposition.

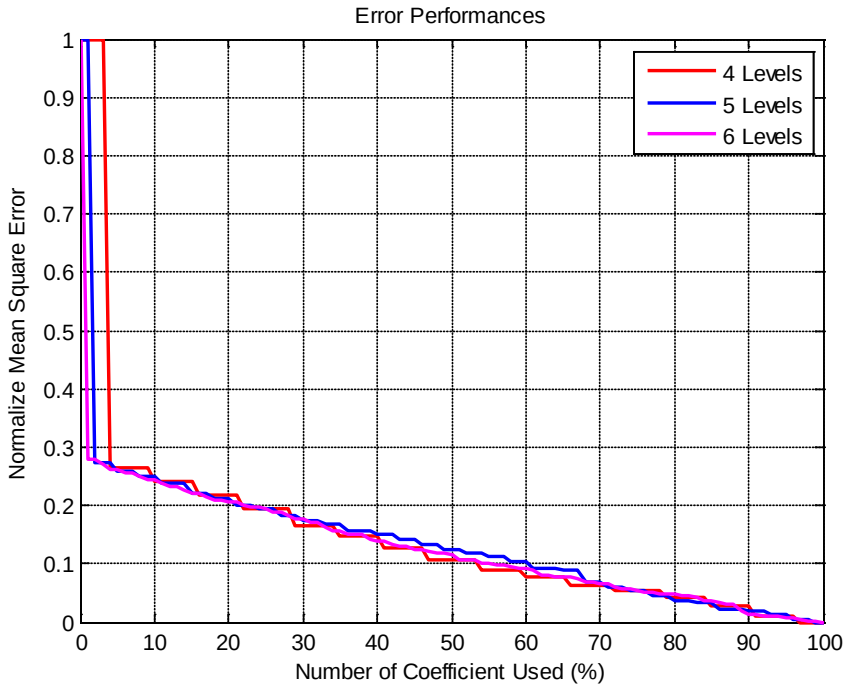

Figure 4.29 Normalized Mean Square Error (NMSE) for Real Process data with different level of decomposition on 1D Wavelet Packet Algorithm

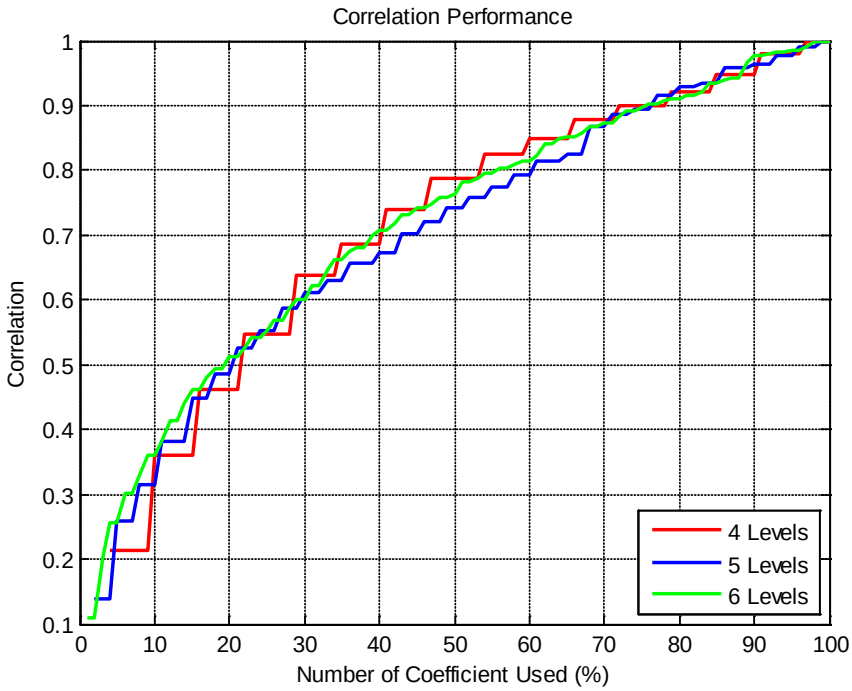

Figure 4.30 Correlation for Real Process data with different level of decomposition on 1D Wavelet Packet Algorithm

B. Wavelet Filter

Besides the level of decomposition which affects the performance of the proposed algorithm, as mentioned in the preceding part, there is also another variable that has to be considered, namely the mother wavelet. In order to have sufficient knowledge to achieve the best signal reconstruction, we also must analyze the behavior of the reconstructed signal for different type of wavelet and different length of filter.

In this simulation, several types of mother wavelet are used over different number of coefficients which are used at constant decomposition level of 5. This simulation also uses NMSE and correlation as a metric of performance evaluation. Figure 4.31 and Figure 4.32 show the results of performance evaluation of the proposed algorithm for different type of mother wavelet in terms of these parameters, respectively.

Figure 4.31 shows the error value between original and reconstructed signal. From this figure, generally, the results for different type of wavelets and filter length are still quite similar.

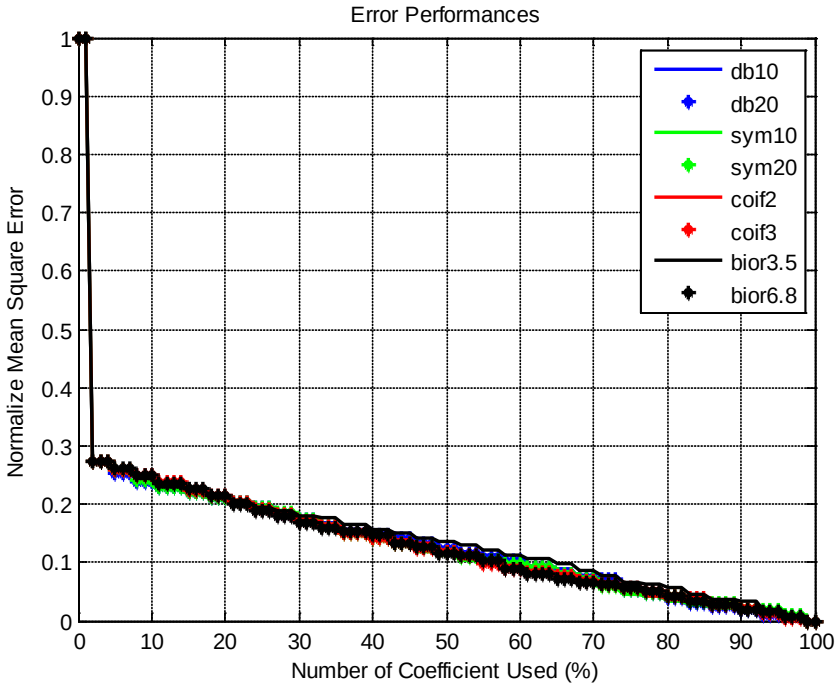

Figure 4.31 Normalized Mean Square Error (NMSE) for Real Process data with different type for wavelet filter on 1D Wavelet Packet Algorithm

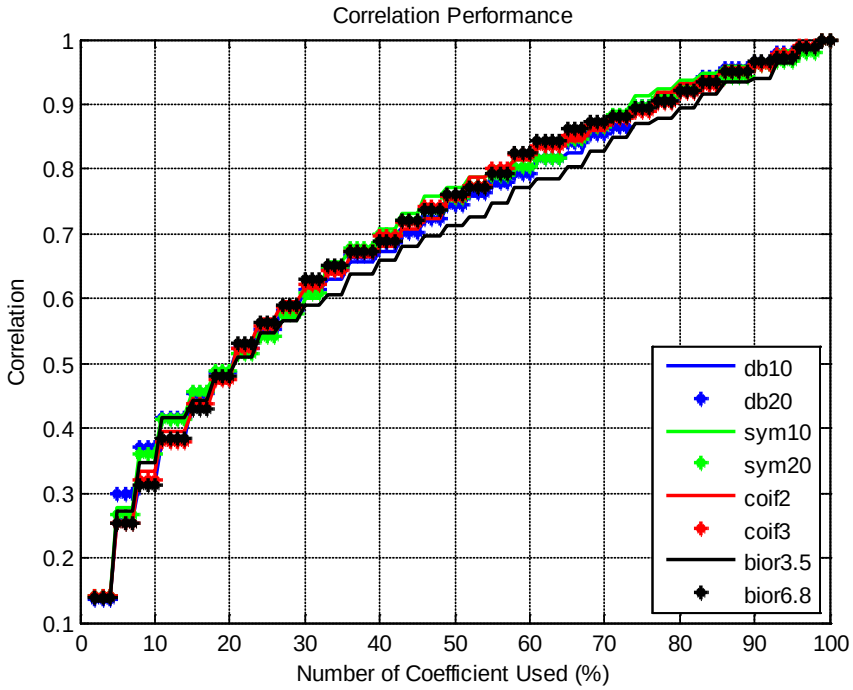

Figure 4.32 Correlation for Real Process data with different type of wavelet filter on 1D Wavelet Packet Algorithm

Beside the result of different level of decomposition, type of mother wavelet and its filter length, we want also to observe the effect of different rate of arrival time which is shown in Figure 4.33 and Figure 4.34. From those results, we can see that although the trend is almost similar, but the exact value of each observation point is different.

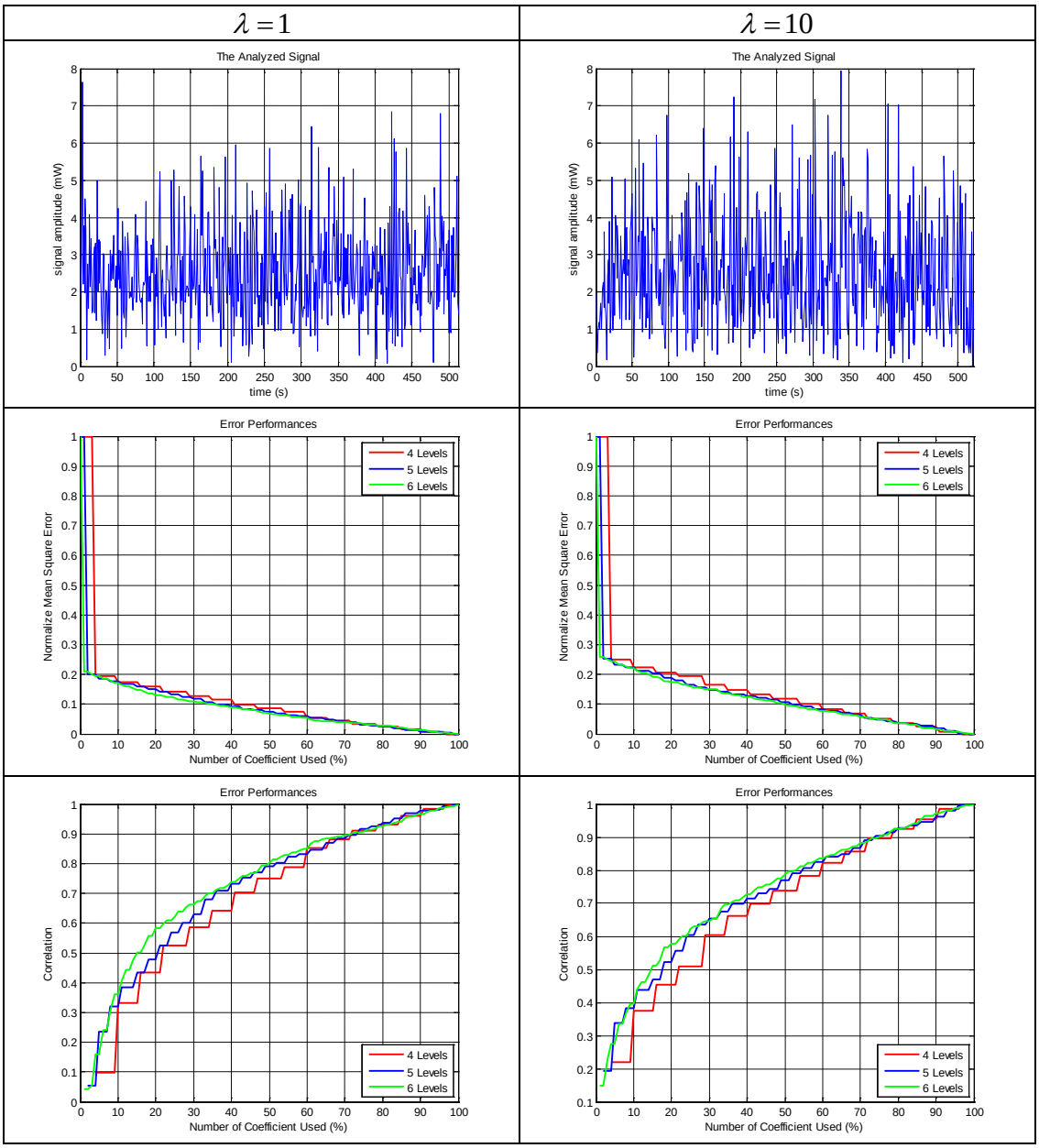

Figure 4.33 Performance comparison of real process with different level of decomposition on 1D Wavelet Packet Algorithm.

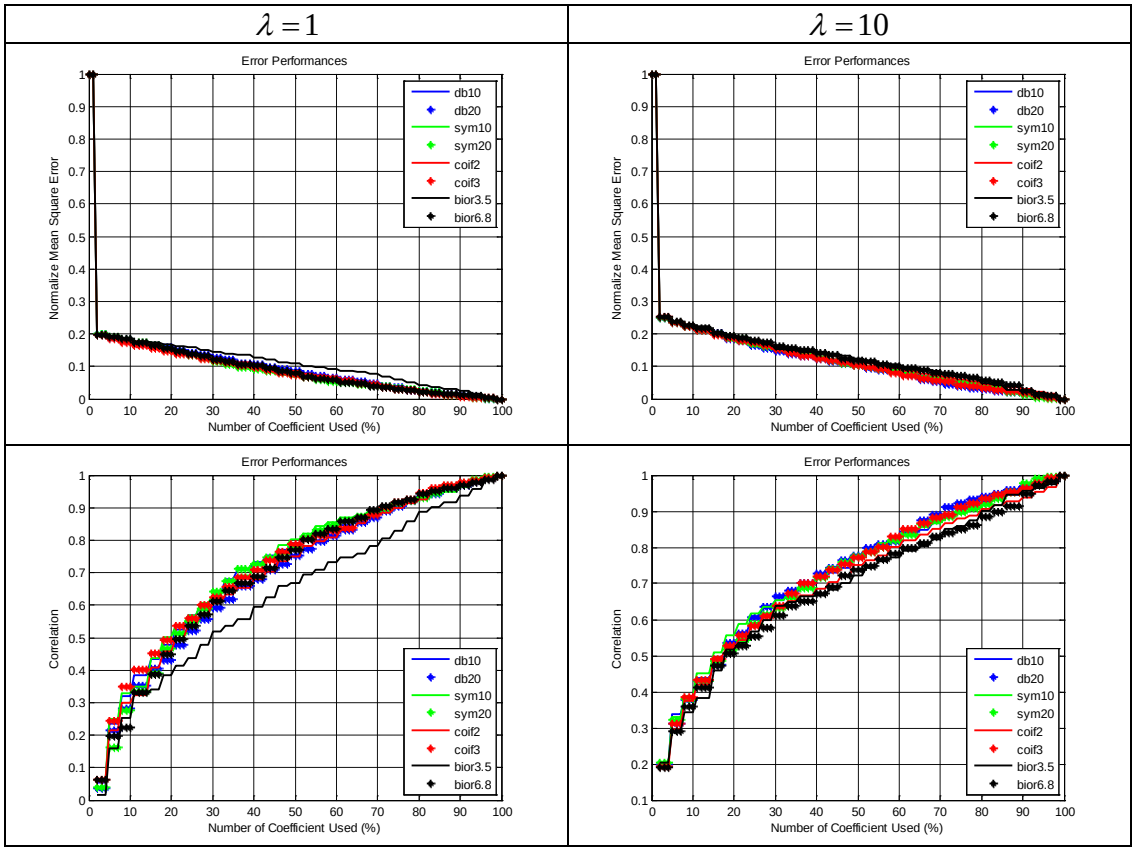

Figure 4.34 Performance comparison of real process with different type of wavelet filter on 1D Wavelet Packet Algorithm.

4.4.2 Tree Pruning Algorithm

In this section, the results of channel representation based on wavelet packet with tree pruning technique are presented. As described in section 4.2, that the process of tree pruning is splitting all of nodes iteratively until all of child nodes cannot be split anymore until certain level of decomposition which is determined at the beginning of process. The node splitting is done by considering the entropy value summation of two child nodes compared to entropy value of their mother node. If the summation is less than the entropy value of the mother node, then the node is split. Contrary, if summation is more than the entropy value of mother node, the node is rejoined. The wavelet packet tree structure as a result of this process is depicted in Figure 4.35, by using daubhecies10 as a mother wavelet and 5 levels of decomposition. The comparison of the reconstructed signal to the original signal is shown in Figure 4.36 with NMSE = 1.0550e-022. Due to the comparison yields similar results, we then plot the statistical characteristic of this signal by analyzing

cumulative distribution function (CDF) as shown in Figure 4.37. With reducing some WP Coefficient, this method produce 18 terminal nodes indicate the number of WP Coefficient.

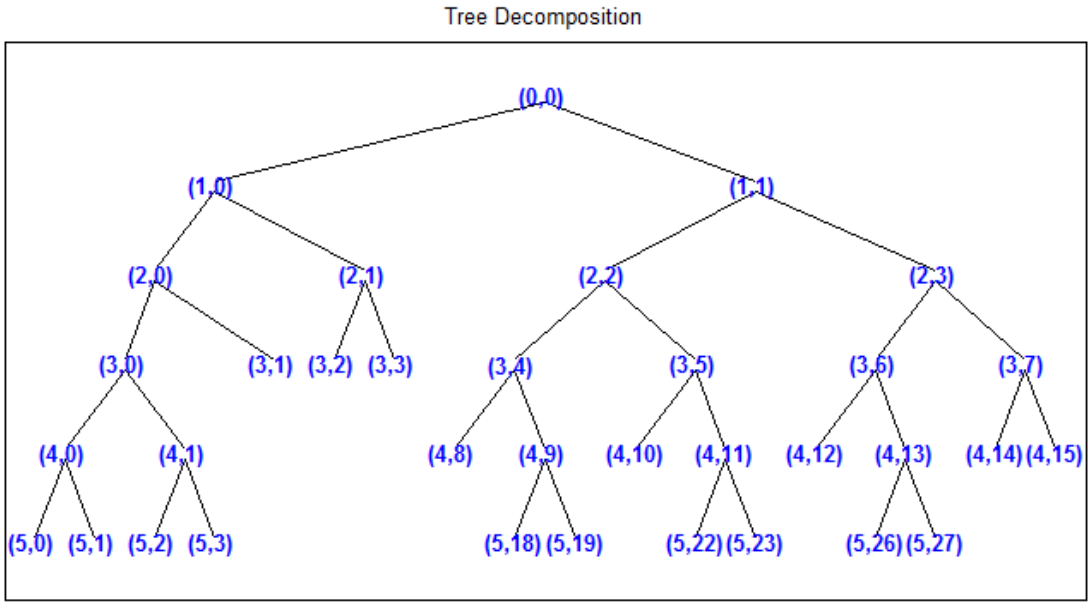

Figure 4.35 Wavelet Packet Tree for Tree Pruning

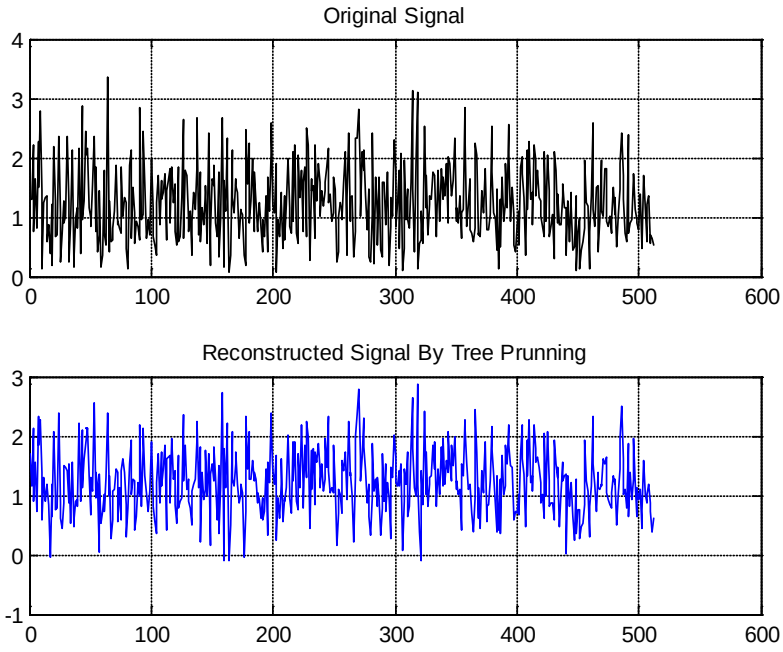

Figure 4.36 Comparison between original and reconstructed signal for Rayleigh Distribution Data using Tree Pruning Method

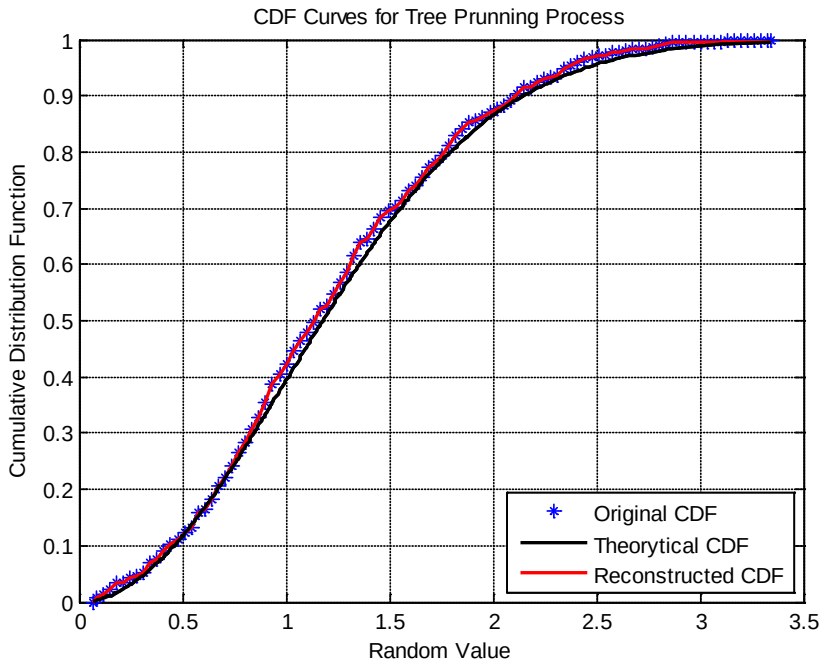

Figure 4.37 CDF for Rayleigh Distribution Data using Tree Pruning Method

4.4.3 Performance Comparison

The performance of two candidate methods, presented in subsection 4.4.1 and 4.4.2, are now compared in this subsection. We have known that tree pruning method can represent the channel or signal more efficient than coefficient reduction. This condition can be considered in term of WP Coefficients which are used for representing kind of input.

For fairness of comparison the same system parameters have been used for both methods – Daubechies-10 is the mother wavelet of choice; the levels of decomposition is fixed at 5; 100% of significant coefficients to reconstruct kind of input, resulting different number of terminal nodes which indicating the number of coefficient which are used to represent the input. In this scenario, the coefficient reduction method produce 32 terminal nodes due to decomposing the input uniformly which is yielded by 2^5, while tree pruning method produces 18 terminal nodes. This representation yields similar NMSE is around 1.0550e-022

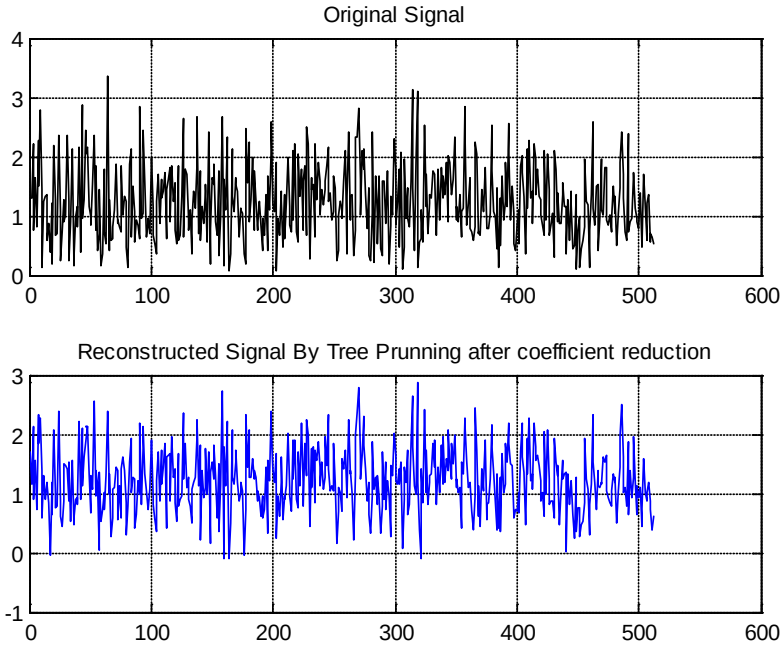

Figure 4.38 Comparison between original and reconstructed signal for Rayleigh Distribution Data using Tree Pruning Method with removing several coefficients

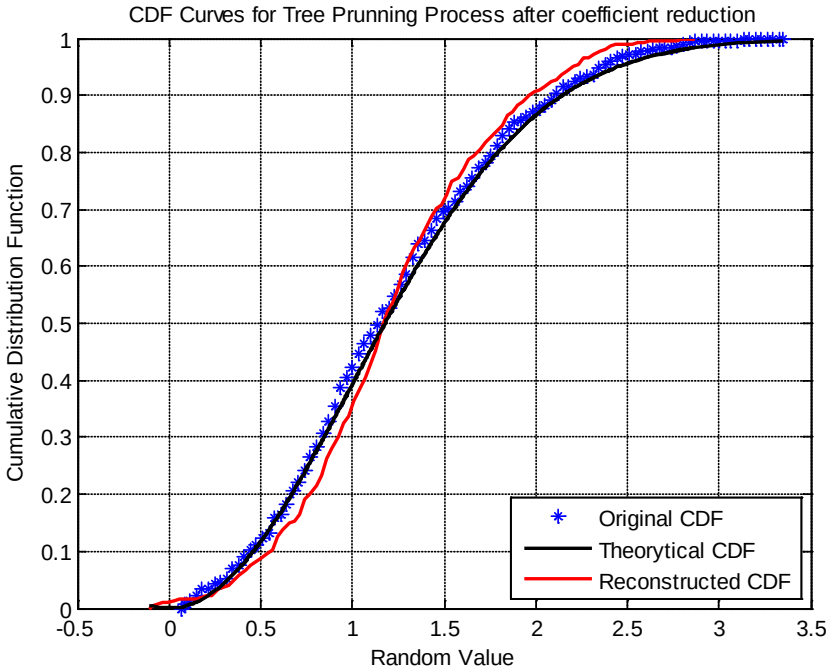

Figure 4.39 CDF for Rayleigh Distribution Data using Tree Pruning Method with removing several coefficients

Another way to analyze the property of the two proposed methods, we can consider same number of terminal nodes as a result of decomposition which are

yielded by both of methods. For tree pruning method, we apply daubechies10 as mother wavelet, 5 levels of decomposition and 75% of significant coefficients to be used for reconstructing the input. By this method, the number of branches which are used is 13. This method yield the value of MSE is 0.0992. To ensure the similar behavior which is depicted in Figure 4.38, we consider statistical data in term of cumulative distribution function (CDF) as shown in Figure 4.39. Although the CDF curve of original and reconstructed signal is slightly different, but the trend of curve is still reasonable to be considered as Rayleigh distribution.

After we know the performance of tree pruning method for such scenario, we then apply same scenario to coefficient reduction method. But in this scenario, we use 40% of significant coefficients instead of using 75% of significant coefficients which are used in tree pruning. This modification is done in order to use same number of significant coefficient to be reconstructed.

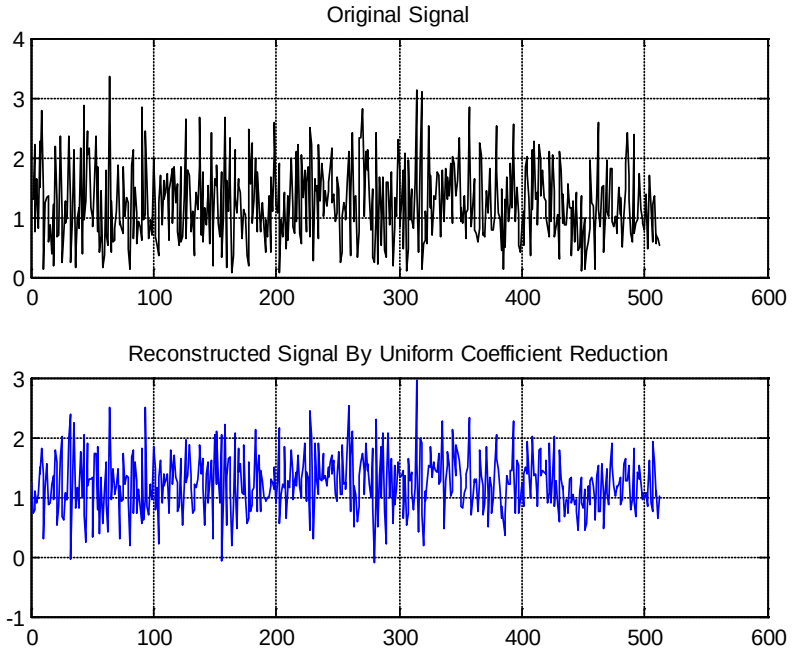

Figure 4.40 Comparison between original and reconstructed signal for Rayleigh Distribution Data Coefficients reduction compare to tree pruning method

This method resulting MSE of 0.1845 which is almost twice that of the previous method. We show the cumulative distribution function (CDF) in Figure 4.41. We can see from the figure that the CDFs of the original and reconstructed signal is more different if we compare to the same previous figure. This can be

understood that the different results is caused that the coefficient reduction loss more information regarding the component of original signal when remove a lot of coefficient.

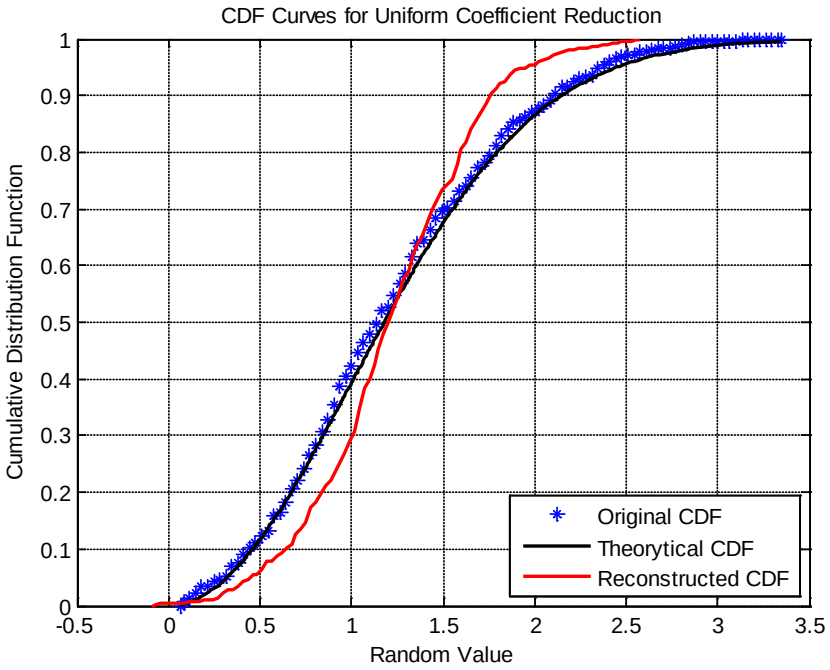

Figure 4.41 CDF for Rayleigh Distribution Data using Tree Pruning Method with removing several coefficients

4.5 Summary

In this chapter, the application of wavelet packet based algorithms for representing channels is described. The possibility of using wavelet packet transform for sparse representation of channels was studied. Preliminary results illustrating the efficacy of the WP approach were shown. To improve the performance of the proposed system two optimizations, namely, coefficient-reduction and tree-pruning were implemented. The proposed methods were compared and contrasted. It was shown that the tree-pruning algorithm performed better in accurate and sparse representation of channels. Furthermore, the impact of the number of levels of WP decomposition and the type of mother wavelet employed were also investigated. To gauge the system performance first and second order stochastic metrics such as MSE, LCR and correlation were employed. The results of the study demonstrated the efficacy of the proposed WP method in efficient representation of radio channels.

5

Wavelet Packet Based Algorithm for Representation of Time-Varying Wireless Channel

In the fourth chapter, the advantages of one-dimensional wavelet packet to represent wireless channel have been studied. The description in that chapter is focused on time-invariant wireless channel. Unfortunately, many signals encountered in real life are non-stationary, which are varying in time. In this chapter, the possibility of two-dimensional wavelet packet to represent time-varying wireless model is investigated and described.

We start with the description of time-varying wireless channel as well as two-dimensional wavelet packet, in section 5.1 and 5.2, respectively. In section 5.3, the discussion on how the properties of two-dimensional wavelet can be used for representation of time-varying wireless channel is presented. This implementation uses similar methods which are described in chapter 4, namely Coefficient-Reduction and Tree-Pruning algorithm based on entropy theory. The simulation setup of this implementation is elaborated in section 5.4. The performance of each those algorithms are analyzed in Section 5.5. Finally, section 5.6 summarizes the entire discussion on two-dimensional wavelet packet algorithm for efficient representation of time-varying wireless channel.

5.1 Time-Varying Wireless Channel

Before representing wireless channel model varying in time, an engineer has to have an adequate knowledge on the characteristic of time-varying wireless channel model. We may recall the basic knowledge of time-variant wireless channel model from chapter 2 to give an overview about it.

The nature of wireless channel is not stationary either in space or time. Many signals are encountered varying in time due to reasons such as [2],

1. The position of transmitter and/or receiver may be varied in space, time-by-time. For instance, in mobile wireless communication, the receiver is not standing in one position but also moving following the movement of user.
2. The motion of objects within propagation path between transmitter and receiver. For example, if one standing beside the road with heavy traffic, the motion of car on the road influences the propagation of signal to be received at receiver.

Such time-varying wireless channels are usually modeled using two-dimensional representation. One of these dimensions represents the time delay of signal due to the existence of multipath propagation and the other represents the variation of channel behavior during the observation time. In [4], Hashemi derived the impulse response for time-varying wireless channel, which can be represented as

$$h(t,\tau) = \sum_{n=0}^{N(\tau)-1} a_n(t)\,\delta\left[\tau - \tau(t)\right] e^{j\theta_n(t)}. \tag{5.1}$$

Variables $a_n(t)$ and $e^{j\theta_n(t)}$ represents the magnitude and phase of the contribution from scatterer n, and τ_i is its associated propagation time (delay). Delays can be interchanged with path lengths using $\tau_i = {}^{d_i}\!/_{c}$.

5.2 Two-Dimensional Wavelet Transforms

Many applications encountered not only in one dimension (e.g. data stream or signal) but also in two dimensions (e.g. Image). Wavelet Transform as a linear tool to analyze data has been widely used for such application. However, conventional wavelet transforms, which are derived in one-dimensional manner, are not quite

suitable to be applied for two-dimensional application. To cope with this circumstance, in [27], Meyer generalized the wavelet model to any dimension $n > 0$. This work was also used by Mallat in [24] for Multiresolution Signal Decomposition. More applications based on two-dimensional wavelet are reported in [55]-[59].

In wavelet transform, beside one-dimensional wavelet transform there is another kind of process called *two-dimensional wavelet transform*. Such transformation gives more flexibility but has more complexity in term of analysis. Basically, two-dimensional wavelet transform is similar to one-dimensional wavelet transform, but there is a minor modification in the decomposition process which leads to quaternary tree structure instead of binary tree structure. The example of this process, the quaternary tree structure and frequency plan for 2 levels decomposition are depicted in Figure 5.1 and Figure 5.2, respectively

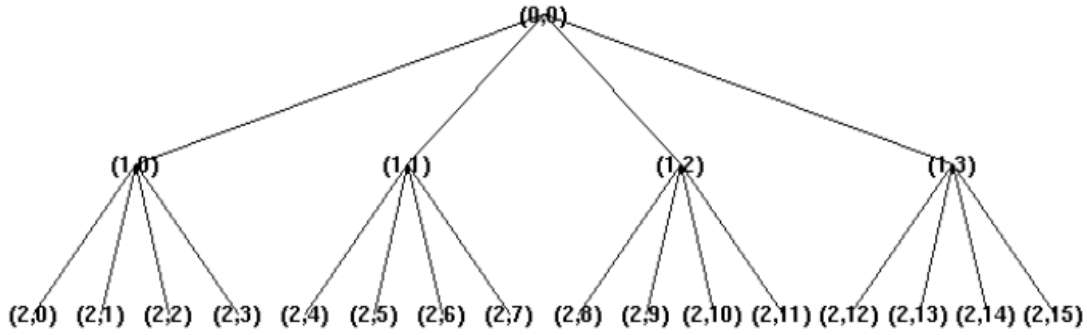

Figure 5.1 Quartenary tree structure of depth 2 [59]

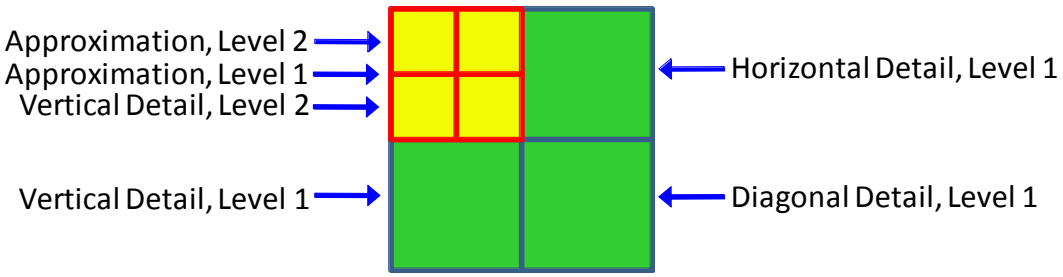

Figure 5.2 Frequency Plan of two-dimensional wavelet

Figure 5.1 shows that in every level of decomposition, each branch yields four child-branches, which is then called *two-dimensional wavelet coefficient*. These two-dimensional wavelet coefficients are obtained from multistage tree structure of two-dimensional filter banks [24]. Figure 5.3 shows one level of two-

dimensional filter banks for decomposition a two-dimensional input. Instead of decompose one side of input as in one-dimensional decomposition, two-dimensional decomposition is applied into two sides of two-dimensional input; rows and columns. In the first step, the rows of such input is convolved with one-dimensional filter banks to obtain low and high frequencies of row components which is then represented in two row-branches, and then each branch of rows representation are convolved again in columns side of input by using another one-dimensional filter banks to acquire low and high frequencies of column components. Each branch of rows representation results two branches of column representation. So that, at the end of this decomposition resulting four branches which then refer as wavelet coefficient. An example of this decomposition is shown in Figure 5.4. The two-dimensional input (Figure 5.4 (a)) is passed to the one level of two-dimensional wavelet decomposition in Figure 5.3. The result of such decomposition is depicted in Figure 5.4 (b). Each index in the frequency plan (Figure 5.4 (b)) refers to the coefficient indexes in Figure 5.3.

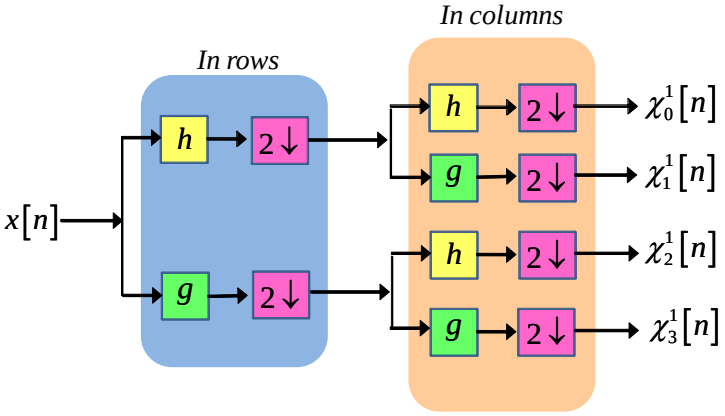

Figure 5.3 Decomposition Step in 1 Level of Decomposition

In order to obtain mathematical approach of the two-dimensional wavelet transform for either two-dimensional discrete wavelet transform (2D-DWT) or two-dimensional wavelet packet transform (2D-WPT), the one-dimensional (1D) version of each wavelet transform in chapter 3 has to be recalled.

Due to the two-dimensional input (e.g. image) can be modeled as finite energy function $f(x,y) \in L^2(\mathbb{R}^2)$ [57], [24], an obvious way to get two-dimensional wavelet transform from one-dimensional is to use separable wavelets [57] which are

obtain from scaling function $\phi(x)$ and its associated wavelet $\psi(x)$ in one-dimensional. These functions are modified that satisfies to the orthonormal basis of $L^2(\mathbb{R}^2)$. The two-dimensional scaling and its associated wavelet function are given as follow [24]

$$\begin{aligned} \Phi(x,y) &= \phi(x)\phi(y), & \Psi_1(x,y) &= \phi(x)\psi(y), \\ \Psi_2(x,y) &= \psi(x)\phi(y), & \Psi_3(x,y) &= \psi(x)\psi(y). \end{aligned} \tag{5.2}$$

The function of Φ and Ψ_i are orthogonal to each other with respect to integer shifts. The function Φ is a separable two-dimensional scaling function, and the set of wavelet Ψ_i such that $\left\{2^{-j}\Psi_i\left(2^{-j}x-k, 2^{-j}y-l\right)\right\}$ is an orthonormal basis of $L^2(\mathbb{R}^2)$, where $i=1,2,3$ and $(j,k,l)\in\mathbb{Z}^3$.

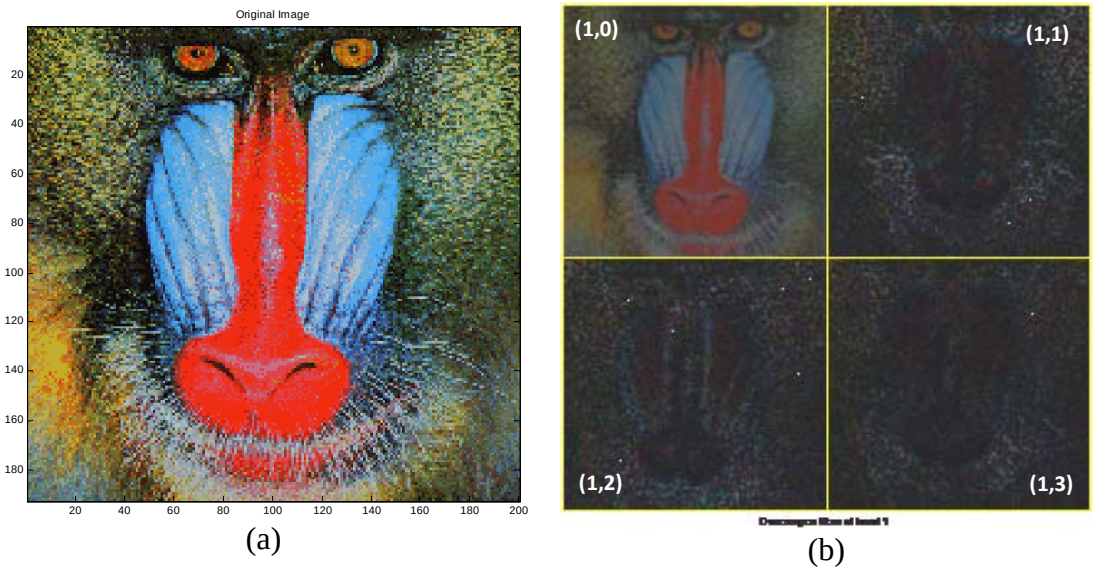

(a) (b)

Figure 5.4 Frequency Plan (b) at one Level of Decomposition of input in (a)

For the case of 2D-DWT, the approximation $A^j f$ and details $D_i^j f$ of the signal $f(x,y)$ at resolution 2^{-2j} is characterized by the set of inner products as follow

$$A^j f = \left(\left\langle f(x,y), 2^{-j}\Phi\left(2^{-j}x-k, 2^{-j}y-l\right)\right\rangle\right)_{(k,l)\in\mathbb{Z}^2} \tag{5.3}$$

$$D_i^j f = \left(\left\langle f(x,y), 2^{-j}\Psi_i\left(2^{-j}x-k, 2^{-j}y-l\right)\right\rangle\right)_{(k,l)\in\mathbb{Z}^2, i=1,2,3} \tag{5.4}$$

An example of two-level tree structure for 2D-DWT in term of two-dimensional filter banks and its frequency plan are depicted in Figure 5.5 and Figure 5.6, respectively.

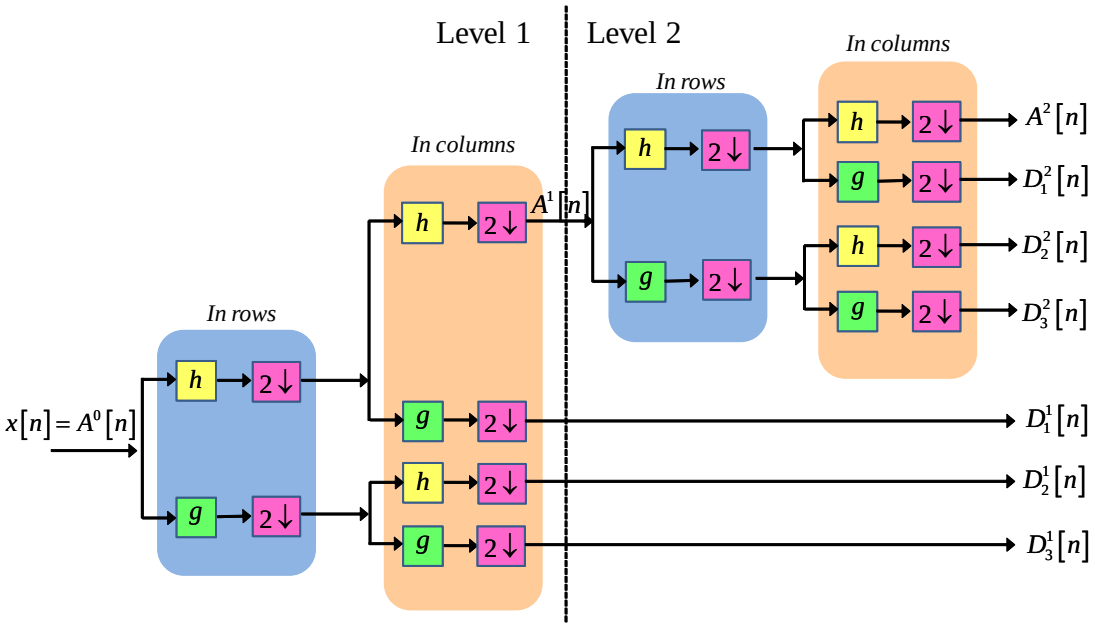

Figure 5.5 Two Level of Filter Banks for 2D-DWT

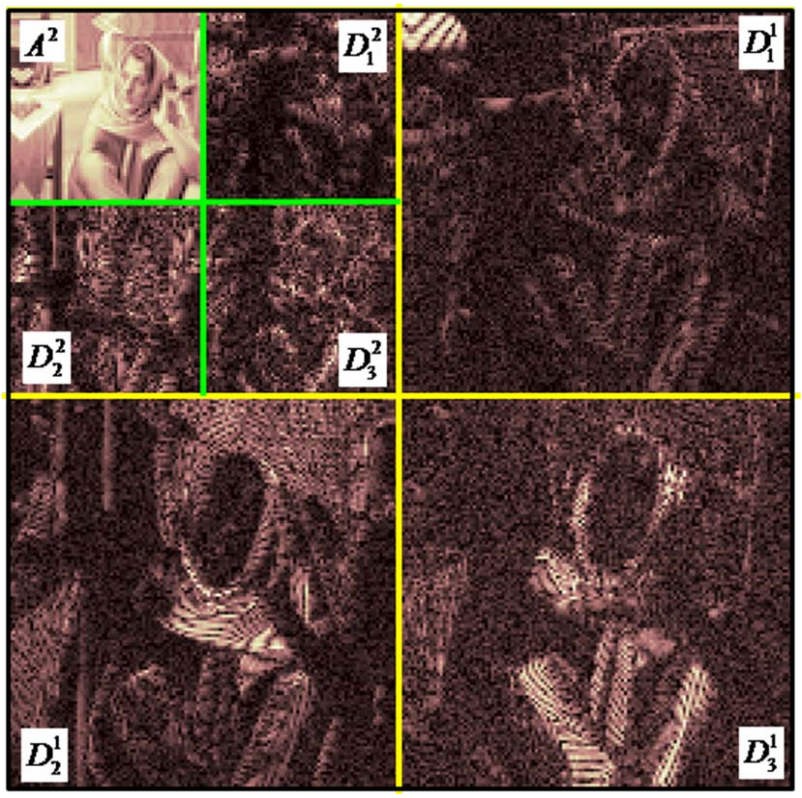

Figure 5.6 Frequency plan of two levels 2D-DWT

For the purpose of representing an input using wavelet packet transform, we must extend two-dimensional discrete wavelet transform to two-dimensional wavelet packet transform. The extension of two-dimensional wavelet packet transform is derived from one-dimensional wavelet packet transform. Considering the wavelet packet basis $(\xi_m)_{m\in\mathrm{N}}$ which can be generated from a given function ξ_0 according to

$$\xi_{2m}(x) = \sqrt{2}\sum_n h[n]\xi_m(2x-n)$$
$$\xi_{2m+1}(x) = \sqrt{2}\sum_n g[n]\xi_m(2x-n)$$

Where the function ξ_0 can be identified with the scaling function ϕ and ξ_1 with the mother wavelet ψ. Then, the WP bases can be defined to be the collection of orthonormal bases of $L^2(\mathbb{R}^2)$ composed of functions of the form $\xi_{j,k,m}(x) = 2^{-j/2}\xi_m(2^{-j}x-k)$ with $j,k,m\in\mathbb{Z}^2\times\mathrm{N}$. Each element of the bases is determined by a subset of the indexes *j*, *k* and *m* (for instance, a conventional wavelet basis corresponds to the collection of indexes $(j,k,1),(j,k)\in\mathbb{Z}^2$). The set $(\xi_{j,k,m}(x))_{k\in\mathbb{Z}}$ is an orthonormal basis of a subspace $V_{j,m}$ of $L^2(\mathbb{R})$ such that $V_{j,2m+1}$ is the orthogonal complement of $V_{j,2m}$ in $V_{j-1,m}$, where $V_{j,0}$ can be identified with closed subspace V_j and $V_{j,1}$ with W_j.

By analogy with (5.2), one can construct the set of functions as follow [57]

$$(\chi_{m,n}(x,y) = \xi_m(x)\xi_n(y))_{(m,n)\in\mathrm{N}^2} \tag{5.5}$$

Where $\chi_{0,0} = \Phi$, $\chi_{0,1} = \Psi_1$, $\chi_{1,0} = \Psi_2$ and $\chi_{1,1} = \Psi_3$ stand as particular cases. A two-dimensional wavelet packet basis is then composed of function of the form

$$\chi_{j,k,l,m,n}(x,y) = 2^{-j}\chi_{m,n}(2^{-j}x-k, 2^{-j}y-l) \tag{5.6}$$

Where the collection of indexes $(j,k,l,m,n)\in\mathbb{Z}^3\times\mathrm{N}^2$ is such that the intervals $[2^{-j}m, 2^{-j}(m+1))\times[2^{-j}n, 2^{-j}(n+1))$ form a disjoint cover of $[0,+\infty)\times[0,+\infty)$ and k,l range over all the integers. Hence, any triplet $(j,m,n),(m,n)\neq(0,0)$ thus defined gives rise to a detail image

$$D^j_{m,n} f = (\langle f(x,y), 2^{-j}\chi_{j,k,l,m,n}(x,y)\rangle)_{(k,l)\in\mathbb{Z}^2} \tag{5.7}$$

An example of two-level tree structure for 2D-WPT in term of two-dimensional filter banks and its frequency plan are depicted in Figure 5.7 and Figure 5.8, respectively.

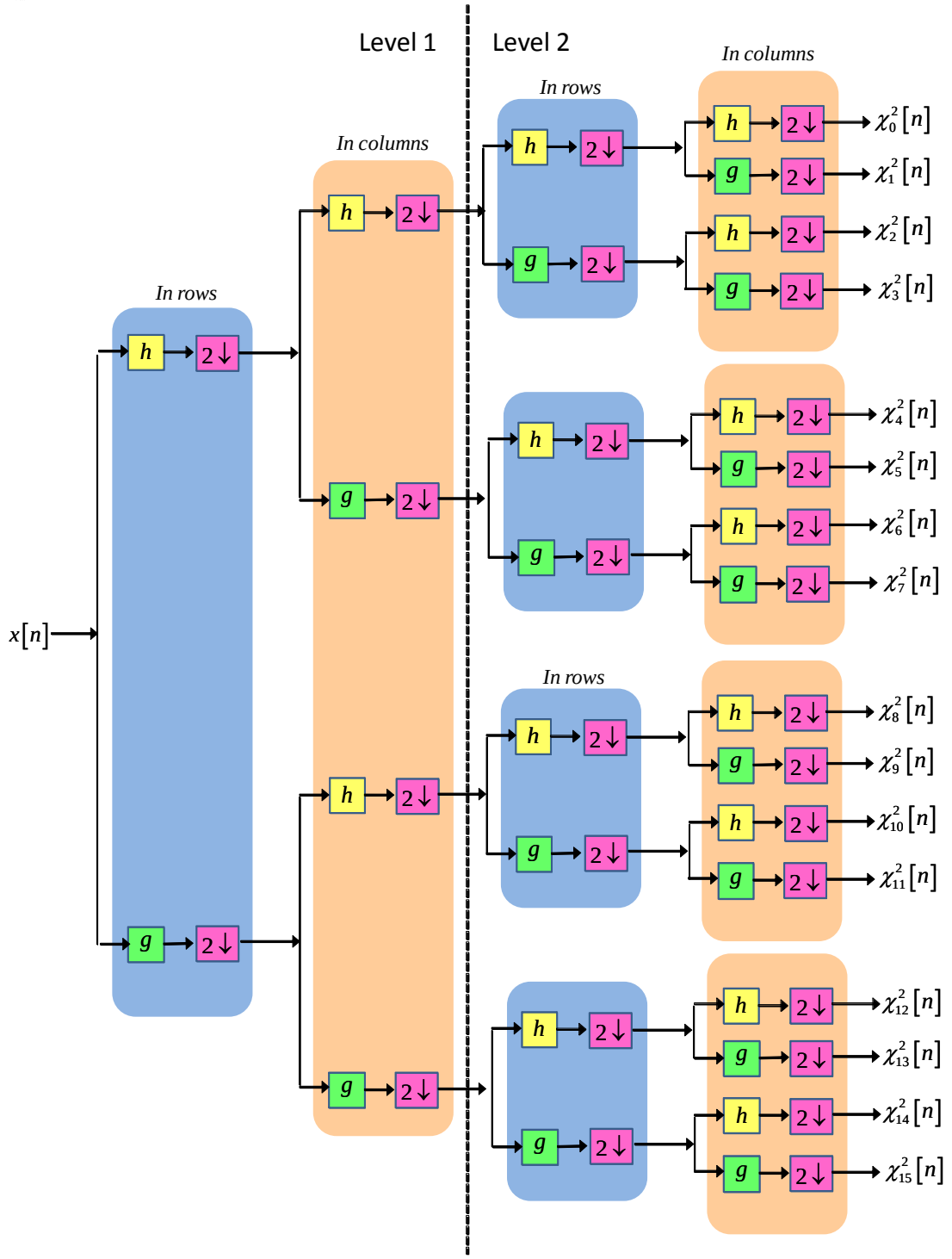

Figure 5.7 2-Levels Two Dimensional Wavelet Packet Tree Structure

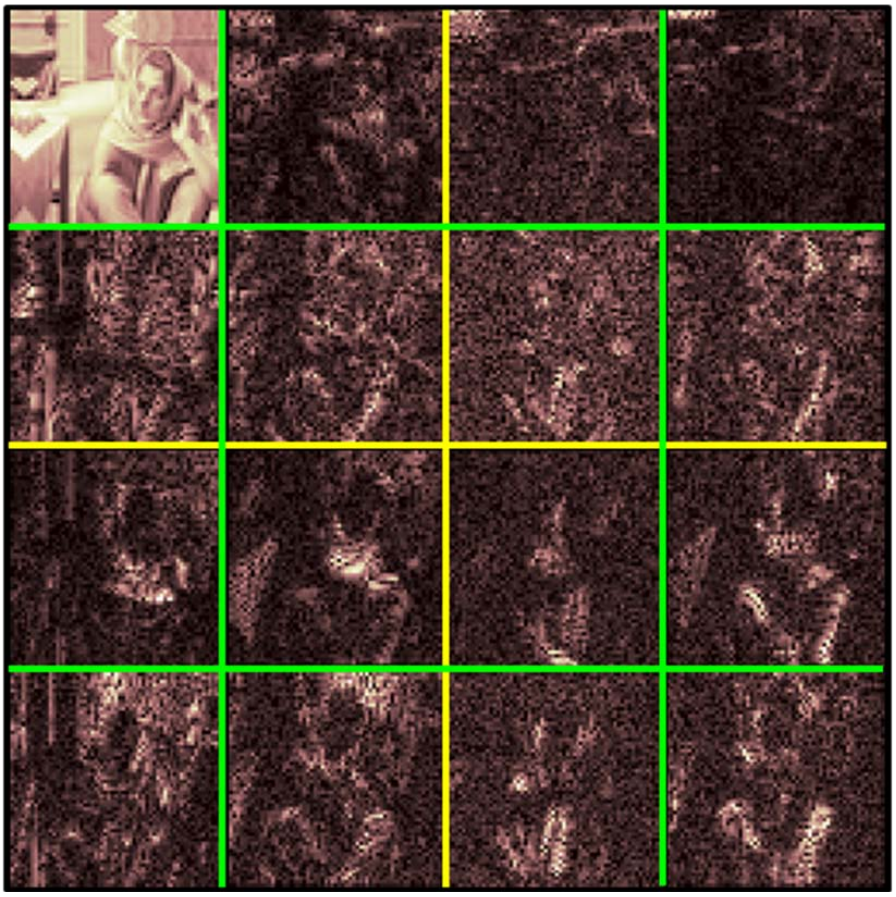

Figure 5.8 Frequency plan of two levels 2D-WPT

5.3 Two-Dimensional Wavelet Packet Based Wireless Channel Representation

In section 4.2, the representation of time-invariant wireless channel based on wavelet packet algorithm has been successfully implemented. In this section, the algorithm will be extended to the two-dimensional form in such a way that the algorithm is able to represent time-varying wireless channel efficiently. Such algorithm is then called *two-dimensional wavelet packet algorithm* which is developed based on two-dimensional wavelet packet transform (2D-WPT).

Due to the fact that the 2D-WPT is widely used in image representation, hence the representation of time-varying wireless channel based on wavelet packet algorithm can be treated as image representation. Analogous to an image, time-varying wireless channel representation $h(t,\tau)$ usually has two dimensions; τ in x-

axes which represent the time delay of each received radio propagation and t in y-axes which represents the time observation of channel behavior.

As with the representation of time-invariant wireless channel, the idea behind the proposed system is to represent an unknown time-varying wireless channel in term of a set of known two-dimensional wavelet packet (2D-WP) bases. Once such channel is mapped onto 2D-WP bases, only those bases which contain significant information are retained. The proposed system is then evaluated using performance metrics, such as correlation and level crossing rate, which have hitherto not been considered in the literature.

The proposed system primarily performs three major tasks, namely, 2D-WP decomposition, selection of best 2D-WP representation and 2D-WP reconstruction. 2D-WP Decomposition and 2D-WP reconstruction are implemented using two-dimensional filter banks which has been described in the section 5.2. The methods of selecting the best 2D-WP representation are similar to the methods which are used for selecting the best one-dimensional WP representation. The details of these methods are described in section 4.2 –

a) *Coefficient-reduction*, where the channel is uniformly decomposed using WP transform and the best components are selected based on their entropy values,
b) *Tree-pruning*, where an arbitrary decomposition of the input is conducted to arrive at the WP tree structure with lowest entropy [33].

The complete procedure for the two-dimensional wavelet packet based wireless channel representation is described in Algorithm 2.

Algorithm 2: Wavelet Packet algorithm for signal representation.

1. Choose type of channel to be represented, such as
   a. Rayleigh Distribution Data
   b. Sine function
2. Wavelet Packet Algorithm Setup
   a. Set Type of Wavelet Filter
   b. Set Levels of Decomposition
3. Calculating entropy value of each wavelet packet branches
4. Set number of wavelet packet coefficient which will be reduced
5. Choose number of the lowest branches which will be eliminated proportionally to point 4.
6. Set eliminated branches to zero

7. Reconstruct the rest of wavelet packet coefficient to be considered as reconstructed signal for the representation.
8. Comparing the reconstructed signal to the original signal.

5.4 Simulation Setup

To evaluate the ability of the proposed two-dimensional wavelet packet based algorithm for representation of time-varying wireless channel, different kind of inputs are chosen-

1. Image, this input is used in order to obtain a fundamental insight on two-dimensional wavelet packet for processing data.
2. Rayleigh Distribution, this input is used as a further input to represent channel model varying in time.
3. Sine Function, this input is used to exploit and analyze the advantages of time-frequency localization for time-varying channel representation.

To evaluate the ability of the proposed wavelet packet algorithms to accurately represent channels stochastic metrics such as Normalize Mean Square Error, Level Crossing Rate and correlation value are employed. Each of those parameters can be defined as follow

(a) Mean Square Error (MSE)

MSE is a second order of error, which quantifies the difference between values implied by an estimator and the true values of the quantity being estimated [52]. The equation of MSE in term of two-dimensional representation is given as [60]

$$MSE_{2D} = E\left[\left|y(m,n) - \hat{y}(m,n)\right|^2\right] \tag{5.8}$$

where y and $\hat{y}$ are the function of original and reconstructed signal, respectively. For comparing all of performance in this simulation with equal standard, all of MSE values are normalized to the maximum one, which then called *Normalized Mean Square Error (NMSE).*

(b) Correlation

Correlation ratio is a measure of the relationship between two sets of data. This parameter is referred to first statistical moment to quantify the

dependence of a data to another [53]. In term of two dimensional data, correlation can be defined as follow

$$r = \frac{\sum_m \sum_n \left(y_{mn} - \bar{y}\right)\left(\hat{y}_{mn} - \bar{\hat{y}}\right)}{\sqrt{\left(\sum_m \sum_n \left(y_{mn} - \bar{y}\right)^2\right)\left(\sum_m \sum_n \left(\hat{y}_{mn} - \bar{\hat{y}}\right)^2\right)}} \tag{5.9}$$

where $\bar{y}$ and $\bar{\hat{y}}$ are the mean value of two-dimensional original and reconstructed signal, respectively. For comparing all of performance in this simulation with equal standard, all of correlation values are normalized to the maximum one.

Some of scenarios will be used to measure all of performance parameters above with all of the possible number of coefficient reduction. Such scenarios are,

(a) Different level characteristic for constant wavelet filter

(b) Different wavelet filter characteristic for constant decomposition.

5.5 Numerical results

5.5.1 Coefficients Reduction Algorithm

In this subsection, the results of channel representation based on wavelet packet with coefficient reduction technique will be described. The explanation are classified based on the type of input and scenarios in each type.

5.5.1.1 Image

In order to obtain an insight in channel model representation, we first apply an image to two-dimensional wavelet packet. An image can be modeled as finite energy function $f(x,y)$, channel models which have function $h(\tau,t)$ can then be intrepreted has similar behavior to an image. The image which is used for this process is shown in Figure 5.9. The dimension of this image is 256x256. In practical, we must define the level of decomposition, mother of wavelet, and the number of coefficient which are retained. Consequently, we must know the effect of these system parameters to the performance of signal reconstruction.

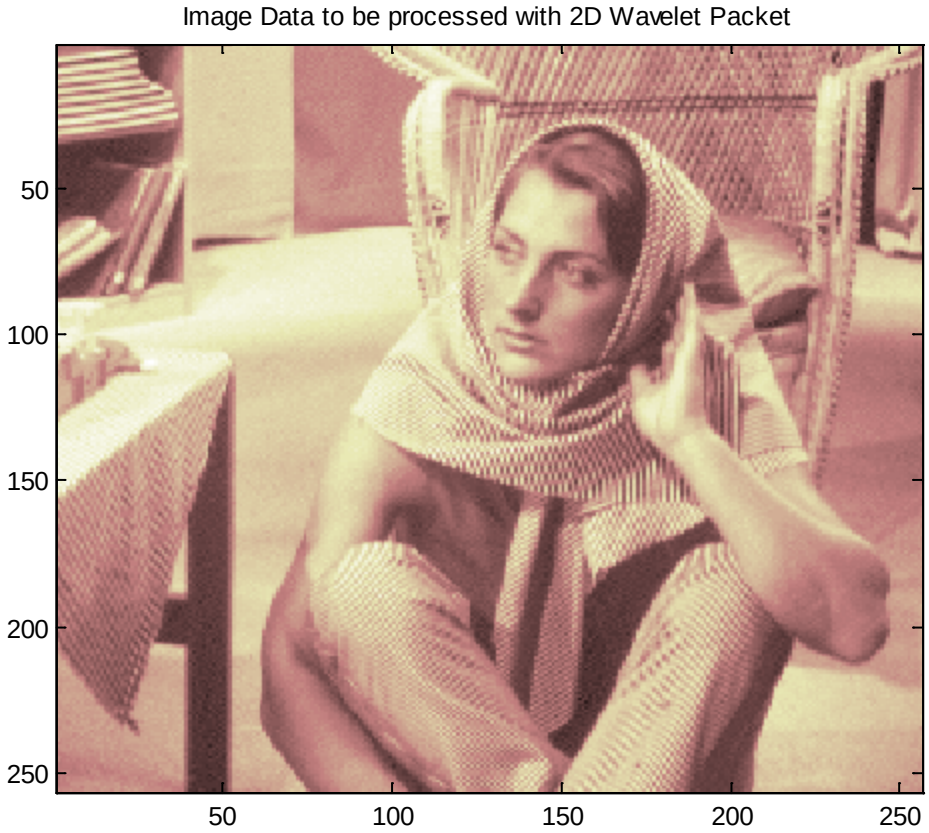

Figure 5.9 An image input for 2D Wavelet Packet Based Algorithm

A. Level of Decomposition

In order to know the effect of decomposition level to the performance, various level of decomposition is simulated with constant mother wavelet of Daubechies10, compared to different number of coefficients which are used to be reconstructed. The reason of choosing Daubechies10 as a mother wavelet is that Daubechies10 has a support of minimum size for a given vanishing moment [40]. The results of these scenarios are depicted in Figure 5.10 and Figure 5.11 for NMSE and correlation evaluation parameter, respectively.

From both figures, we can understand immediately that there are slightly differences of the reconstructed signal performance. To assists us understanding the differences, we can refer to Figure 5.12. The numerical representative of some such values are shown in Table 5.1 and Table 5.2, respectively, for NMSE and correlation. A significant difference can be observed from the curve of 2 level of decomposition.

This can be occurred caused by limited number 2D-WP Bases in such a way if some bases are removed, many information are lost.

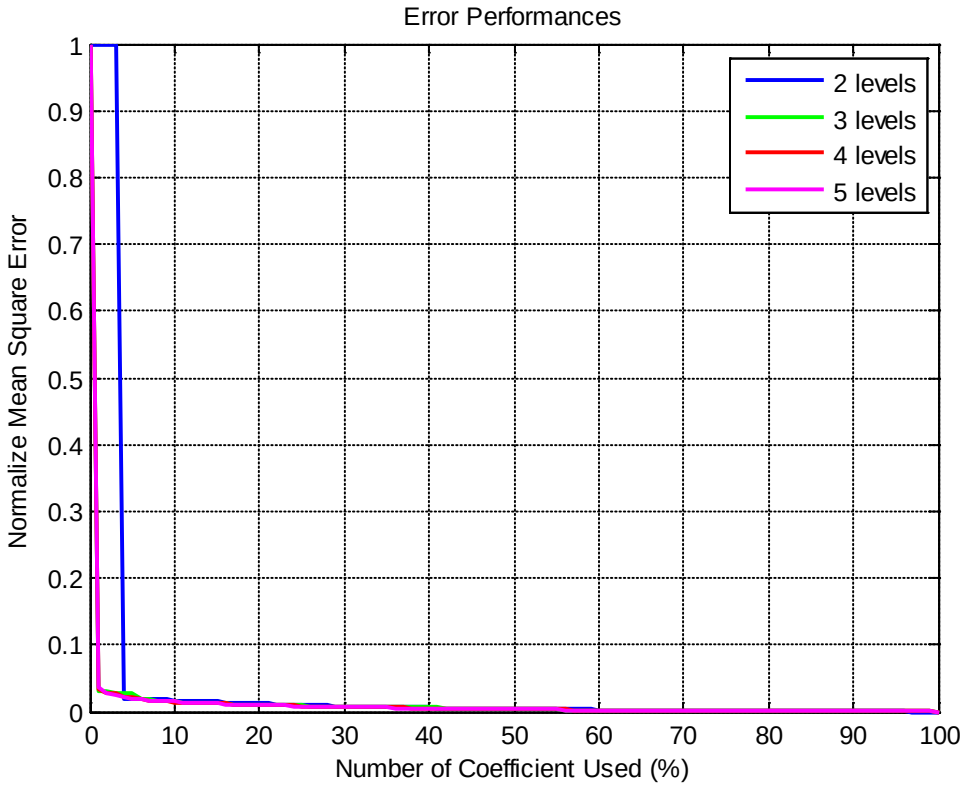

Figure 5.10 Normalize Mean Square Error (NMSE) for Image data with different level of decomposition on 2D Wavelet Packet Algorithm

Table 5.1 Representative of some values of NMSE for Image data with different level of decomposition on 2D Wavelet Packet Algorithm

Level	0%	1%	2%	3%	4%	5%	6%
2	1	1	1	1	0.017785	0.017785	0.017785
3	1	0.031476	0.031476	0.027698	0.026505	0.026505	0.018057
4	1	0.03443	0.027809	0.026663	0.023285	0.020702	0.018527
5	1	0.036964	0.027498	0.024349	0.020946	0.019523	0.018206

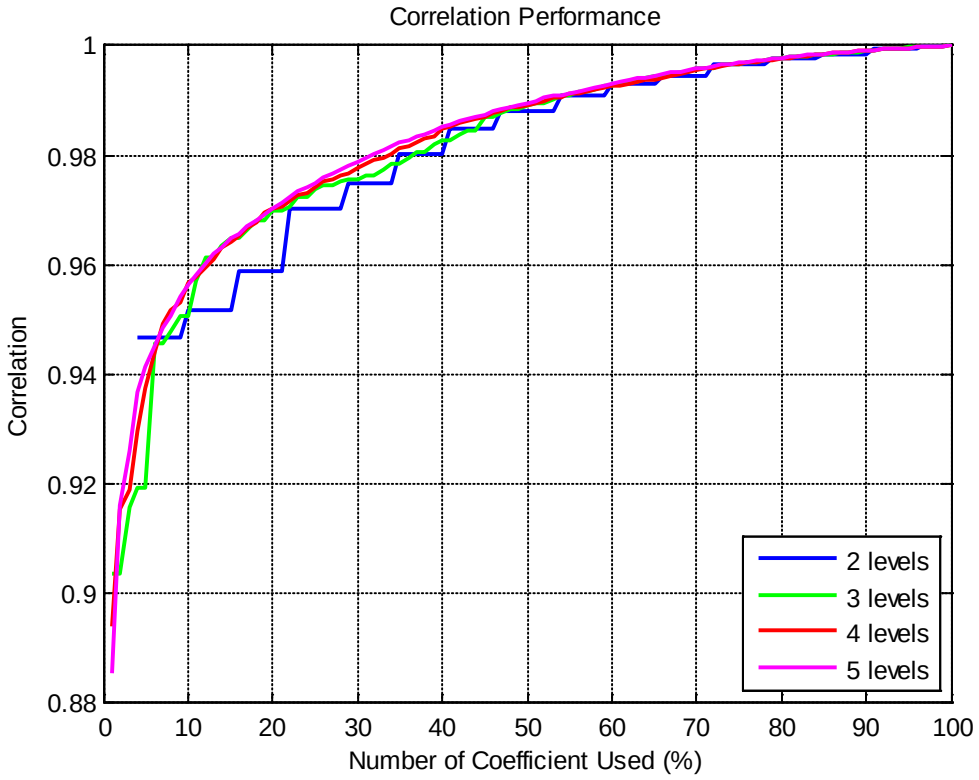

Figure 5.11 Correlation for Image data with different level of decomposition on 2D Wavelet Packet Algorithm.

Table 5.2 Representative of some values of Correlation for Image data with different level of decomposition on 2D Wavelet Packet Algorithm

Level	4%	10%	20%	30%	40%	50%
2	0.95	0.951847	0.958889	0.974868	0.980379	0.988041
3	0.92	0.950567	0.969918	0.97571	0.982776	0.989278
4	0.93	0.956599	0.970179	0.977664	0.985043	0.989303
5	0.94	0.956217	0.970377	0.978658	0.985077	0.989552

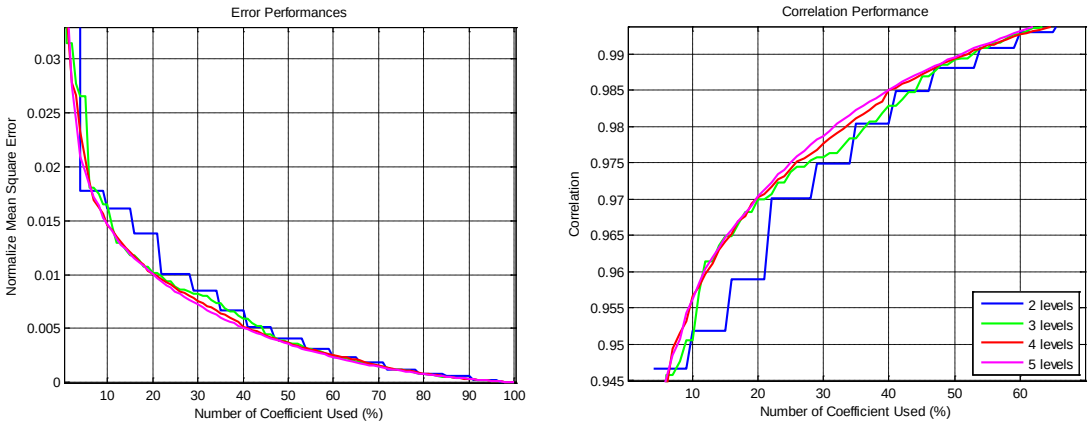

(a) (b)

Figure 5.12 Zoom version of (a) NMSE and (b) correlation for Image data with different level of decomposition on 2D Wavelet Packet Algorithm

B. Wavelet Filter

Moreover, in order to have adequate knowledge to ensure the best signal reconstruction, we also have to analyze the behavior of the reconstructed signal for different type of wavelet and different length of filter. This scenario is simulated by using constant decomposition level of 4. The reason of choosing 4 as level of decomposition is that, refer to Figure 5.10 and Figure 5.11, 4 levels of decomposition gives better result than others in term of NMSE and correlation. If consider the zoom version of these version in Figure 5.12, we see that there is another value of decomposition level which has similar performance, namely 5. However, compared to the 4 levels, 5 levels of decomposition has more complexity in term of whole process, especially for bases selection algorithm.

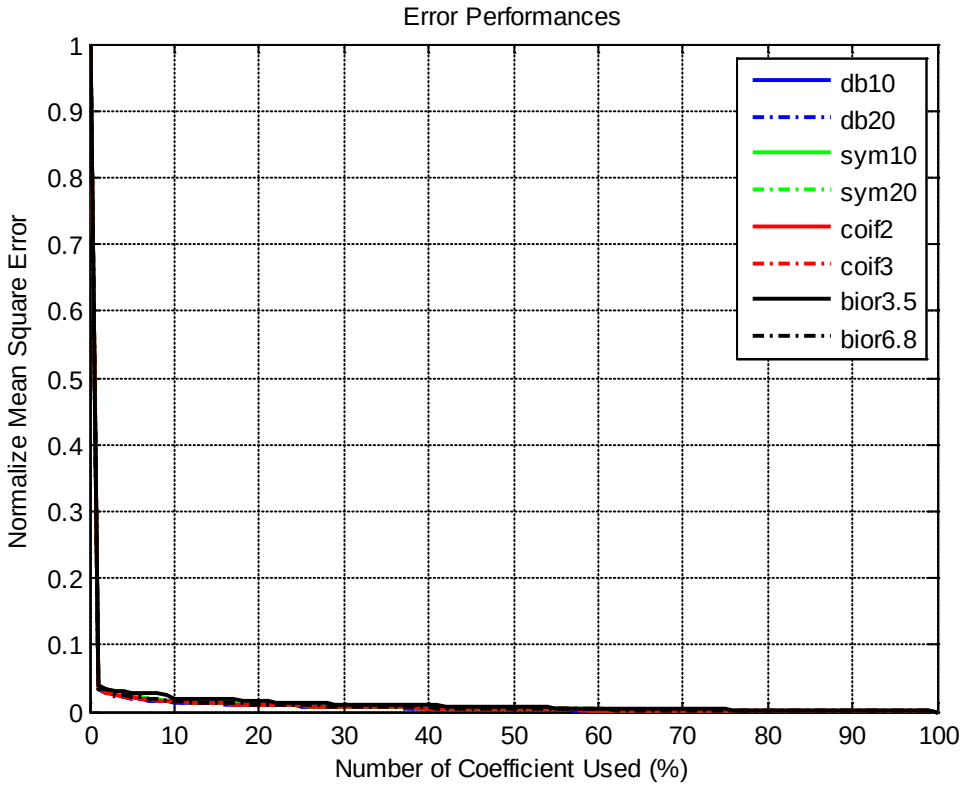

Figure 5.13 Normalize Mean Square Error (NMSE) for Image data with different mother of wavelet on 2D Wavelet Packet Algorithm

Generally, the results for different type of wavelets and filters length are quite similar as depicted in Figure 5.13 and Figure 5.14, respectively, for NMSE and correlation value. The zoom version of these figures which are shown in Figure 5.15 give more impression about the similarity of these results. The numerical representative of some such values are shown in Table 5.3 and Table 5.5,

respectively, for NMSE and correlation. The performance differences between each mother of wavelet are around 0.7%, a small value which can be neglected.

Table 5.3 Representative of some values of NMSE for Image data with different level of decomposition on 2D Wavelet Packet Algorithm

Wavelet	48%	49%	50%	51%	52%
Daubhecies10	0.00388	0.003796	0.003647	0.003521	0.003413
Daubhecies20	0.003859	0.003768	0.003653	0.003496	0.003431
Symlett10	0.004492	0.004192	0.004046	0.003923	0.003816
Symlett20	0.00481	0.004712	0.004552	0.00433	0.004229
Coiflet2	0.004341	0.004093	0.003941	0.003812	0.003719
Coiflet3	0.004257	0.004146	0.003931	0.003784	0.003659
Bi-orthogonal3.5	0.007203	0.007088	0.006885	0.0065	0.006407
Bi-orthogonal6.8	0.004642	0.004528	0.004338	0.004151	0.004059

Nevertheless, if we consider Figure 5.14, there is a difference of channel behavior when Bi-orthogonal 3.5 and 6.8 are applied as mother wavelet in the decomposition process. These differences are due to the different lengths of filter to the two initial type of wavelet (see Table 5.4)

However, the differences are also seen when wavelet mothers of coiflets are applied and compared to others. For example, if we consider coiflet2 which has filter length of 12, the accuracy of reconstruction is quite similar to the two initial wavelet mothers but different with bi-orthogonal 6.8 which also has same length of filter. These descriptions can be also supported by considering Figure 5.14.

Table 5.4 Filter length of certain wavelet filter

Wavelet Type	**Filter Length**
Daubechis 10	20
Daubechis 20	40
Symlet 10	20
Symlet 20	40
Coiflet 2	12
Coiflet 3	18
Bi-ortoghonal 3.5	12
Bi-orthogonal 6.8	18

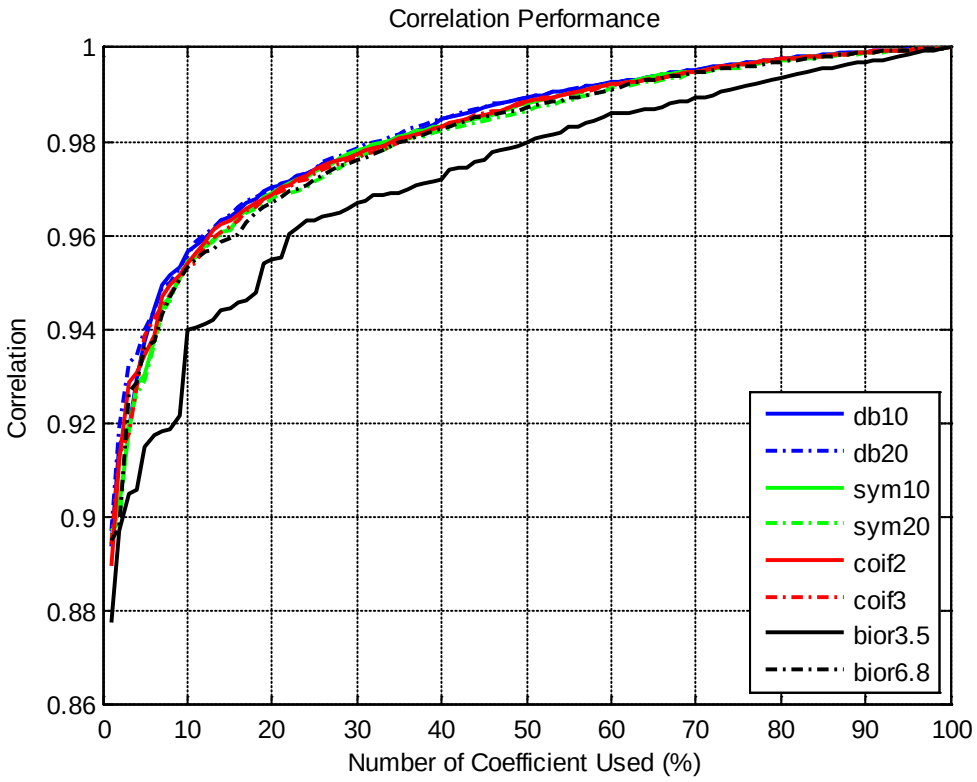

Figure 5.14 Correlation for Image data with different mother of wavelet on 2D Wavelet Packet Algorithm

Table 5.5 Representative of some values of Correlation for Image data with different mother of wavele on 2D Wavelet Packet Algorithm

Wavelet	48	49	50	51	52
Daubhecies10	0.988615	0.988864	0.989303	0.989673	0.989991
Daubhecies20	0.988677	0.988947	0.989285	0.989748	0.989938
Symlett10	0.986808	0.987694	0.988124	0.988489	0.988804
Symlett20	0.985868	0.986156	0.986629	0.987285	0.987585
Coiflet2	0.987254	0.987987	0.988435	0.988815	0.98909
Coiflet3	0.987503	0.98783	0.988465	0.988898	0.989266
Bi-orthogonal3.5	0.978762	0.979104	0.979707	0.980855	0.981131
Bi-orthogonal6.8	0.986364	0.9867	0.987264	0.987814	0.988087

5.5.1.2Rayleigh Distribution

The behavior of nature cannot be predicted by anyone and is usually assumed as random behavior. Hence, this condition implies to the model of channel which is also has to be assumed as a random process. Due to the random process in such channel, the model of channel is usually represented statistically. One of that randomness is amplitude of channel which is represented using Rayleigh

Distribution. And because of the nature of channel is changing in time, that distribution is also represented in time-variant as shown in Figure 5.16**.** This input is generated randomly both in $x-$axes and $y-$axes, based on Rayleigh distribution with length of 256 at both of side. For this type of input, the similar scenarios in the previous subsection will be used, and analyze the behavior of the results afterwards.

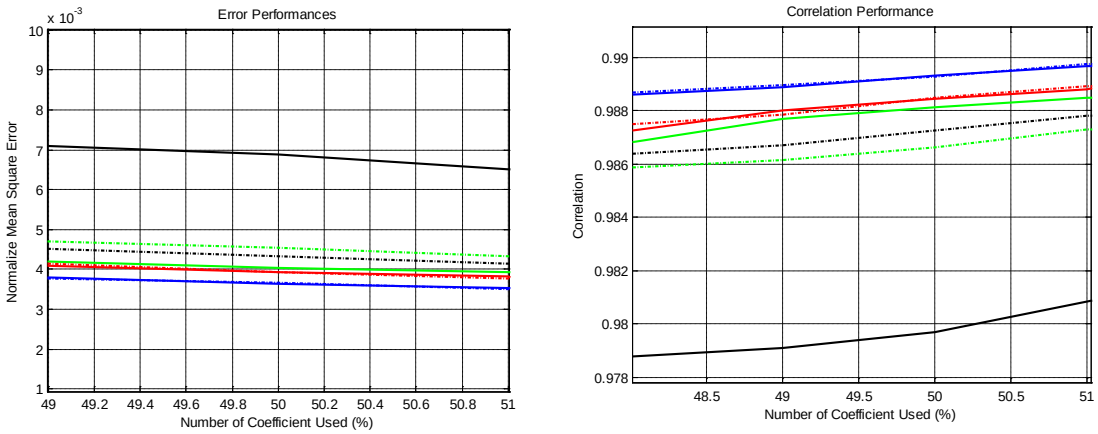

(a) (b)

Figure 5.15 Zoom version of (a) NMSE and (b) correlation for Image data with different mother wavelet on 2D Wavelet Packet Algorithm

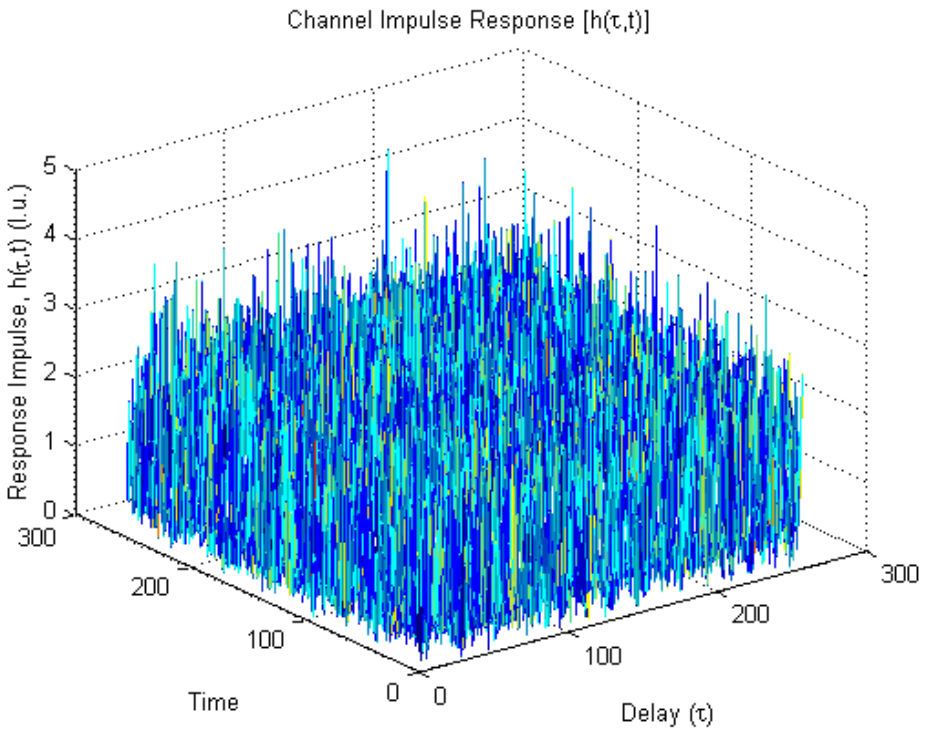

Figure 5.16 Rayleigh Distribution as an input 2D Wavelet Packet Based Algorithm

A. Level of Decomposition

In this part, the effect of decomposition level to the performance of signal reconstruction are observed over various number of coefficients which are used to be reconstructed, with the mother of wavelet is keep constant, i.e. Daubechies10. The results of these scenarios are depicted in Figure 5.17 and Figure 5.18 for NMSE and correlation evaluation parameter, respectively. The numerical representative of some such values are shown in Table 5.6 and Table 5.7, respectively, for NMSE and correlation. From these figures and tables, we can see that there is no significant difference between various levels of decomposition over various numbers of coefficients which are used to be reconstructed. The differences in term of NMSE and correlation are around 0.22% and 1.3%, respectively. From Figure 5.18, we can see that the trend is similar to Figure 5.11 where the performance is better as big as the level of decomposition.

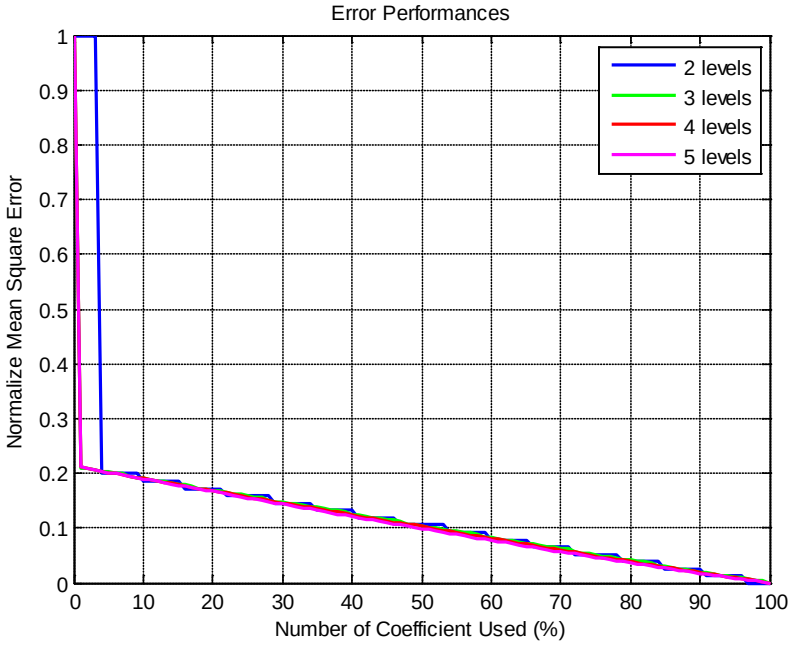

Figure 5.17 Normalize Mean Square Error (NMSE) for Raykeigh Distribution data with different level of decomposition on 2D Wavelet Packet Algorithm

Table 5.6 Representative of some values NMSE for Raykeigh Distribution data with different level of decomposition on 2D Wavelet Packet Algorithm

Level	48%	49%	50%	51%	52%	53%	54%
2	0.004074	0.004074	0.004074	0.004074	0.004074	0.004074	0.003127
3	0.003911	0.003911	0.003655	0.003624	0.003624	0.003362	0.003147
4	0.00388	0.003796	0.003647	0.003521	0.003413	0.003228	0.003163
5	0.003855	0.003693	0.003562	0.003415	0.003274	0.003139	0.003038

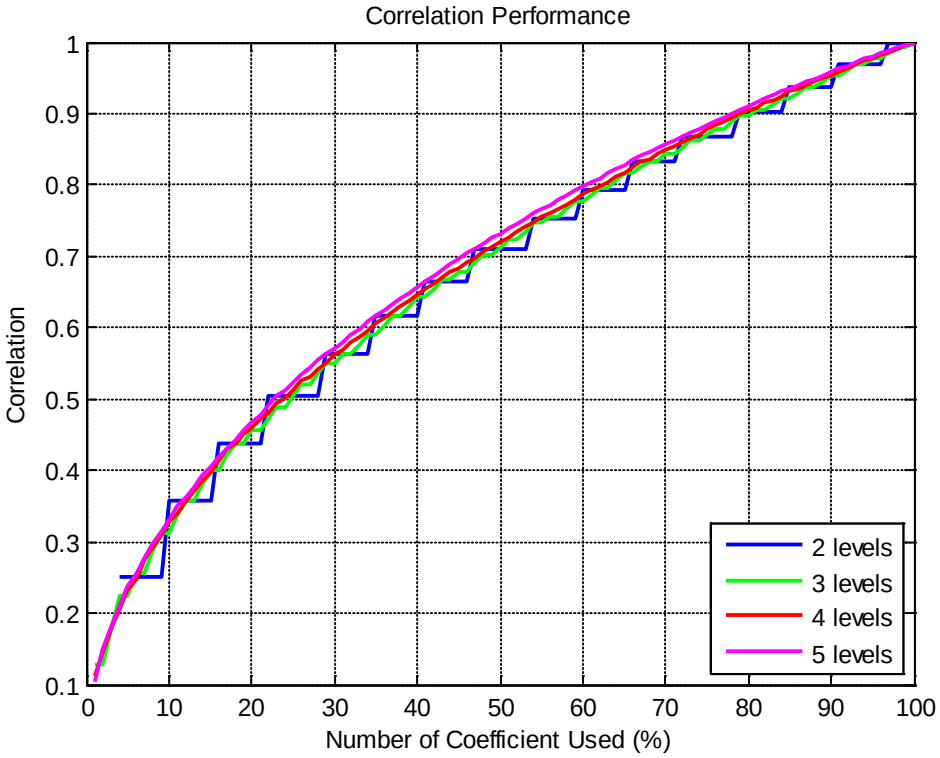

Figure 5.18 Correlaytion for Rayleigh Distribution Data with different level of decomposition on 2D Wavelet Packet Algorithm

Table 5.7 Representative of some values Correlation for Raykeigh Distribution data with different level of decomposition on 2D Wavelet Packet Algorithm

Level	48%	49%	50%	51%	52%	53%	54%
2	0.710266168	0.710266	0.710266	0.710266	0.710266	0.710266	0.7535
3	0.702374247	0.702374	0.713642	0.724771	0.724771	0.735581	0.746303
4	0.706285485	0.711633	0.719843	0.727552	0.73311	0.741419	0.746448
5	0.718519332	0.725391	0.732339	0.739417	0.746264	0.75381	0.759946

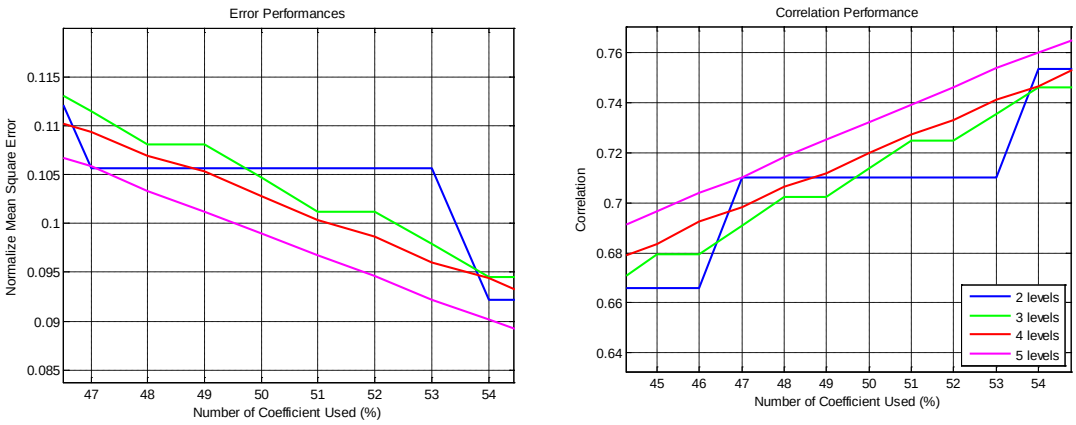

(a) (b)

Figure 5.19 Zoom version of (a) NMSE and (b) correlation for rayelgih distribution data with different level of decomposition on 2D Wavelet Packet Algorithm

B. Wavelet Filter

Furthermore, in this part, the effect of various mother of wavelet and its length to the performance of signal reconstruction are observed over various number of coefficients which are used to be reconstructed, with the level of decomposition is keep constant at 4 levels. The reason of choosing 4 as level of decomposition is that (refer to Figure 5.17 and Figure 5.18) 4 levels of decomposition gives better result than others in term of NMSE and correlation. If we consider the zoomed version of these version in Figure 5.19, we can see that there is another value of decomposition level which has similar performance, namely 5. However, compared to the 4 levels, 5 levels of decomposition has more complexity in term of whole process, especially for bases selection algorithm.

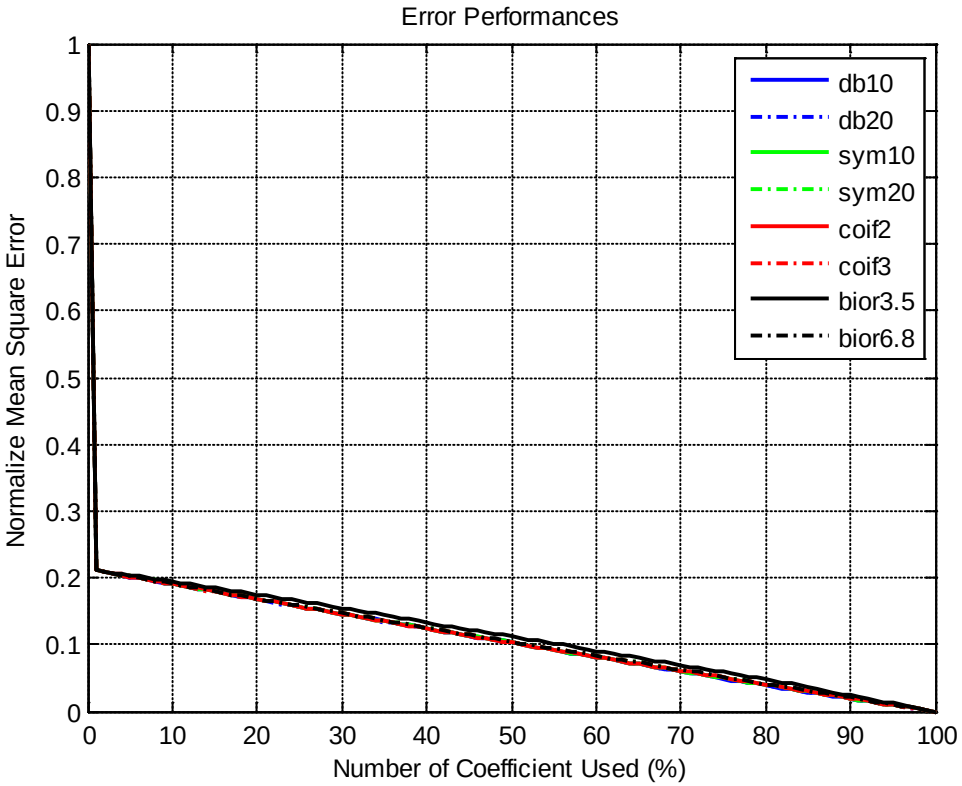

Figure 5.20 Normalize Mean Square Error (NMSE) for Rayleigh Distribution Data with different mother of wavelet on 2D Wavelet Packet Algorithm

Generally, the results for different type of wavelets and filters length are quite similar as depicted in Figure 5.20 and Figure 5.21, respectively, for NMSE and correlation value. The zoomed version of these figures which are shown in Figure 5.22 emphasize about the similarity of these results. The numerical representative of

some such values are shown in Table 5.8 and Table 5.9, respectively, for NMSE and correlation. The performance differences between each mother of wavelet in term of NMSE and correlation are around 0.47% and 0.4%, respectively.

Table 5.8 Representative of some values of NMSEfor Rayleigh Distribution data with different mother of wavele on 2D Wavelet Packet Algorithm

Wavelet	48	49	50	51	52
Daubhecies10	0.106891	0.105273	0.102765	0.100385	0.098653
Daubhecies20	0.106766	0.105107	0.102517	0.09999	0.098237
Symlett10	0.107207	0.105554	0.103002	0.100527	0.098817
Symlett20	0.108148	0.106578	0.104078	0.101515	0.099928
Coiflet2	0.106783	0.105138	0.102717	0.100272	0.09853
Coiflet3	0.10753	0.105935	0.103194	0.100789	0.099169
Bi-orthogonal3.5	0.116207	0.11448	0.112106	0.109711	0.108018
Bi-orthogonal6.8	0.108297	0.106646	0.104299	0.101847	0.100104

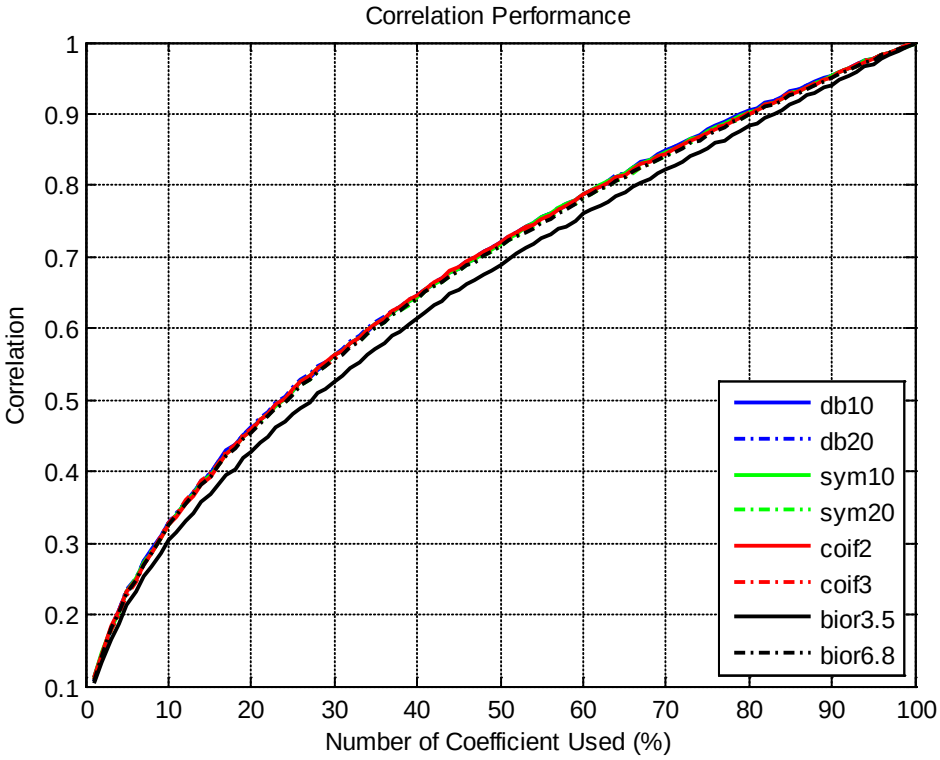

Figure 5.21 Correlation for Rayleigh Distribution Data with different mother of wavelet on 2D Wavelet Packet Algorithm

Nevertheless, if we consider Figure 5.21 and its zoomed version in Figure 5.22, there is a difference of channel behavior when Bi-orthogonal 3.5 and 6.8 are applied as mother wavelet in the decomposition process. These differences can be

occurred due to the different length of filter to the two initial type of wavelet (see Table 5.4)

However, the differences are also seen when wavelet mothers of coiflets are applied and compared to others. For example, if we consider coiflet2 which has filter length of 12, the accuracy of reconstruction is quite similar to the two initial wavelet mothers but different with bi-orthogonal 6.8 which also has same length of filter. These descriptions can be also supported by considering Figure 5.21.

Table 5.9 Representative of some values of Correlation for Rayleigh Distribution data with different mother of wavele on 2D Wavelet Packet Algorithm

Wavelet	48%	49%	50%	51%	52%
Daubhecies10	0.706285	0.711633	0.719843	0.727552	0.73311
Daubhecies20	0.706618	0.712105	0.720583	0.728756	0.734376
Symlett10	0.705159	0.710634	0.719006	0.727031	0.732525
Symlett20	0.702012	0.707237	0.715477	0.723827	0.728949
Coiflet2	0.706571	0.712005	0.719936	0.727854	0.733442
Coiflet3	0.704073	0.709365	0.71837	0.726176	0.731391
Bi-orthogonal3.5	0.675961	0.6818	0.689905	0.697983	0.703634
Bi-orthogonal6.8	0.701517	0.707015	0.714754	0.722753	0.728388

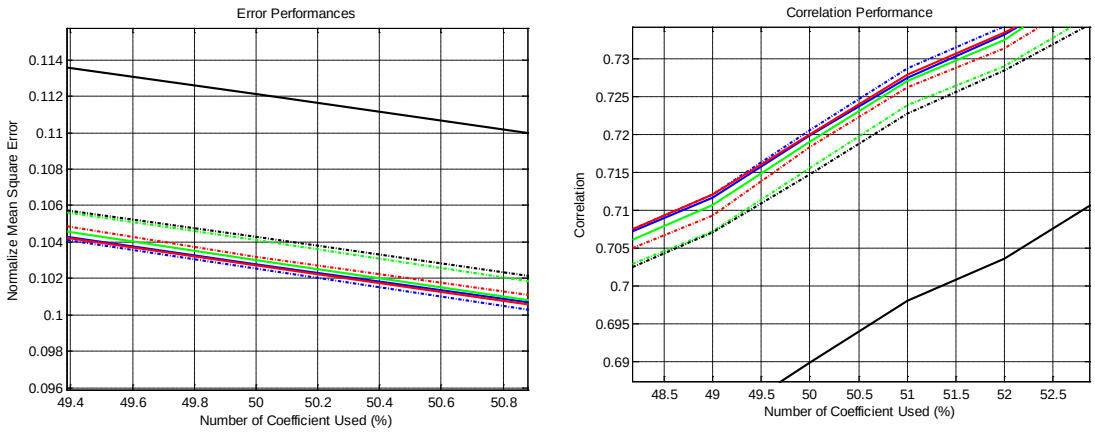

(a) (b)

Figure 5.22 Zoom version of (a) NMSE and (b) correlation for Rayleigh Distribution data with different mother of wavelet on 2D Wavelet Packet Algorithm

5.5.1.3 Sine Function

The last kind of input considered in this chapter is the mixed sine functions which contains different frequency. The idea behind generating this input is that in

real life, beside the random behavior, the signals are also contained different information of frequency which has to be considered.

This sine function used in the study is given as follows:

$$x_1(t) = \sin 2\pi t + \sin 4\pi t + \sin 6\pi t + \sin 8\pi t$$
$$x_2(t) = \sin 10\pi t + \sin 4\pi t + \sin 6\pi t + \sin 8\pi t$$
$$x_3(t) = \sin 14\pi t + \sin 4\pi t + \sin 6\pi t + \sin 8\pi t$$
$$x_4(t) = \sin 18\pi t + \sin 4\pi t + \sin 6\pi t + \sin 8\pi t$$
$$X(t,i) = x_i(t) \quad ,i = 1,2,3,4$$

A plot of the studied signal is given in Figure 5.23.

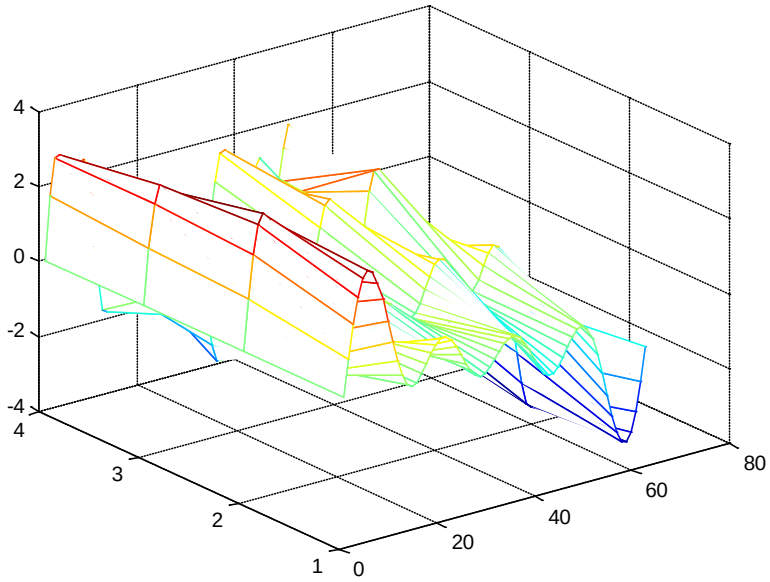

Figure 5.23 Sine Functions as input for 2D Wavelet Packet Based Algorithm

This input is passed through the algorithm to be decomposed with wavelet mother of Daubechies10 and decomposition level of 1. The reason of choosing daubechies10 has been described in the preceding part and the reason of choosing 1 level is due to the limitation of input data length. Actually, the level of decomposition can be increased by enlarging the input data length. However, due to the objectives of this part is to only observing the frequency information of the signal, hence the length of data is remain. After decomposing such signal, the 1 level 2D-WP bases is presented in Figure 5.24.

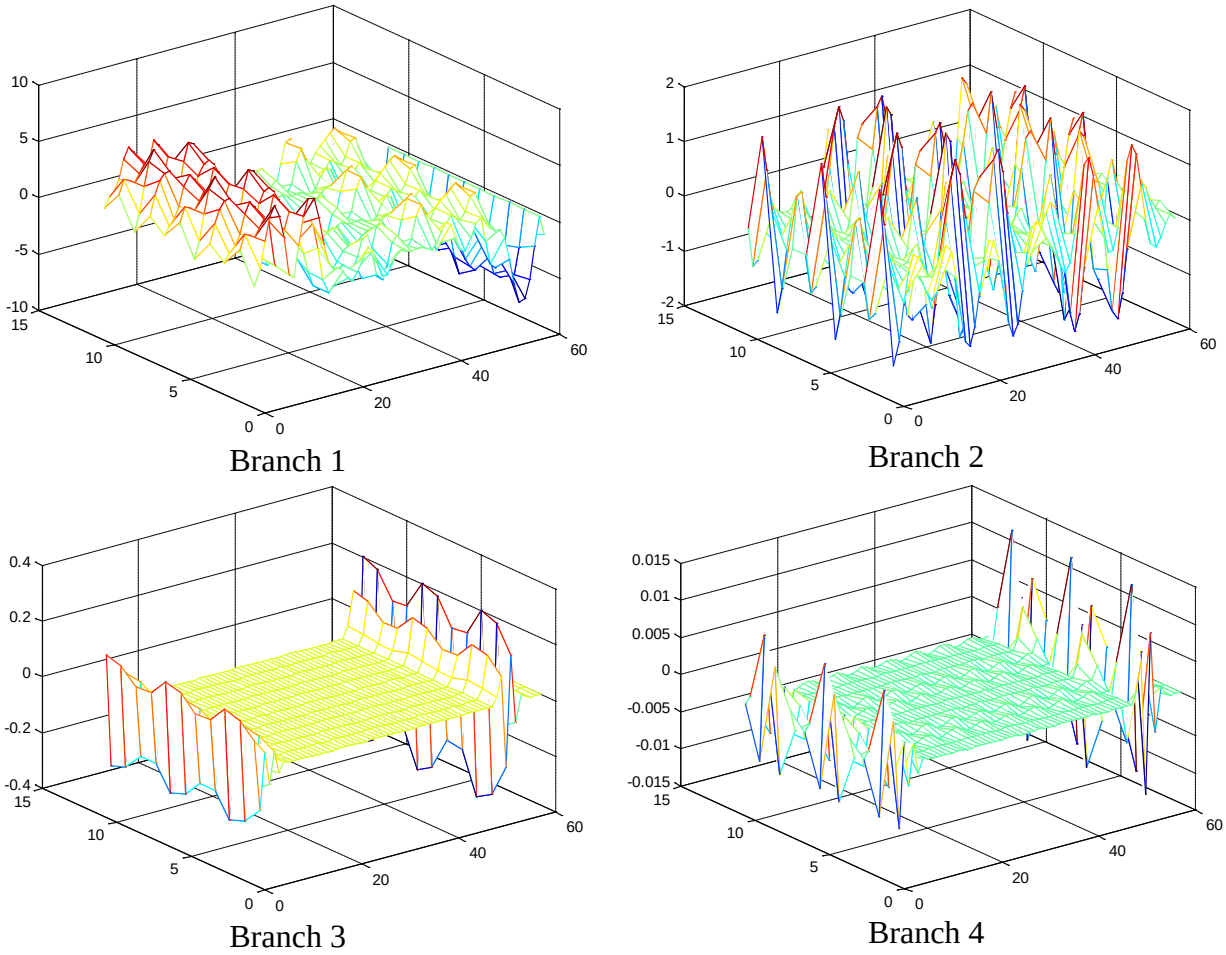

Figure 5.24 1 Level 2D-WP Bases of sine functions for 2D Wavelet Packet Algorithm

The result of these representations are depicted in Figure 5.25. From these figures, we can see that if the approximation which is situated in branch 1 is excluded in the signal reconstruction, the reconstructed signal is different to the original with NMSE of 0.9117. This condition occurs because the approximation branch contains all the information on the signal. Different to the rest of results which have almost similar shape with the original signal, the reconstruction which removed one of detail branch yields almost similar shape of signal due to less information about the signal is contained in the detail of 2D-WP bases.

5.6 Summary

In this chapter, the application of wavelet packet based algorithms for representing time-varying wireless channels is addressed. The possibility of using two-dimensional wavelet packet (2D-WP) transform for sparse representation of time-varying wireless channels was studied. Preliminary results illustrating the

efficacy of the 2D-WP approach were presented. Improving the performance of the proposed system an optimizations, namely, coefficient-reduction was implemented. Furthermore, the impact of the number of levels of 2D-WP decomposition and the type of mother wavelet employed were also investigated. To gauge the system performance first and second order stochastic metrics such as MSE, LCR and correlation were employed. The results of the study demonstrated the efficacy of the proposed 2D-WP method in efficient representation of radio channels.

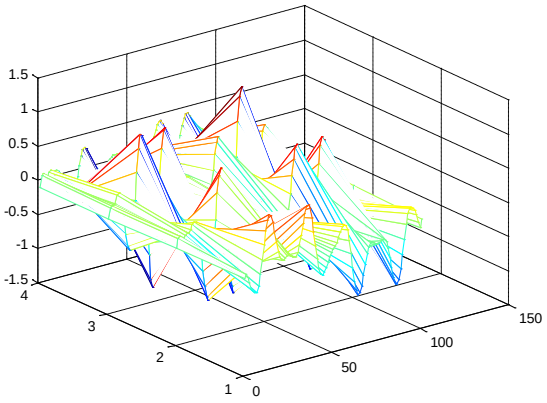

MSE = 1.8053
(Branch 1)

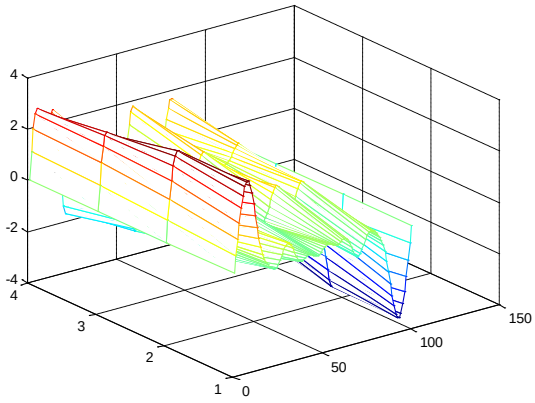

MSE = 0.1733
(Branch 2)

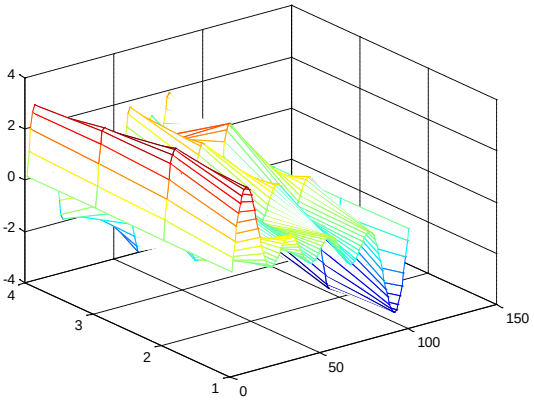

MSE = 5.2206e-04
(Branch 3)

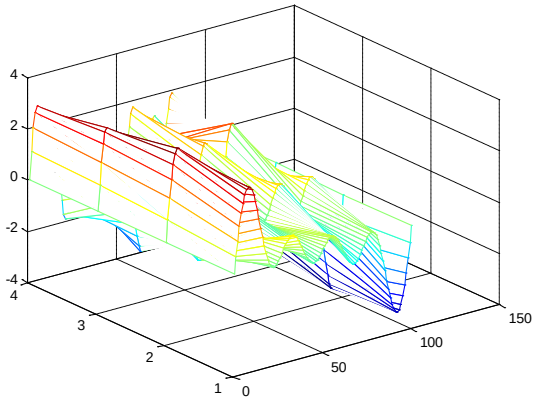

MSE = 4.4253e-07
(Branch 4)

Figure 5.25 2D-WP Reconstruction with one 2D-WP Bases removed

6

Conclusions and Recommendations

6.1 Conclusions

In this thesis report, the applicability of wireless channel representation based on wavelet packet algorithm is addressed. The possibility of one-dimensional and two-dimensional wavelet packet algorithm for time-invariant and time-varying representation, respectively, is investigated. The results illustrating the efficiency of one-dimensional and two-dimensional approach were presented. To improve the performance of the proposed system, two optimization methods, namely coefficient reduction and tree pruning were implemented. Furthermore, the impact of the number of decomposition level and the type of mother wavelet employed were also investigated. To measure the system performance, first and second order stochastic metrics such as MSE, LCR and correlation were employed.

From the whole study, represent the wireless channel using wavelet packet based algorithm is applicable and shows promising results on the efficiency and accuracy. Besides that, two optimization methods which are implemented in this algorithm also show promising result.

Through the simulation, time-invariant wireless channel can be well modeled using one-dimensional wavelet packet algorithm with implement either coefficient reduction methods or tree pruning. The accuracy and dependence between original and reconstructed signal over different number of coefficient reduction are similar when different level of decomposition and different type of mother wavelet are

employed. Hence, there is no significant impact on the performance from the use of different level of decomposition, the type of mother wavelet and different length of wavelet. The performance of the two methods is shown that when same number of coefficients which are used in the signal reconstruction, tree pruning yields better performance than coefficient reduction.

On the other side, two-dimensional wavelet packet algorithm can also represent the time-varying wireless channel, efficiently. Similar to the one-dimensional algorithm to represent time-invariant, the results of representations using two-dimensional algorithm show no significant effects on the performance by applying different level of decomposition and type of mother wavelet.

6.2 Future Research

1. Exploit the property of time-frequency tiling to obtain more information about the characteristic or behavior of the wireless channel.

   In this context, the information of frequency selectivity on the wireless channel is very important to guarantee a good quality of wireless communication. On the other side, time-frequency tiling offers the flexibility to obtain more information on the channel.

2. Develop an algorithm to determine the best level of decomposition based on the length of wireless channel response impulse.

   From the study in this thesis report, there is a big relation between length of data and level of decomposition. When length of data is longer, then the level of decomposition is also high. The increasing of decomposition level leads to the increasing of the number of coefficients which are obtained and also increase the load of computation. However, if the decomposition level is too low, it brings on the bad performance of representation. Hence, having a knowledge on the best level of decomposition is very important.

3. Develop an algorithm to represent different type of wireless channel by removing the redundant coefficient on their representation.

   On the data compression, there are to terms that are always considered to be taken into account, namely reducing the insignificant coefficient and reducing the redundancy of data. In this report, removal the insignificant coefficient has been well conducted. However, reducing the redundancy is not considered, whereas the duplicity of coefficient always occurs. Combining these two terms into the algorithm perhaps will give better performance in the representation.

4. Investigate the performance of wavelet based wireless communication system by implementation wavelet based channel modeling together with other related results.

   Wavelet transform holds prominent characteristic that can be used to obtain the information on the signal. On the other side, wavelet transform has been also widely used in other fields of wireless communication systems, such as wavelet packet based multicarrier modulation, wavelet packet based synchronization, and wavelet packet based equalization. Investigating the performance of those applications together with wireless channel modeling based wavelet packet will leads to incredible knowledge on the possible future system of communication.

5. Validation of proposed algorithm with real-time data analysis.

   Many channel models are derived from the empirical method which comes from the channel measurements at several locations. The results of this thesis only consider the behavior of characteristic certain parameters of the channel which haven proposed. In order to know the quality of the proposed algorithm, we have to change the input with the real-time measured data. For example, the measurement at TU Delft by Dr. Zoubir Irahhauten for his dissertation.

References

[1] T.S. Rappaport, *Wireless Communication – Principles & Practice*, Prentice Hall PTR, New Jersey, 1996.

[2] K. Pahlavan, A.H. Levesque, *Wireless Information Networks*. John Wiley & Sons, Inc. New York, 1995.

[3] G.L. Turin, F.D. Clapp, T.L. Johnston, S.B. Fine and D. Lavry, "A Statistical model of urban multipath propagation," IEEE Transaction on Vehicular Technology, Vol. VT-21, No.1, Feb 1972, pp.1-9.

[4] H.Hashemi, "The indoor radio propagation channel," Proceedings of the IEEE, vol.81, no. 7, July 1993, pp.943-968.

[5] S.J.Howard and K.Pahlavan, "Autoregressive modeling of wide-band indoor radio propagation," IEEE Transaction on Communication, vol. 40, no. 9, Sept. 1992, pp. 1540-1552.

[6] A. Goldsmith, *Wireless Communications*. Cambridge University Press, 2005.

[7] B. Sklar, "Rayleigh fading channels in mobile digital communication systems .I. Characterization," *Communications Magazine, IEEE,* vol. 35, pp. 90-100, 1997.

[8] M.Nakagami, "The *m*-distribution, a general formula of intensity distribution for rapid fading," in Statistical Methods of Radio Wave Propagation, Pergamon Press, 1960.

[9] A. Papoulis, Probability, *Random Variables, and Stochastic Processes*. Third Edition, McGraw-Hill International Editions, 1991.

[10] H.Suzuki,"A statistical model for urban radio propagation," IEEE Trans.Commun., vol. COM-25, pp.673-680, July 1977.

[11] W.C.Y. Lee, *Mobile Communication Engineering : Theory and Applications*. 2nd Edition," McGraw-Hill Telecommunication. 1997.

[12] A. Saleh and R. Valenzuela, "A statistical model for indoor multipath propagation," IEEE Journal on Selected Areas in Communications, vol. 5, pp. 128-137, Feb. 1987.

[13] Q. Spencer, M. Rice, B. Jeffs, and M. Jensen, "A statistical model for angle of arrival in indoor multipath propagation," IEEE Vehicular Technology Conference, vol. 3, no. 47, pp. 1415-1429, May 1997.

[14] G.Strang, T.Nquyen, “Wavelets and Filter Banks”, Wellesley-Cambridge Press, 1996

[15] B.Burke, The World According to Wavelets: The Story of a Mathematical Technique in the Making, Second Edition, A K Peters, May 1998

[16] R. Polikar, “The Engineer’s Ultimate Guide to Wavelet Analysis”, http://users.rowan.edu/~polikar/WAVELETS/WTtutorial.html

[17] S.G. Mallat, “A Theory for Multiresolution Signal Decomposition: The Wavelet Representation”, IEEE Trans. Pattern Anal. Machine Intell., Vol.11, pp.674-693, July 1989

[18] I. Daubechies, “Ten Lectures on Wavelets”, Philadelphia : SIAM, 1992.

[19] Online Encyclopedia - http://en.wikipedia.org/wiki/STFT

[20] H. Nikokaar, “Short Course: Wavelets for Wireless Communication”, European Conference and Wireless Technology, Munich, Germany, October 9-12, 2007

[21] A. Graps, “An Introduction to Wavelets”, IEEE Computational Science and Engineering, vol. 2, no.2, pp.50-61, 1995. (also available on http://www.amara.com/current/wavelet.html)

[22] M.K. Lakshmanan, and H. Nikookar, “A Review of Wavelets for Digital Wireless Communication”, Wireless Personal Communication, Vol. 37, No. 3-4, May 2006, pp.387-420, Springer.

[23] M. Vetterli and C. Harley, “Wavelets and Filter Banks: Theory and Design”, IEEE Transaction on Signal Processing, vol. 40, no. 9, pp. 2207-2232, September 1992.

[24] S. Mallat, “A theory for multiresolution signal decomposition: The wavelet representation,” *IEEE Transactions on Pattern Analysis and Machine Intelligence*, vol.11, no.7, pp.674-693, Jul 1989.

[25] A. Grossmann and J. Morlet, “Decomposition of Hardy functions into square integrable wavelets of constant shape,” SIAM J. Math.. vol. 15. pp. 723-736. 1984.

[26] M. Vetterli,and I. Kovacevic, "Wavelets and subband coding," Prentice Hall PTR, Englewood Cliffs, New Jersey, 1995.

[27] Y. Meyer. “Ondelettes et functtons splines,” Srm. Equarions aux Derivees Partielles. Ecole Polytechnique. Paris, France, Dec. 1986.

[28] C. S. Burrus, R. A. Gopinath, and H. Guo, Introduction to Wavelets and Wavelet Transforms, a Primer. Upper Saddle River, NJ: Prentice Hall, Inc, 1998.

[29] W. J. Phillips, “Wavelet and Filter Banks Course Notes”, 2003 [Available Online] http://www.engmath.dal.ca/courses/engm6610/notes/notes.html

[30] R.R. Coifman and Y. Meyer,"Orthonormal Wave Packet Bases," preprint, Numerical Algorithms Research Group, Yale University, 1989.

[31] R.R. Coifman, Y. Meyer and V. Wickethauser, "Adapted Waveform Analysis, Wavelet Packets and Applications," preprint, Numerical Algorithms Research Group, Yale University, 1992.

[32] M.V. Wickerhauser Adapted Wavelet Analysis from Theory to Software, A.K. Peters, Wellesley, MA (1994).

[33] A.R. Lindsey, Generalized Orthogonally Multiplexed Communication via Wavelet Packet Basis, Ph.D. dissertation, Faculty of the Russ College of Engineering and Technology, Ohio University, 1995.

[34] A.Lindsay, “Wavelet Packet Modulation for Orthogonally Transmultiplexed Communications”, IEEE Transaction on Communications, Vol.45, pp.1336-1339, May 1997.

[35] A.Jamin and P. Mahonen, “Wavelet packet modulation for wireless communications”, Published In Wireless Communications & Mobile Computing Journal, Vol. 5, Issue 2, pp. 123-137, John Wiley and Sons Ltd. March 2005.

[36] T.S. Rappaport et al, “Statistical channel impulse response models for factory and open plan building radio communication system design” , IEEE trans. on Communications, vol. 39, no. 5, pp795-807, May 1991

[37] H. Hashemi, “Impulse response modeling of indoor radio propagation channels”, IEEE JSAC vol. 11, no. 7,pp967-977, Sept. 1993.

[38] M. Sayeed and B. Aazhang, “Joint multipath-Doppler diversity in mobile wireless communications”, IEEE trans. on Communications, vol. 47, no. 1, pp 123-132, Jan. 1999.

[39] H. Nikookar, R. Prasad, "Simulation of mobile radio channel by Karhunen-Loeve analysis", Proceeding of MTT-S European Wireless, pp 128-133, Amsterdam, The Netherlands, 1998.

[40] R.R. Coifman and M.V.Wickerhauser, “Entropy-based algorithms for best basis selection”, IEEE Trans. on 1nfor.mation Theory, vol. 38, no. 2, pp 713-718, March 1992.

[41] G. Kantor, P.S. Krishnaprasad, “Efficient Implementation of Controllers for Large Scale Linear Systems via Wavelet Packet Transforms”, Proceeding of Conference on Information Sciences and Systems (CISS) 1998.

[42] D. Vautrin, X. Artusi, M.F. Lucas, D. Farina, “A Novel Criterion of Wavelet Packet Best Basis Selection for Signal Classification With Application to Brain–Computer Interfaces,” IEEE Transactions on Biomedical Engineering, Vol. 56, No. 11, Nov 2009

[43] F. Chen, W. Li; X. Li, “Audio Quality-Based Authentication Using Wavelet Packet Decomposition and Best Tree Selection,” Proceeding of International Conference on Intelligent Information Hiding and Multimedia Signal Processing (IIHMSP), 2008.

[44] H. Zhang and H. Fan, “An indoor wireless channel model based on wavelet packets”, Proceeding of the 34th Asilomar Conference on Signals, Systems, & Computers, Pacific Grove, CA, USA, October 2000.

[45] H. Zhang, H. Fan, and A. Lindsey, "A wavelet packet based model for time-varying wireless communication channels," Proc. 3rd IEEE SPAWC Workshop, Taiwan, March 2001.

[46] S.M.S Sadough and E. Jaffrot, “A Wavelet Packet Based Model For And Ultra-Wide Band Indoor Propagation Channel,“ Proceeding of ECPS Conference, France, March 2005.

[47] Laidler, Keith J. (1995). *The Physical World of Chemistry*. Oxford University Press. pp. 104–105. ISBN 0-19-855919-4.

[48] Oxford English Dictionary, Second Edition, 1989.

[49] Avery, John (2003). *Information Theory and Evolution*. World Scientific. ISBN 981-238-400-6

[50] C.E. Shannon, "A Mathematical Theory of Communication", *Bell System Technical Journal*, vol. 27, pp. 379-423, 623-656, July, October, 1948.

[51] K. Ramchandran and M. Vetterli, “Best wavelet packet bases in a rate distortion sense,” IEEE Trans. Image Processing, vol. 2, pp. 160–175, Apr. 1993.

[52] Online Encyclopedia – http://en.wikipedia.org/wiki/Mean_squared_error.

[53] Online Encyclopedia – http://en.wikipedia.org/wiki/Correlation_and_dependence.

[54] F. Pérez Fontán and P. Mariño Espiñeira “Modeling the wireless propagation channel : a simulation approach with MATLAB”. John Wiley & Sons, Ltd. United Kingdom, 2008.

[55] B. Liu, X. Ping, T. Zhang, M. Shao, “A new two-dimensional signal decomposition scheme using the extreme-lifting scheme,” *Proceeding of The 5th International Conference on Signal Processing, WCCC-ICSP 2000,* Vol.1, 21-25 Augst 2000.

[56] L. Zhou, X. Tong, "Application of two-dimension wavelet transform in image process of pets in stored grain," *Proceeding of 2008 International Conference on Machine Learning and Cybernetics*, vol.5, 12-15 July 2008

[57] M.C. Robini, I.E. Magnin, H.Benoit-Cattin, and Atilla Baskurt, "Two-Dimensional Ultrasonic Flaw Detection Based on the Wavelet Packet Transform," *IEEE Transaction On Ultrasonic, Ferroelectrics, and Frequency Control*, Vol. 44, NO. 6, November 1997, pp.1382-1394.

[58] F.G. Meyer, A.Z. Averbuch, J.-O. Stromberg, "Fast adaptive wavelet packet image compression," *IEEE Transactions on Image Processing*, vol.9, no.5, May 2000, pp.792-800.

[59] M. Misiti, Y. Misiti, G. Oppenhiem, J. Poggi, “MATLAB Wavelet Toolbox: Getting Started Guide” The Mathworks. (Also available on http://www.mathworks.com/help/toolbox/wavelet/wavelet_product_page.html)

[60] T.Q. Nguyen, J.S. Walker, “Wavelet-Based Image Compression,” Chapter on The Trasfrom And Data Compression Handbook, CRC Press, 2001.

Appendix

One of the important things in the modeling is validation, undeniable for wireless channel modeling. It needs also validation to ensure that the model stands in the right manner. Accordingly, while finishing this thesis, an effort towards validating the proposed algorithm to represent wireless channel model is also considered. The brief description in this appendix, hopefully, can be used to enrich the coverage of this research.

Firstly, the author has prescribed the data which will be used to validate the proposed algorithm in this thesis. The measurement data presented by Zoubir Irrahauten in his dissertation[2] is chosen to be used for validating the proposed algorithm. The measurement is conducted at EWI Building of Technische Universiteit Delft. The measurement data which are used in this thesis located at,

1. A Coridor which has LOS condition
2. An Office which has LOS condition
3. NLOS Condition between coridor and office
4. NLOS Condition inside an office with 1 wall of obstacle.

Each of measured data has 49 point of observation which refer to the number of channel impulse response and data length of 8000.

To evaluate the perfomance of the proposed algorithm, some variables are determined in this validation as follow,

1. Using 7 levels of decomposition
2. Iterate in 0-100% of significant coefficient with 8 types of mother wavelet
3. Represent the behavior of coefficient reduction in term of NMSE, Correlation and Time Delay Spread.

[2] Z. Irrahauten, "Ultra-Wideband Wireless Channel : Measurements, Analysis, and Modeling," Ph.D Dissertation. TU Delft. 2009

Besides that, several scenario are also considered in this validation to ensure that the proposed algorithm is working well. These scenarios are,

1. Using the theoritical distribution which are used in the measurement campaign as an input to the proposed algorithm, such as log-normal distribution, Gamma Distribution and Poisson distribution.
2. Using the statiscal distribution data of the measurement with the parameters which are obtained from the measurement.
3. Using the measured data directly as an input of algorithm.

All of the scenarios are measured their performnace in term of NMSE, Correlation dan RMS Delay Spread.

For initial validation, the author only consider one of the measured data which is located at a coridor with LOS condition. This measured data is directly passed to the proposed algorithm. From the simulation, it is shown that the proposed algorithm can be also used to represent the real measurement data. The result of this scenario is classified based on the variables of the proposed algorithm in terms of NMSE, Correlation and RMS Delay Spread, as follow.

A. Level of Decomposition

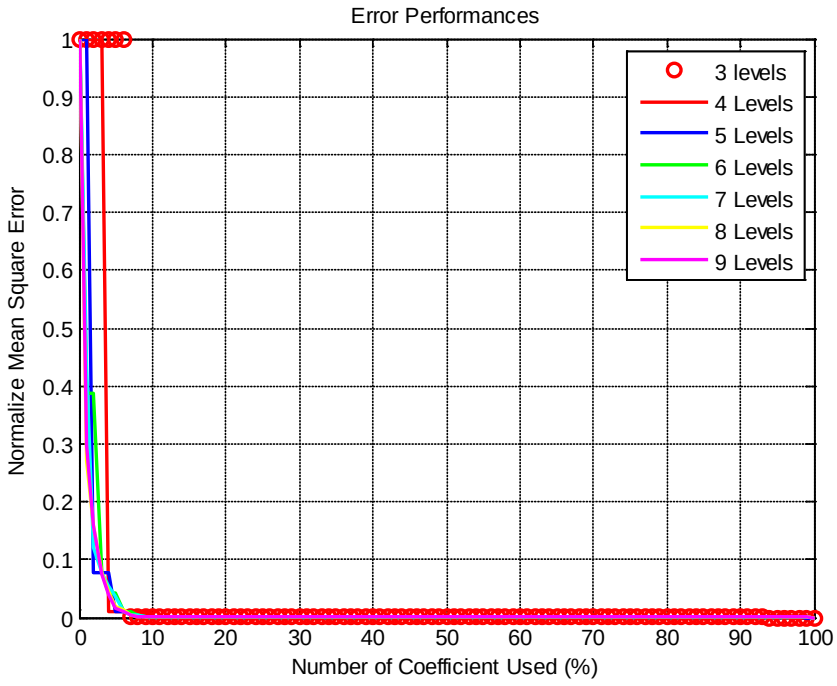

Figure 26 The Normalized Mean-Square Error for different level of decomposition

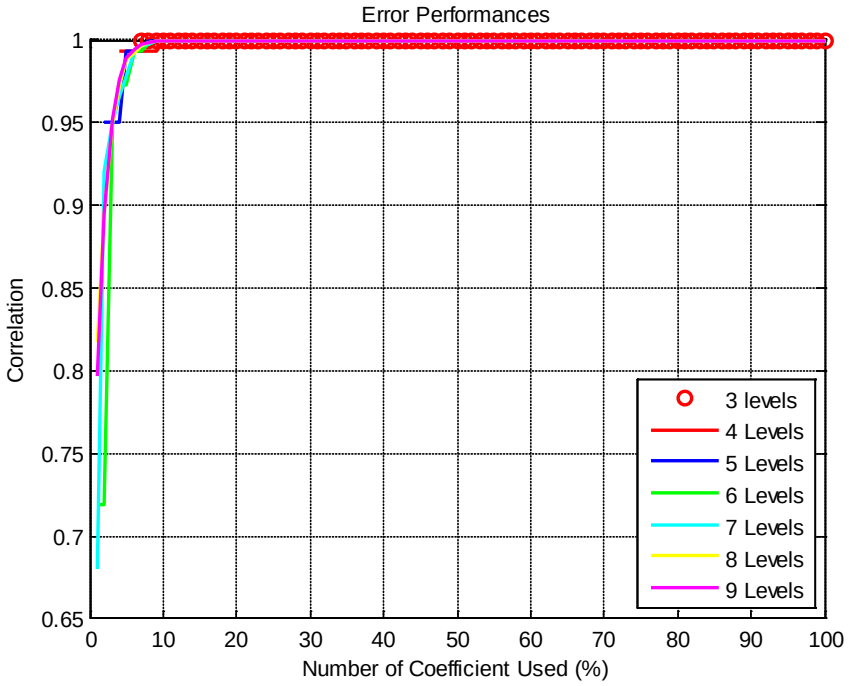

Figure 27 The Correlation for different level of decomposition

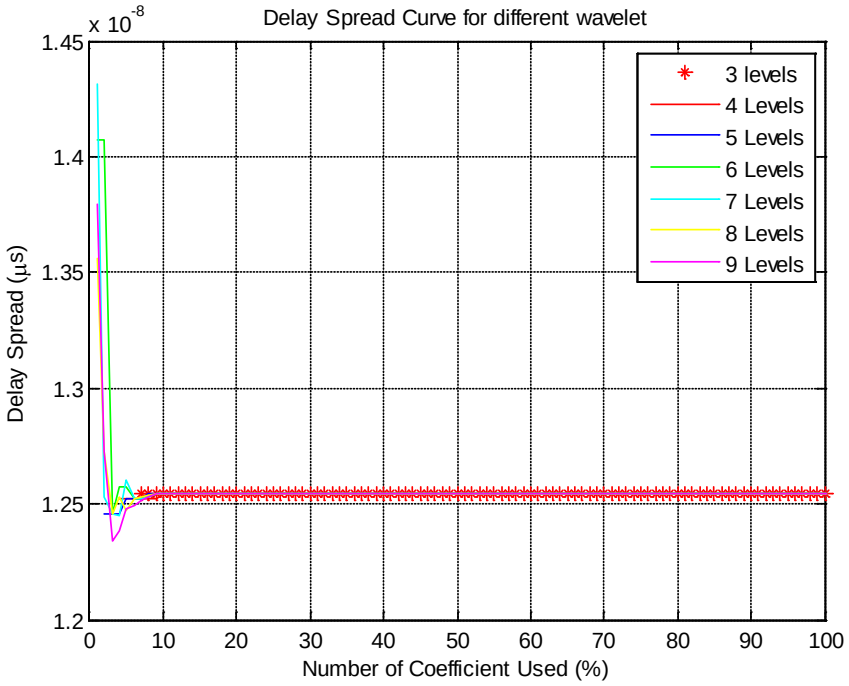

Figure 28 The RMS Delay Spread for different level of decomposition

B. Wavelet Filter

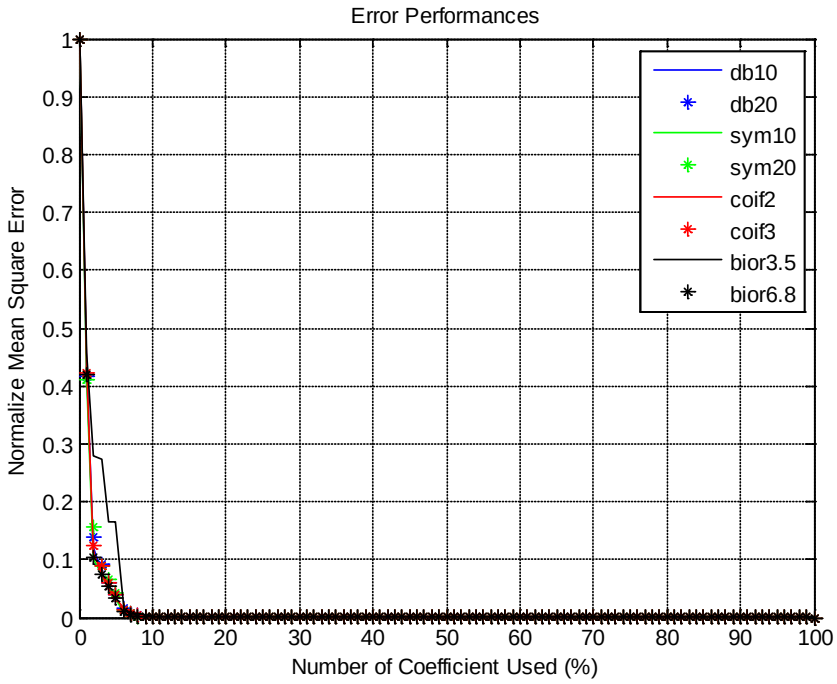

Figure 29 The Normalized Mean-Square Error for different type of Wavelet Filter

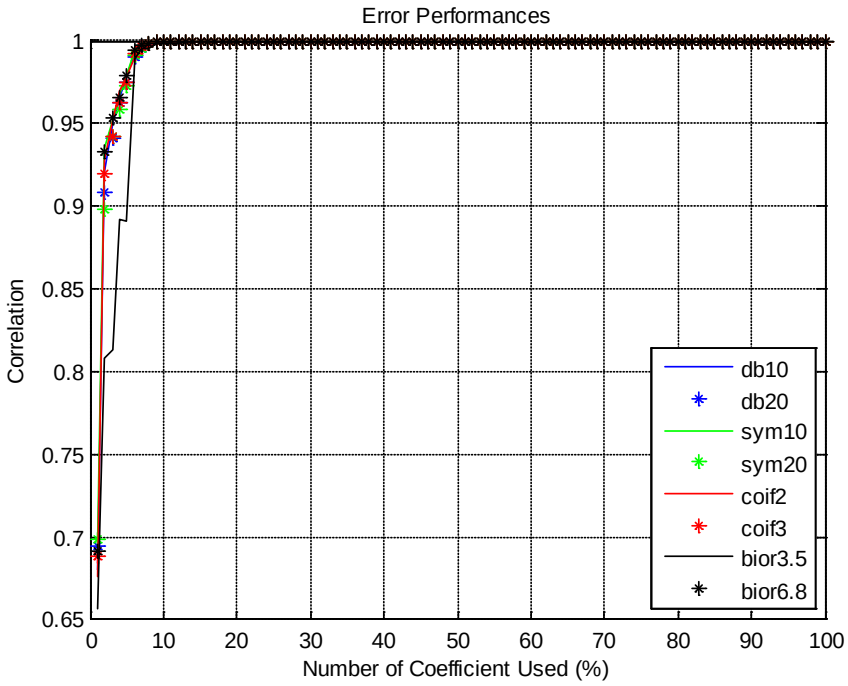

Figure 30 The Correlation for different type of Wavelet Filter

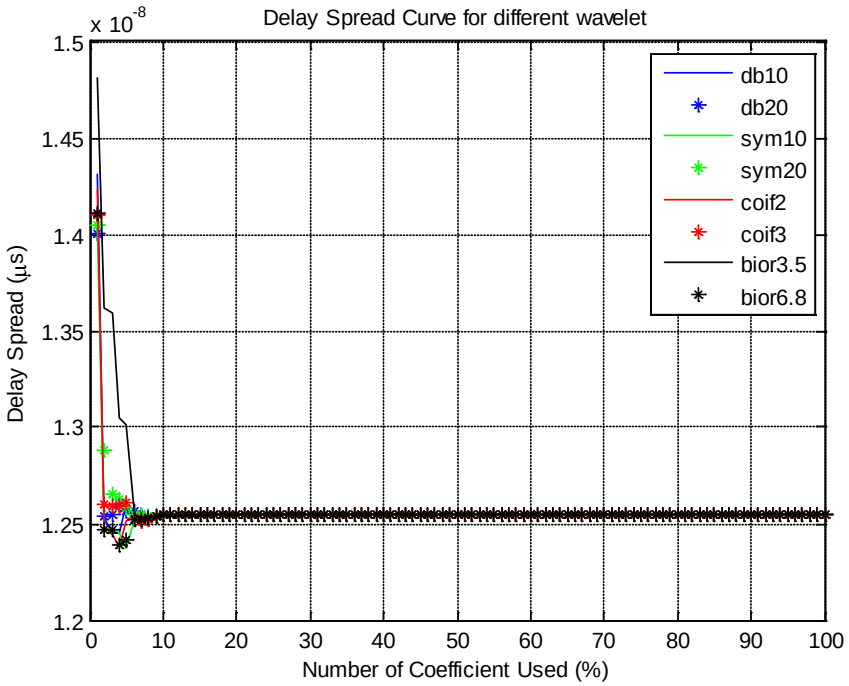

Figure 31 The RMS Delay Spread for different type of Wavelet Filter

From the results above, we can see that the proposed algorithm can be used to represent the real condition of the channel (in this case obtained from the measurement). Almost all of the figures show that the realible performance is started around 10% coefficient which are used to be reconstructed. Pleaseto be noted that it is only preliminary results to see the effect of input to the algorithm. The main challenges in this validation campaign which want to be achieved is that represent the statistical model obtained from the measurement. Besides that, the validation must also consider all of locations which are used to conduct the meaurement.